SIMULTANEOUS HYDRODENITROGENATION AND DEEP HYDRODESULFURIZATION

M. Egorova and R. Prins

Laboratory for Technical Chemistry, Federal Institute of Technology (ETH), Zurich, Switzerland

The hydrodenitrogenation (HDN) of 2-methylpyridine and 2-methylpiperidine and the hydrodesulfurization (HDS) of dibenzothiophene (DBT) and 4,6-dimethyl-dibenzothiophene (4,6-DMDBT) were studied separately and simultaneously over a sulfided NiMo/Al$_2$O$_3$ catalyst. Reaction conditions were 5 MPa total pressure, 300-340°C, and 35 kPa H$_2$S to minimize the influence of the H$_2$S formed during HDS. The first product in the HDN of 2-methylpyridine is 2-methylpiperidine, which reacts by ring opening to 2-aminohexane rather than hexylamine.

The same ring-opening pattern was observed for 2-ethylpiperidine, which demonstrates that the piperidine ring opens on the sterically less hindered side of the molecule and not on the side with the most   H atoms. This, and the small number of olefins formed, suggests that   elimination does not play an important role in the HDN of piperidine. In accordance with our HDN studies of dihexylamine, we therefore assume that piperidine mainly undergoes HDN by nucleophilic substitution by H$_2$S, followed by elimination and hydrogenolysis of the resulting alkanethiol.

2-Methylpyridine and 2-methylpiperidine completely blocked the hydrogenation pathway of the HDS of DBT (leading to cyclohexylbenzene) and inhibited the direct desulfurization route (leading to biphenyl). The inhibitory effect of 2-methylpyridine on the direct desulfurization was stronger than that of 2-methylpiperidine.

The main route in the HDS of 4,6-DMDBT was hydrogenation to tetrahydro-4,6-DMDBT followed by desulfurization, whereas in the HDS of DBT the selectivity towards hydrogenation was only 15%. Both the direct desulfurization and the hydrogenation pathway in the HDS of 4,6-DMDBT were strongly inhibited by 2-methylpyridine and 2-methylpiperidine. The hydrogenation to tetrahydro-4,6-DMDBT was slow and further hydrogenation and HDS were blocked.

The only remaining HDS pathway, direct desulfurization to 3,3'-dimethylbiphenyl, was very slow. The inhibitory effect of 2-methylpyridine on the HDS of 4,6-DMDBT was equal to that of 2-methylpiperidine. Thus, the HDS of di-alkyldibenzothiophenes in the presence of nitrogen-containing molecules is extremely difficult.

H$_2$S promoted the hydrogenation of 2-methylpyridine up to 10 kPa and inhibited it at higher H$_2$S partial pressures. H$_2$S, however, had a positive influence on the HDN of 2-methylpiperidine at all pressures. DBT and 4,6-DMDBT had a negative effect on the hydrogenation of 2-methylpyridine but did not influence the C-N bond cleavage in the HDN of 2-methylpiperidine. Therefore, C-N and C-S bond breaking take place at different active sites, whereas the hydrogenation sites for N- and S-containing molecules may be the same.

INFLUENCES OF NITROGEN SPECIES ON THE HYDRODESULFURIZATION REACTIVITY OF A GAS OIL OVER SULFIDE SPENT CATALYSTS.

SRI DJANGKUNG SUMBOGO MURTI, KI-HYOUK CHOI, YOZO KORAI and ISAO MOCHIDA
Institute of Advanced Material Study, Kyushu University, Kasuga, Fukuoka 816-8580, Japan

INTRODUCTION

The recent trend to tighten the regulation very rapidly to 10ppm S in gas oil requires better ways to achieve such a very low level of sulfur content at the least increase of cost. The major task is to hydrodesulfurize effectively and deeply the refractory sulfur species, which have been identified to be 4-methyl (4M), 4,6-dimethyl (4,6-DM), and 4,6,x-trimethyl (4,6,x-TM) dibenzothiophenes (DBTs). Such species are of very low reactivity apparently because of their methyl groups located to the neighbor of sulfur atoms in the center ring. In addition, they suffer marked inhibition by H_2S and NH_3 produced from the reactive sulfur species, nitrogen and aromatic species especially at their very low concentration below 500ppm, which makes further difficult their deep desulfurization. Hence removal of nitrogen species before the HDS is very effective [1].

Catalyst deactivation is an important fact in petroleum industries, from both economic and technological points of view. Coke deposition on the catalyst is generally believed to be the primary cause of catalyst deactivation in hydrotreating petroleum [2]. The loss of catalyst activity makes necessary to terminate the operation to regenerate the catalyst. Sintering during coke oxidation complicates regeneration of the supported catalyst.

In the present study, spent NiMo and CoMo alumina catalysts were evaluated in the hydrodesulfurization (HDS) reactivities of gas oil and its nitrogen species-free oil, in term of gross and molecular based desulfurization behaviors. The effects of nitrogen species removal and roles of the catalysts in the deep HDS of the gas oils and their respective sulfur species were discussed. Additionally, the reactivity of nitrogen species briefly discussed over the spent catalyst in HDS.

EXPERIMENTAL

I. Gas Oil sample and catalysts.

Some representative properties of gas oil and its nitrogen free one are summarized in Table 1. Spent $NiMo/Al_2O_3$ and $CoMo/Al_2O_3$ catalysts were provided in the test runs of a catalyst vendor. The catalyst was presulfided before reaction by H_2S (5vol%)/H_2 flow at 360 ^{o}C for 2 hours.

Table 1. Composition of original and N-free GOs

|	Gas Oil (GO)	N free Gas Oil (NF-GO)
Carbon (wt%)	85.95	86.08
Hydrogen (wt%)	12.30	12.30
Sulfur (wt%)	1.64	1.60
Nitrogen (ppm)	300	0

II. Hydrotreatment

HDS was performed in a 100 ml autoclave-type reactor. Gas oil (10 g) was hydrotreated at 340 ^{o}C under 50 kg/m^2 H_2 (initial H_2 pressure at room temperature) over 1 g of pre-sulfided catalyst by single and two-stage reaction configurations. The reaction times for the single stage were 30 and 60 min, while the two-stage reaction was consisted of two 30 min reactions. The second stage was operated after refreshing the reaction atmosphere with fresh H_2 at room temperature. The hydrotreated product was analyzed by GC-AED (Atomic Emission Detector, HP5890P, G2350A).

RESULTS AND DISCUSSION

1) Molecular composition of gas oils

Figure 1 illustrates carbon, sulfur and nitrogen chromatograms of feed gas oil (GO). GO consisted basically of paraffinic hydrocarbons as shown by spike peaks. Sulfur species found in GO were alkylbenzothiophenes (BTs), dibenzothiophene (DBT), and alkylated-dibenzothiophenes. Considerable amounts of 4-DBT, 4,6-DMDBT and 4,6,X-TMDBT were found in the oil. Most of the nitrogen species in the oil were non-basic species as carbazole and alkylated carbazoles.
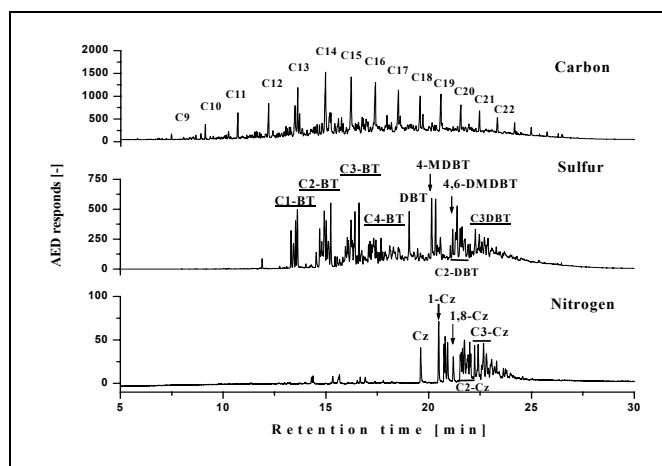
Figure 1. Carbon, sulfur and nitrogen chromatograms of gas oil.

2) HDS of total sulfur

HDS of GO and NF-GO over virgin and spent NiMoS and CoMoS catalysts is showed in Table 2. Relatively reactive sulfur species (benzothiophenes) were easily removed by 30 min HDS, however, refractory sulfur species still remained after 60 min of reaction. HDS activity of spent NiMo and CoMo catalysts decreased compare to the virgin ones. HDS over spent NiMo and CoMo left 1440 and 940ppmS, respectively, which are lower than both the virgin one 900 and 420ppmS, respectively. Nitrogen removal and two-stage reaction enhanced the HDS over spent NiMo and CoMo to 550 and 310ppmS, respectively, less than that of over virgin ones to be 130 and 160ppmS, respectively. It can be noted that nitrogen inhibition over spent catalysts is smaller than that of over virgin ones.

Table 2 HDS activity for total sulfur removal

Catalysts	GO			NF-GO		
	30	60	2st	30	60	2st
NiMo Virgin	2245	901	349	1079	260	129
Spent	5733	1439	1090	5244	958	594
CoMoVirgin	1177	421	333	686	194	161
Spent	3525	943	493	2810	689	310

3) HDS of refractory sulfur species

HDS activity of spent catalysts decreased more against refractory sulfur species (DBTs) as listed in Table 3. These catalysts suffer to much inhibition product gases such H_2S and NH3 especially spent NiMo one. HDS of refractory species in the first 30 min of reaction over spent NiMo and CoMo achieved 2300 (29%) and 1430 (56%) much lower than that over virgin one. Nitrogen removal and two-stage reaction enhanced the HDS over spent NiMo and CoMo catalysts up to 94 and 95% conversion, respectively.

Table 3 HDS activity for refractory sulfur removal

Catalysts	GO			NF-GO		
	30	60	2st	30	60	2st
NiMo Virgin	2116	885	194	605	161	139
Spent	2303	798	692	2150	576	195
CoMo Virgin	691	264	229	384	120	93
Spent	1432	455	270	1284	207	161

Among refractory sulfur species, 46DMDBT and 4E6MDBT were the most refractory ones. 46DMDBT over spent NiMo catalysts exhibited nuch the same reactivity than that over virgin one by single reaction, while that over spent CoMo was certainly lower than that over virgin one. Two stage reaction enhanced HDS over virgin NiMo to be much more active than the spent one. The same trend was observed in the HDS of 4E6MDBT as summarized in Table 4.

**Table 4** HDS activity for 46DMDBT and 4E6MDBT removal

	46DMDBT			4E6MDBT		
Catalysts	30	60	2st	30	60	2st
NiMo Virgin	123	77	33	59	39	16
Spent	121	76	71	59	33	32
CoMo Virgin	69	48	45	28	20	20
Spent	113	80	52	49	33	24
NiMo Virgin	63	25	24	29	12	11
Spent	114	58	19	57	28	10
CoMo Virgin	56	28	24	24	13	12
Spent	98	62	41	42	29	19

Nitrogen free oil enhanced the HDS of 46DMDBT over spent NiMo and CoMo, although the extent was smaller.

Carbon deposited on the spent catalysts was detected by RAMAN. The carbonization extent of carbon on the NiMo and CoMo catalysts was indicated by relative intensity of 1580 and 1360 cm^{-1} peaks. NH3 desorption measured by TPD suggested the spent NiMo lost the acidity while spent CoMo maintained acidity.

4) HDN over spent catalysts

HDN conversion of GO over virgin and spent NiMoS, CoMoS catalysts is illustrated in Figure 2. HDN activity of spent NiMo and CoMo catalysts was much decreased compared to that of the virgin ones, although the reactivity of nitrogen species was much the same.
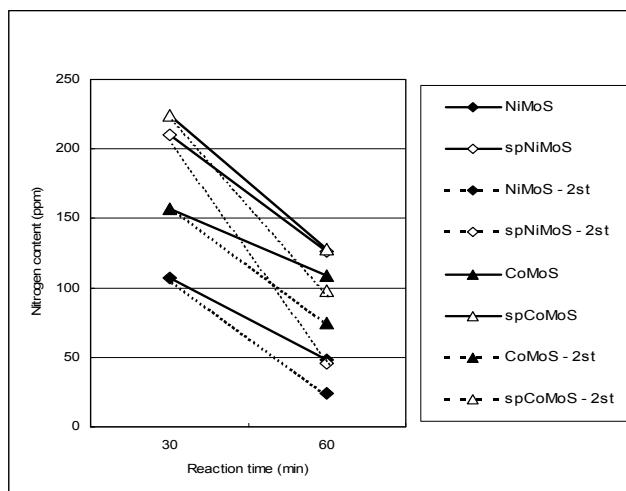
Figure 2. HDN conversion of GO over virgin and spent NiMoS, CoMoS alumina catalysts

Discussion

Spent catalysts lost their activity apparently due to the carbon deposition, which covered the active sites. Such carbon deposition reduced the acidity of NiMo catalyst while activity of CoMo can survive. Such carbon deposition changed the catalyst performances for the HDS against reactive and refractory sulfur species of original and NF oil in single and two-stage reaction.

The activity for refractory sulfur species is reduced more than that for the reactive species. The effect of two-stage and n-removal were markedly reduced over spent NiMo while rather limited over spent CoMo. Loss of activity by carbon deposition may be related with such changes in catalytic selectivity.

References
1. D. D. Whitehurst, T. Isoda, and I. Mochida, *Adv. Catal*. **42** (1998)345.
2. E. Furimsky, F.E. Massoth, *Catal. Today* **17** (1993) 537

Hydrodesulfurization of DBT over a NiMo catalyst: Inhibition by sulfur and aromatic compounds

Edd A. Blekkan[1], Anastasia Virnovskaia[1], Håkon Bergem[2], Petr Steiner[1]

1. Department of Chemical Engineering, The Norwegian University of Science and Technology (NTNU), N-7491 Trondheim, Norway
2. SINTEF Applied Chemistry, N-7465 Trondheim, Norway

Introduction

The key to achieving deep hydrodesulfurization (HDS) is the removal of complex sulfur molecules like dibenzothiophene (DBT) and the alkyl-substituted analogues of DBT, compounds that have a very low reactivity in catalytic HDS. In this paper we describe experimental work aimed at understanding the influence of sulfur and aromatic compounds in the oil on the activity of a Ni-Mo catalyst. DBT was used as a model compound for the HDS reaction.

Experimental

The experimental work was done in a fixed-bed microreactor using a model feed consisting of DBT in a hydrocarbon solvent (n-heptane). The feed was spiked with sulfur as dimethyldisulfide (DMDS) or thiophene or with aromatics (toluene or naphtalene) in varying concentrations. The hydrodesulfurisation of DBT was investigated, especially with respect to the products of the desulfurization. The catalyst used was a commercial Ni-Mo sample, which was crushed and sieved to 75-125 μm and presulfided according to the instructions from the manufacturer prior to the experiments.

Results and Discussion

After an initial period of stabilization in DBT/n-heptane, the catalytic activity for HDS of DBT was investigated as a function of the composition of the solvent. Fig. 1 shows the conversion of DBT as a function of the sulfur concentration in the feed. Added sulfur
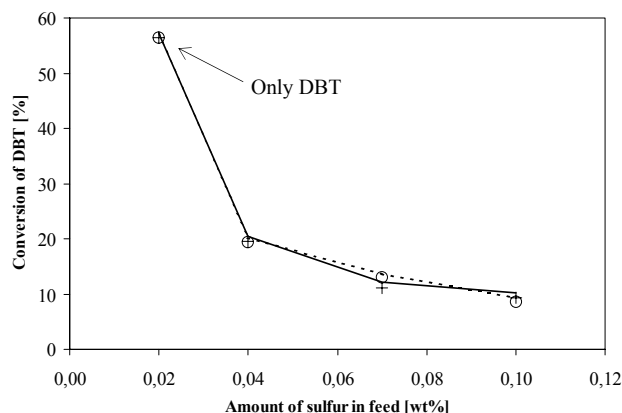
Figure 1. Effect of total sulfur concentration on catalytic conversion of DBT. Conditions: 2 MPa, 200 °C, LHSV=21.4 hr^{-1}, 0.1 wt% DBT in n-heptane. Extra sulfur added as DMDS (solid line) or thiophene (dashed line)

clearly inhibits the HDS, and there is no difference between the sulfur compounds added. This probably indicates that both compounds are rapidly converted to H_2S, and that the inhibition in this case is due to a competitive effect of H_2S. The order with respect to sulfur was determined, and found to be −0.6, a value that corresponds well with widely used LHHW-type rate expressions for HDS of DBT, where the H_2S-concentration appears in the denominator of the expression.

Fig. 2 shows the effect of added aromatics in the feed, keeping
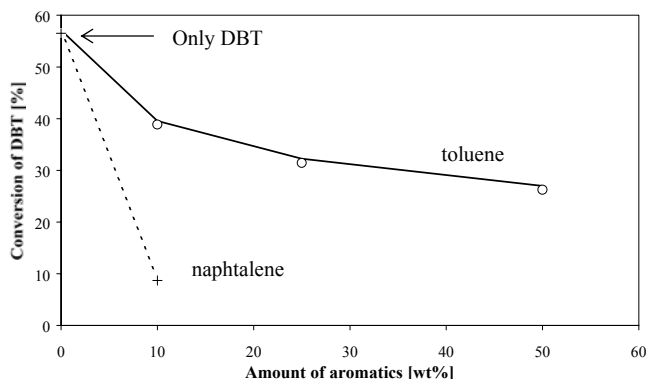
Figure 2. Effect of added aromatics on the catalytic conversion of DBT. Conditions: 2 MPa, 200 °C, LHSV=21,4 hr^{-1}, 0,1 wt% DBT in n-heptane or n-heptane/aromatic solvent.

DBT concentration constant. The order with respect to toluene was estimated to be approximately −0.2, again a value that can be rationalized in terms of a classical LHHW rate-equation with the aromatic compound as an inhibitor in the denominator. A stronger inhibition by naphtalene was observed, but further experiments were not performed due to a strong, irreversible deactivation, probably due to coking. The same effect, though even more pronounced, was observed for 1-methyl-naphtalene.

The products of the DBT reaction were identified to be cyclohexylbenzene (CHB), biphenyl (BP) and partially hydrogenated DBT (TetrahydroDBT, THDBT and hexahydroDBT, HHDBT). All these products were observed in all experiments, but their concentrations varied according to conversion and the use of the added components. These products are usually ascribed to a direct desulfurization of DBT, giving BP as the product, or a route involving hydrogenation of the aromatic ring to THDBT/HHDBT as intermediates followed by desulfurization to CHB. BP can also be hydrogenated to CHB, but this is reported to be a slow process (1). The final hydrogenation product, bicyclohexyl (BCH) was not observed here.

BP was the main product in all cases, indicating that the direct desulfurization route is the most important also over NiMo, as has been concluded earlier for CoMo catalysts (1). In general, the ratio between CHB and BP increased with increasing DBT conversion. However, the influence of the inhibitors on the overall activity was different. Even though the effect of DMDS and thiophene on the overall DBT conversion was similar there were subtle differences in the selectivities. Small amounts of thiophene seemed to favour the direct desulfurization, seen as an increased selectivity to BP. With DMDS as the source of the added sulfur the opposite effect was observed, at least at low conversions. Addition of toluene led to a higher selectivity to BP at the expense of CHB, apparently inhibiting the hydrogenation stronger than the hydrogenolysis sites on the catalyst.

(1) H. Topsøe, B.S. Clausen, F.E. Massoth, Hydrotreating Catalysis, Springer-Verlag, Berlin Heidelberg, 1996, and references cited therein.

HYDRODESULFURIZATION OF LIGHT CYCLE OIL

Ki-Hyouk Choi, Yosuke Kinoshita, Yozo Korai, and Isao Mochida*

Institute of Advanced Material Study, Kyushu University
Kasuga-Koen, Kasuga, Fukuoka 816-8580 JAPAN
*e-mail : mochida@cm.kyushu-u.ac.jp

INTRODUCTION

Light cycle oil from fluid catalytic cracker(FCC) is one of the main streams for diesel oil pool. About one-third of the total diesel product was reported to be from cracked feedstocks in America[1]. As the regulations on the sulfur content of diesel fuel become stricter, hydrotreating of LCO to meet forecasted specifications has been urgent issue in refinery industry. It has been well-known that hydrodesulfurization of LCO is much more difficult than that of straight run gas oil due to its large content of aromatic components[2]. Nitrogen species is also strong inhibitor for HDS reaction. Fundamental properties of LCO strongly depend on the feed and operating conditions of FCC.

In this study, LCO having different aromatic contents, distillation ranges and nitrogen contents were hydrodesulfurized by using sulfide catalysts supported on alumina and silica-alumina-zeolite as an effort to find a better way to hydrodesulfurize LCO to meet the future regulations on sulfur content of diesel fuel.

EXPERIMENTS

ALCO, BLCO and CLCO were provided from refiners. Their basic properties were summarized in Table 1. Hydrodesulfurization experiments were conducted by using autoclave-type reactor(100 ml internal volume) at 340 ^{o}C and 360 ^{o}C. Initial hydrogen pressure was adjusted to 50 kg/cm^2. The catalysts, which were obtained from commercial catalyst vendors, were CoMo and NiMo supported on alumina(-A) and silica-alumina-zeolite(-SAZ). Pre-sulfidation was performed at 360 ^{o}C for 2 hours under 5% H$_2$S/H$_2$ stream

Reaction products were analyzed by GC-AED(HP5890P and G2350A).

Table 1. Basic Properties of LCO.

Property	ALCO	BLCO	CLCO
Total Sulfur Content	9,070 ppmS	9,156 ppmS	8,928 ppmS
Total Nitrogen Content	230 ppmN	1,322 ppmN	825 ppmN
Non-aromatics[*1]	22.2 wt%	12.6 wt%	13.1 wt%
Aromatics[*1]	77.8 wt%	87.4 wt%	86.9 wt%
IBP(^{o}C)	173.0	227.5	
T50(^{o}C)	270.0	323.5	
T90(^{o}C)	358.0	345.5	
FBP(^{o}C)	-	374.5	

*1: ASTM D2549-91

RESULTS AND DISCUSSIONS

Although total sulfur contents were almost same for each other, BLCO and CLCO had much higher nitrogen content as shown in Table 1. BLCO and CLCO contained more aromatic fraction and high boiling-point species than ALCO. Fig. 1 showed carbon, sulfur, nitrogen chromatograms of ALCO and BLCO. Although total nitrogen content of CLCO was 62% of that of BLCO, carbon and sulfur chromatograms of CLCO were not different from those of BLCO. Most of sulfur species present in LCO samples were analyzed to be aromatic. Alkylated benzothiophenes were found in BLCO and CLCO as in trace level while ALCO contained small amount of them. BLCO and CLCO showed dominant presence of alkylated DBT such
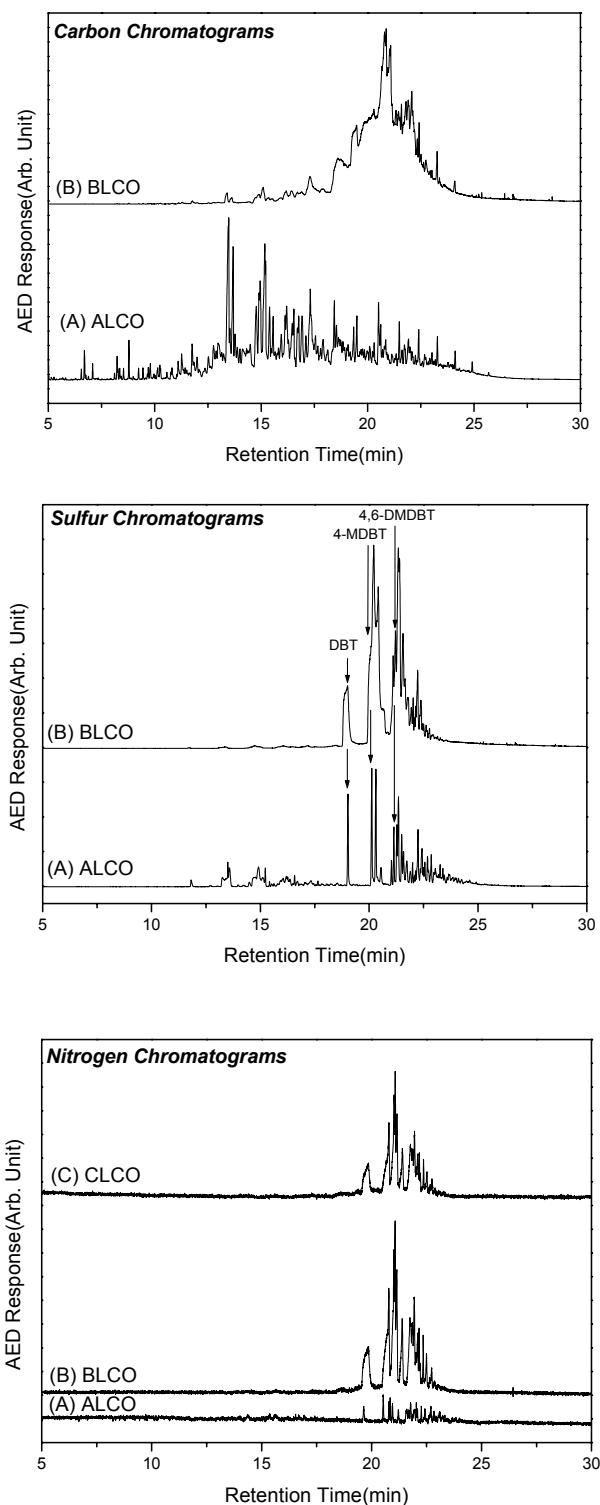

Figure 1. Carbon, sulfur, and nitrogen chromatograms of (A) ALCO, (B) BLCO, (C) CLCO.

as 4-MDBT, 4,6-DMDBT, 4,6,X-TMDBT. Broad peaks on sulfur chromatograms of BLCO seems to be from the non-aromatic sulfur species. Most of nitrogen species found in LCO samples were Carbazoles.

Table 2 is the total sulfur, total nitrogen, DBT, 4-MDBT, and 4,6-DMDBT contents remained after 2 hours hydrodesulfurization. The HDS of SRGO having total sulfur and nitrogen contents of 14,354 ppmS and 250 ppmN, respectively, by the same conditions(340°C and CoMo-A catalyst for 2 hours) resulted in 95% conversion(661 ppmS) of total sulfur content. As can be seen in Table 2, the reactivity order of HDS is ALCO >> CLCO > BLCO for all catalysts. Remained sulfur content in ALCO was around 14 - 25%. However, BLCO and CLCO resulted in the total sulfur content of 26 - 47% after reaction at 340 °C. While the reaction at higher temperature of 360 °C gave less sulfur contents, the lowest sulfur content was 953 ppmS by NiMo-A from CLCO. Remained sulfur species from ALCO were 4-MDBT, 4,6-DMDBT, 4,6,X-TMDBT and DBT was less than detectable level as in Table 2 in the case of NiMo-A and CoMo-A. Although quantification of each sulfur species in HDS products of BLCO and CLCO had some uncertainty due to broad peaks as in Fig. 1, HDS conversion of DBT was much higher than those of 4-MDBT and 4,6-DMDBT. Furthermore, remained content of 4-MDBT and 4,6-DMDBT was not much different in the case of 340 °C reactions of BLCO and CLCO although HDS at 360 °C resulted in lower content of 4-MDBT than that of 4,6-DMDBT.

HDN activity also depended on the LCO type. ALCO showed much lower nitrogen content of HDS products than BLCO and CLCO. The difference in HDN activity between BLCO and CLCO was small except for CoMo-SAZ. HDS activity was higher over CoMo catalyst for all cases irregardless of support type except for BLCO HDS at 360°C. HDS of 4-MDBT and 4,6-DMDBT in ALCO were more active over CoMo and NiMo catalyst respectively. However, NiMo catalyst showed higher activity for HDS of 4-MDBT and 4,6-DMDBT in BLCO and CLCO except for CLCO at 360 °C over -SAZ catalyst. HDS of DBT was faster over NiMo catalyst than CoMo catalyst in the case of BLCO and CLCO. HDN Activity was higher over NiMo catalyst in all reactions. -SAZ catalysts, which are more acidic than -A catalyst, were inferior to those supported on alumina in HDS reaction. HDN activity order was NiMo-A>NiMo-SAZ>CoMo-SAZ>CoMo-A for BLCO and CLCO. HDS and HDN of gas oil was reported to be strongly inhibited by the aromatic species[3, 4]. In this study, LCO having larger content of aromatic fraction showed much lower HDS and HDN activity.

CoMo catalyst, which has been reported to have higher activity for direct desulfurization than NiMo catalyst, showed higher activity in the HDS of all LCO samples. In contrast, HDS of 4,6-DMDBT was higher over NiMo catalyst than CoMo catalyst. This observation could be rationalized by higher activity of NiMo catalyst toward hydrogenative route in the HDS of hindered DBT[4]. Zeolite has been known to be active for hydrogenation, hence could enhance HDS by partial hydrogenating aromatic partner of dibenzothiophene.

However, catalytic function of zeolite components for the HDS of LCO was blocked by large content of aromatic species. Although nitrogen species was also inhibitor for HDS, their effects was not distinct in this study when compared to aromatic content. In spite nitrogen species was reported to have more inhibiting effect than aromatic species in HDS of model gas oil[5], much higher aromatic content of LCO might hinder the observation of the effect of nitrogen content. Nevertheless, CLCO showed slightly higher HDS activity than BLCO. This different activity became more definite at the HDS of 360 °C. HDN of carbazoles was believed to proceed via hydrogenative ways. Hence, NiMo catalyst showed higher activity to HDN of LCO samples.

CONCLUSIONS

LCO showed very limited activity for HDS when compared to that of SRGO. LCO having larger aromatic content showed much lower activity. Nitrogen content in LCO had relatively small effects on HDS. CoMo and alumina showed better performance than NiMo silica-alumina-zeolite for HDS.

REFERENCES
(1) U. S. E.P.A. IN *Regulatory Impact Analysis: Heavy-Duty Engine and Vehicle Standards and Highway Diesel Fuel Sulfur requirements*, EPA 420-R-00-026, Washington DC., **2000**.
(2) Turaga, U and Song, C. Prepr. Pap. -*Am. Chem. Soc., Div. Petrol. Chem.*, **2002**, *47(1)*, 97.
(3) Ma, X; Sakanishi, K; Isoda, T.; Mochida, I. *Ind. Eng. Chem. Res.* **1995**, *34*, 748.
(4) Whitehurst, D. D; Isoda, T.; Mochida, I. *Adv. Catal.* **1998,** *42*, 345.
(5) Koltai, T; Macaud, M; Guevara, A; Schulz, E; Lemaire, M; Bacaud, R; Vrinat, M. *Appl. Catal. A.* **2002**, *231*, 253.

Table 2. Remained total sulfur content of hydrodesulfurized LCO samples after 2 hours reaction at 340°C and 360°C.

Catalyst	Temp. (°C)	ALCO					BLCO					CLCO				
		S (%)	N (%)	DBT	4-MDBT	4,6-DMDBT	S (%)	N (%)	DBT	4-MDBT	4,6-DMDBT	S (%)	N (%)	DBT	4-MDBT	4,6-DMDBT
NiMo-A	340	16%	6%	N.D.	26%	56%	35%	7%	6%	44%	58%	28%	7%	3%	36%	47%
CoMo-A	340	14%	8%	N.D.	20%	71%	30%	41%	2%	46%	64%	26%	35%	2%	39%	51%
NiMo-SAZ	340	25%	4%	2%	48%	69%	47%	17%	17%	50%	49%	43%	15%	16%	48%	48%
CoMo-SAZ	340	20%	5%	1%	39%	76%	40%	32%	16%	52%	53%	34%	16%	10%	47%	51%
NiMo-A	360	–	–		–	–	14%	5%	0%	18%	47%	11%	10%	0%	13%	36%
CoMo-A	360	–	–		–	–	16%	24%	0%	21%	61%	11%	28%	0%	14%	44%
NiMo-SAZ	360	–	–		–	–	28%	18%	4%	37%	60%	23%	18%	2%	30%	43%
CoMo-SAZ	360	–	–		–	–	27%	23%	4%	41%	65%	17%	18%	1%	26%	49%

Kinetic Study of 4,6-Dimethyldibenzothiophene Hydrodesulfurization over Ni Phosphide, NiMo and CoMo Sulfide Catalysts

Jae Hyung Kim[1], Xiaoliang Ma[1], Chunshan Song[1*]
S. Ted Oyama[2] and Yong-Kul Lee[2]

[1] Clean Fuels and Catalysis Program, The Energy Institute and Department of Energy & Geo-Environmental Engineering, Pennsylvania State University, University Park, PA 16802

[2] Environmental Catalysis and Materials Laboratory, Department of Chemical Engineering, Virginia Polytechnic Institute and State University, Blacksburg, VA 24061

Introduction

Ultra-deep hydrodesulfurization (HDS) of diesel fuel is an important research area due to increasingly stringent environmental regulations for fuel sulfur content (1). Alkyl dibenzothiophenes, especially, those with two alkyl groups at the 4- and/or 6-positions of dibenzothiophene (DBT) are still remained in the current commercial diesel fuel, such as 4,6-dimethyldibenzothiophene (4,6-DMDBT), which has been reported as one of the most refractory sulfur compounds in diesel fuel (2,3). HDS of dibenzothiophenes general proceed through two pathways, hydrogenation and hydrogenolysis pathways (4,5). Kinetic data of 4,6- DMDBT HDS for individual reaction pathways are necessary for evaluating new catalysts and for designing new ultra-deep HDS processes. However, such kinetic data are very limited in the literature. In the present study, HDS of 4,6-DMDBT HDS over a Ni_2P/USY phosphide catalyst and two commercial sulfide catalysts was conducted and the rate constants of the three catalysts for the two pathways were measured.

Experimental

4,6-DMDBT was used as the model sulfur compounds in the present study, and decalin was used as solvent. The reactions were carried out in 25-mL, horizontal micro-reactor agitated at 200 strokes/min in a fluidized sand bath within reaction time of 20 min. Reaction temperature was varied from 275˚C to 325˚C under 300 psi H_2 pressure, and H_2 pressure was also varied from 200 psi to 600 psi at 300˚C. In order to examine the effect of aromatic or nitrogen compound on HDS of 4,6-DMDBT, 1-methylnaph-thalene with the same mole as 4,6-DMDBT was added into the feed, and about 800 ppmw quinoline was added. Gas chromatography with a FID detector was used for quantitative analysis of products. GC-MS was used for identification of products.

Two commercial catalysts from Criterion, Cr344 (CoMo/Al_2O_3) and Cr424 (NiMo/Al_2O_3), were used after presulfidation at 350˚C for 4 h with 10 vol % H_2S in H_2 at a flow rate of 200 mL/min. After presulfidation, the catalysts were stored in decalin before use in order to minimize oxidation. Ni_2P/USY catalyst, which was provided by Virginia Tech, was treated in a H_2 flow at 420˚C for 4 h because it has been reduced at 580˚C in H_2 and passivated in 0.5%O_2/Ar flow. After treatment, the reduced Ni phosphide catalyst was also stored in decalin before use.

Results and Discussion

In order to get better kinetic data, the conversion of 4,6-DMDBT was kept below 15%. The main products were tetrahydro-dibenzothiphene (4HDMDBT), dimethlybipheny (DMBP) and meth-ylcyclohexyl-toluene (MCHT). Dimethyldicyclohexane (DMDCH) was also detected when the reaction time was more than 7 min. Hexa-hydrodibenzothiophene (6HDMDBT) was also detected in the HDS reaction over sulfided NiMo and reduced Ni_2P catalysts even

under low hydrogen pressure. 6HDMDBT was observed in the HDS over sulfided CoMo catalyst under high hydrogen pressure. The schematic diagram of 4,6-DMDBT HDS is shown below;
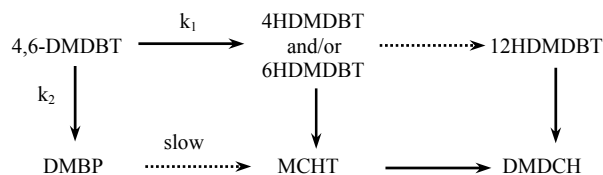

In general, HDS of individual sulfur compound follows the pseudo-first-order kinetics, thus: $\ln(C_{DMDBT}/C_{DMDBT0}) = - (k_1+k_2) \cdot t$, where k_1 is the pseudo first-order rate constant for the hydrogenation pathway, and k_2 is the pseudo first-order rate constant for the hydrogenolysis pathway. The value of (k_1+k_2), overall rate constant, can be calculated from experimental data. **Figure 1** shows the pseudo first order kinetic profile and **Table 1** lists the overall rate constants of 4,6-DMDBT HDS over the NiMo, CoMo and Ni_2P catalysts.
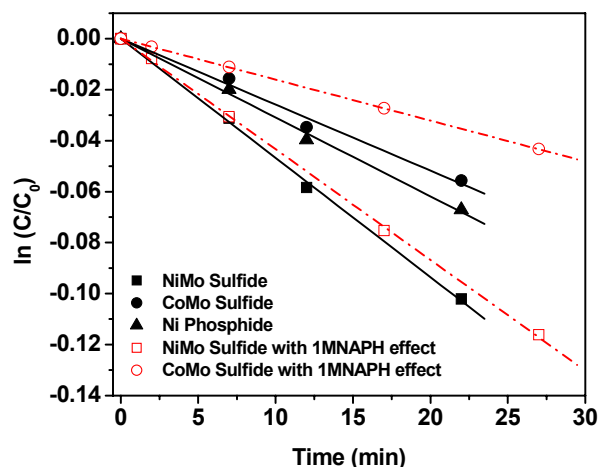
Figure 1. Pseudo first-order kinetics of 4,6-DMDBT HDS over the NiMo, CoMo and Ni_2P catalysts. (Reaction temp. = 300 °C and H_2 pressure = 300 psi).

As shown in **Figure 1,** the NiMo catalyst is more active than the CoMo catalyst in HDS of 4,6-DMDBT. 4HDMDBT and 6HDMDBT, which are the hydrogenated products of 4,6-DMDBT, were found to be dominant over the three catalysts, especially, over the NiMo catalyst and Ni phosphide. It was reported that NiMo catalysts favor HDS of 4,6-DMDBT because Ni catalysts have excellent activity for hydrogenation. After hydrogenation of 4,6-DMDBT, elimination of the sulfur atom becomes easy because hydrogenation reduces the methyl steric hindrance through molecular puckering and increases the electron density on the S atom (6). In general, HDS reaction is inhibited by coexisting aromatics and nitrogen compounds. However, in the present study, 1-methylnaphthalene was found to have only slightly inhibiting effect toward HDS of 4,6-DMDBT as the rate constants and product distributions in the presence of 1-methylnaphthalene and in the absence of 1-methylnaphthalene were similar. Quinoline was found to be a strong inhibitor toward the reaction. The conversion of 4,6-DMDBT was below 5% over both the NiMo and the CoMo catalysts even for the reaction at 300 ˚C over 60 min.

In order to measure the individual value of k_1 and k_2, we tried to measure k_1/k_2 ratio, as k_1 and k_2 values can be calculated by combination of (k_1+k_2) and k_1/k_2 values. We explored three methods to determine k_1/k_2 ratio. In Method 1, k_1/k_2 ratio is considered to be equal to $[C_{HDMDBT}+C_{MCHT}+C_{DMDCH}]/C_{DMBP}$ ratio, assuming that the conversion of DMBP to MCHT is negligible. In Method 2, k_1/k_2 ratio is considered to be equal to the initial selectivity ratio of hydrogenation products to hydrogenolysis products. Initial selectivity of each compound is obtained by extrapolating the selectivity curve to zero conversion as shown in **Figure 2**. **Table 1** lists the kinetic data at different temperatures and pressures, obtained by Method 2.
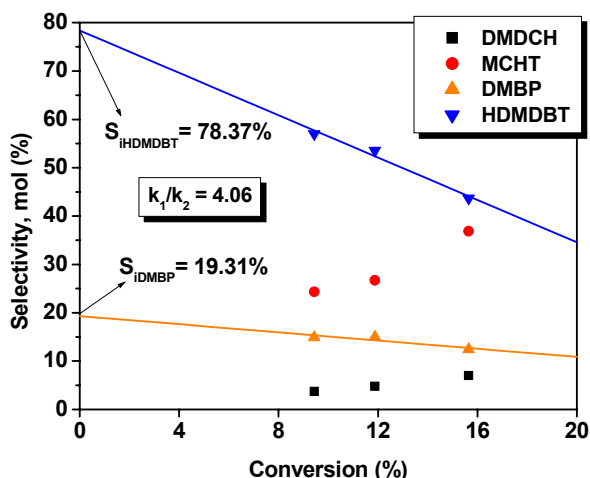
Figure 2. First order fitting of HDMDBT and DMBP products on NiMo sulfide for estimating initial selectivity (Reaction Temp.= 300°C, H_2 Pressure = 300 psi).

In Method 3 (computational simulation method), the formation rate constant of hydrogenation products and hydrogenolysis products can be described respectively as: $C_{HDMMDBT}+C_{MCHT}+C_{DMDCH} = C_o \cdot e^{-k1} \cdot t$, $C_{DMBP} = C_o \cdot e^{-k2} \cdot t$. The optimum k_1/k_2 value was determined by comparing the error between the actual product concentration and the product concentration calculated on the basis of different given k_1/k_2 values. **Table 1** compares rate constants, k_1 and k_2 from three different methods over CoMo, NiMo sulfides and Ni phosphide catalysts. The kinetic data from the three methods are

similar in general. Based on overall rate constants estimated, the total activity of the three catalysts for HDS of 4,6-DMDBT decreases in the order of NiMo > Ni_2P > CoMo. The hydrogenation activity of the catalysts decreases in the order of NiMo > Ni_2P > CoMo, while the hydrogenolysis activity decreases in the order of CoMo ≥ NiMo > Ni_2P. It is clear that the NiMo catalyst is better than CoMo for HDS of 4,6-DMDBT because of its higher hydrogenation activity. However, if ranked based on active sites, then the catalytic activity would appear to be Ni_2P > NiMo > CoMo. This trend also reveals that transition metal phosphides might be more promising catalysts for ultra-deep HDS.

Conclusions

In this study, overall rate constant and individual rate constants of each pathway for HDS of 4,6-DMDBT over the NiMo, CoMo and Ni_2P catalysts were determined by three different methods. The Method 2, which is based on the initial selectivity, appears to be the most reasonable for estimating k_1 and k_2 value among the three methods.

It is clear that NiMo catalyst is better than CoMo for deep HDS of 4,6-DMDBT because of its higher hydrogenation activity. However, if ranked based on active sites, then the catalytic activity would appear to be Ni phosphide > NiMo sulfide > CoMo sulfide.

As shown by the resuts with Ni phosphide, transition metal phosphide can have good activity for HDS of 4,6-DMDBT and may become promising catalyst for deep HDS with some further improvement.

References
(1) C. Song and X. Ma, *Appl. Catal. B*, **2002** in press; C. Song. *Am. Chem. Soc. Div. Fuel Chem. Prepr.*, **2002**, 47 (2), 438.
(2) X. Ma, K, Sakanishi, I. Mochida, *Ind. Eng. Chem, Res.*, **1994**, 33, 218.
(3) B.C. Gates, H. Topsoe, *Polyhedron* **1997**, 16, 3213.
(4) D.H. Broderick and B.C. Gates, *AIChE J.,* **1981**, 27, 663.
(5) K. Sakanishi, T. Nagamatsu, I. Mochida, and D. Whitehurst, *J. Mol. Cat. A* , **2000**, 155, 101.
(6) X. Ma, K, Sakanishi, T. Isoda, I. Mochida, *Energy Fuels.*, **1995**, 9, 33.

Table 1. HDS Rate Constants of 4,6-DMDBT over the NiMo, CoMo and Ni_2P by Method 2

Catalyst	Rate constant 10^5 (s^{-1} g cat^{-1})	300 psi			200 psi	600 psi
		275°C	300°C	325°C	300°C	300°C
NiMo sulfide	k_1+k_2	60.0	78.0 (72.3[2])	159.3	55.2	133.5
	k_1/k_2[1]	4.3	4.1	2.7	4.2	5.1
	k_1	48.6	62.6	115.8	44.6	111.6
	k_2	11.4	15.4	43.5	10.6	21.9
CoMo sulfide	k_1+k_2	14.5	43.2 (26.8[2])	66.5	-	43.8
	k_1/k_2[1]	5.8	1.2	1.6	-	2.7
	k_1	12.4	23.1	35.8	-	31.9
	k_2	2.1	20.1	30.8	-	12.0

[1] k_1/k_2 = [Initial selectivity of HDMDBT]/[Initial selectivity of DMBP]   [2] Overall rate constant of 4,6-DMDBT HDS with 1-methylnaphthalene

New starting CoMo heteropolyoxomolybdates for the preparation of HDS catalysts

C. Martin[1], C. Lamonier[1], E. Payen[1], V. Harlé[2]

[1]Laboratoire de Catalyse de Lille, UMR C.N.R.S N° 8010, Université des Sciences et Technologies de Lille, Bâtiment C3, 59655 Villeneuve d'Ascq, France.
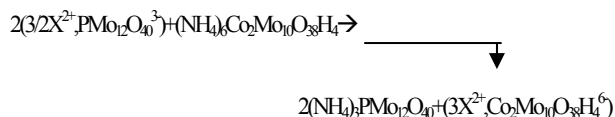[2]Institut Français du Pétrole, 1-4 av de Bois-Préau, 92852 Rueil-Malmaison, France.

Introduction

Hydrodesulfurization (HDS) of petroleum feedstocks is a catalytic process that is based on the use of CoMo/Al$_2$O$_3$ catalysts. It is now well recognized that the active phases are the CoMoS phases [1] that consist of well dispersed MoS$_2$ nanocrystallites decorated with the Co or Ni promotor atoms. These phases are obtained through the sulfidation of an oxidic precursor that is generally prepared by incipient wetness impregnation of an alumina support with ammonium heptamolybdate (AHM) and cobalt (nickel) nitrate. Unfortunately a part of this Co penetrates inside the alumina support, a location considered as detrimental for the activity. That is one of the reasons why the use of complexing agents have been proposed [2]. Direct complexation of the Co or Ni atoms by the molybdenum is also possible to form the 6molybdo-cobaltate anion (H$_6$CoMo$_6$O$_{24}$$^{3-}$), an Anderson type heteropolyanion (HPA). Nevertheless the Co/Mo atomic ratio (1/6) is not sufficient to provide very efficient catalysts. Moreover its solubility limits the total amount of Mo that can be deposited by the incipient wetness impregnation method. The ammonium salt of the decamolybdocobaltate (H$_4$Co$_2$Mo$_{10}$O$_{38}$)$^{6-}$, which is the dimeric form of this Anderson HPA, has a higher solubility and allows us to increase the Mo loading. It appears also very interesting to synthesize Co or Ni salts of these HPA, in order to increase the Co (or Ni)/Mo atomic ratio to the optimum ratio defined for the classical preparation. In the present work we focused on the preparation and characterization of the aforementionned HPA and their use as starting materials for the preparation of new HDS oxidic precursors [3].

Experimental

The synthesis of the ammonium salts, (NH$_4$)$_3$CoMo$_6$O$_{24}$H$_6$,7H$_2$O and (NH$_4$)$_6$Co$_2$Mo$_{10}$O$_{38}$H$_4$,7H$_2$O, were respectively adapted from the method employed by Nomiya et al.[4] and Tsigdinos [5] and the products were checked by XRD, EXAFS, FTIR and Raman spectroscopies. These ammonia salts were dissolved in water and the Ni and Co salts were obtained by cationic exchanges at 50 °C of the ammonium entities using a solution of cobalt or nickel phosphomolybdates. The impregnating solution is directly obtained and contains only Co (and/or Ni) ions and the HPA as shown in the following example where X is the Co or the Ni:

$$2(3/2X^{2+},PMo_{12}O_{40}{}^{3-})+(NH_4)_6Co_2Mo_{10}O_{38}H_4 \rightarrow$$

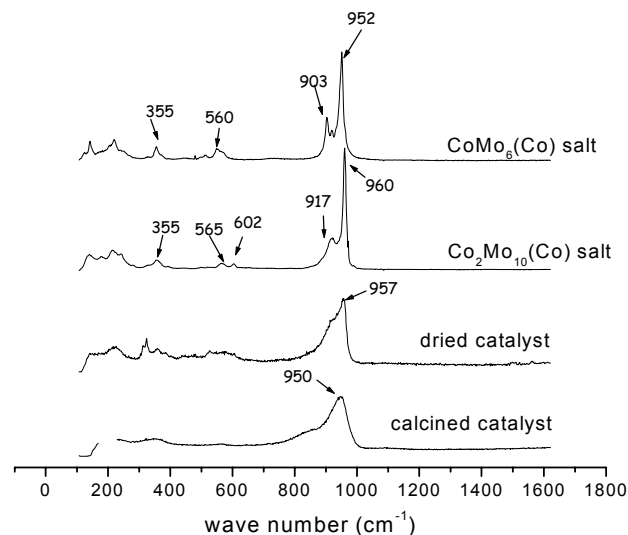$$2(NH_4)_3PMo_{12}O_{40}+(3X^{2+},Co_2Mo_{10}O_{38}H_4{}^{6-})$$

The catalysts were prepared by incipient wetness impregnation of a alumina with these solutions. Reference CoMo solids having the same metal loadings were also prepared for comparison purposes by using the conventional impregnating solutions made of AHM and cobalt (nickel) nitrate. The solids were dried overnight at 100°C and then calcined at 500°C under oxygen.

These oxidic precursors are designated with the formula of the starting material preceded by the Mo loading expressed as MoO$_3$ wt%. These oxidic precursors were then sulfided and their activities were evaluated in HDS of thiophene.
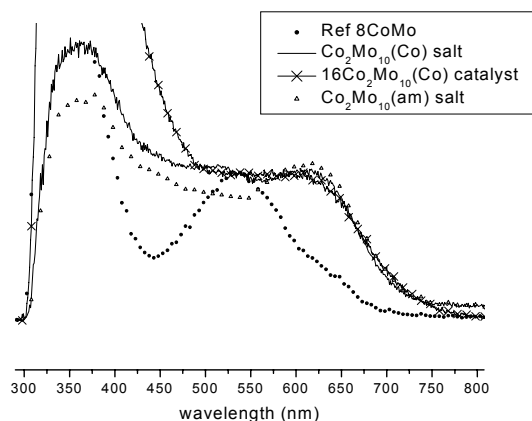
Results and discussion

Raman, UV-visible and EXAFS analysis have been performed on the ammonium and cobalt salts of the HPA. In particular, Raman spectroscopy allowed us to distinguish between CoMo$_6$ and Co$_2$Mo$_{10}$ HPA. Indeed, the Raman spectra differ by a shift of the two most intense lines, corresponding to the symmetric and antisymmetric stretching modes of the Mo-O$_{terminal}$ groups, respectively at 952 and 903 cm^{-1} for CoMo$_6$C$_{3/2}$, and 960 and 917 cm^{-1} for Co$_2$Mo$_{10}$Co$_3$ as shown in figure 1. Characterization of the catalysts at each step of the preparation by various physical techniques (UV-visible, Raman, XPS, EXAFS) allowed us to follow the evolution of the starting materials upon impregnation, drying, and calcination. As an example we focussed here on the Co$_2$Mo$_{10}$Co$_3$ based catalyst. The Raman spectrum of the dried Co$_2$Mo$_{10}$Co$_3$ based catalyst presents a line at 957 cm^{-1} (figure 1). However, its broadness prevents us from concluding unambiguously on the conservation of the HPA structure. Figure 1 also shows the Raman spectrum of 16Co$_2$Mo$_{10}$Co$_3$ catalyst after calcination at 773 K under oxygen. Whatever the atmosphere of calcination the HPA entities are transformed into the classical surface polymolybdate as shown in Raman spectroscopy by a broad line around 950 cm^{-1}.
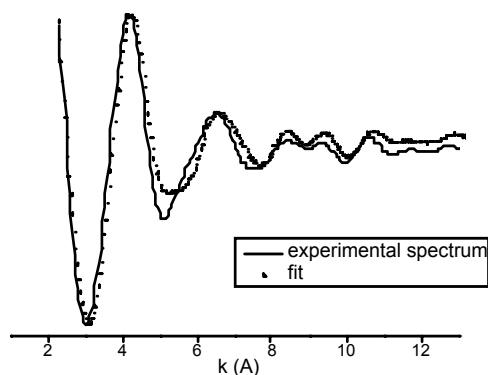

Figure 1. Raman spectra of Co$_2$Mo$_{10}$(Co) and CoMo$_6$(Co) salts and 16Co$_2$Mo$_{10}$(Co) catalyst after drying at 373 K and calcination at 773 K.

In figure 2 are shown the diffuse reflectance spectra (DRS) of the ammonium and cobalt salts of the dimeric HPA, Co$_2$Mo$_{10}$Co$_3$ based dried catalyst and the dried reference one. According to literature data, the absorption feature around 510 nm clearly indicates that the cobalt counter-ion presents an oxidation state of 2+ [6]. The cobalt species in the HPA structure are characterized by the feature around 615 nm, corresponding to the low spin Co^{3+} ion in octahedral coordination. Thus, the DRS spectrum of the dried Co$_2$Mo$_{10}$Co$_3$ catalyst indicates that at least a part of Co^{3+} species are preserved on the support at this stage of the preparation, whereas the conventional catalyst only contains Co^{2+} species.

Figure 2. DRS spectra of $Co_2Mo_{10}(Co)$ and $Co_2Mo_{10}(am)$ salts, $16Co_2Mo_{10}(Co)$ catalyst and a conventionnal catalyst after drying at 373 K.

Complementary results were obtained through XAS experiments. Figure 3 shows the comparison between the experimental EXAFS signal of the dried 16 $Co_2Mo_{10}Co_3$ catalyst and the simulation obtained using the FEFF calculated contributions. These contributions were calculated using the crystallographic data derived from the structure resolution of the monocrystal HPA salt. The simulation is in good agreement with the experience. Thus, analysis of the EXAFS data showed that the dimeric HPA structure is maintained upon impregnation and after drying.

Figure 3. Comparison between the experimental EXAFS of $16Co_2Mo_{10}(Co)$ catalyst and its fit.

These solids were characterized after sulfidation. XPS results confirmed that, after treatment at 673 K under H_2S/H_2, this polymolybdate phase is well sulfided. Moreover, HREM micrographs of the solids showed the presence of well-dispersed MoS_2 crystallites. The comparison between HPA based catalysts and reference solids showed that these crystallites were more stacked and had a shorter size on the first ones.

Table 1 shows the thiophene conversion of these HPA-based catalysts, compared with those of the reference solids.

Table1: metal loading and HDS conversion of typical $CoMo/Al_2O_3$ catalysts

Catalysts Nomenclature	Precursor	MoO₃ loading (wt %)	CoO loading (wt %)	Conversion (%)
8 $CoMo_6C_{3/2}$	$Co_2CoMo_6O_{24}H_6$	8.0	1.7	20.0
Ref8CoMo	AHM, Co nitrate	8.0	1.5	15.0
8 $Co_2Mo_{10}Co_3$	$Co_5Co_2Mo_{10}O_{38}H_4$	8.0	2.1	27
16 $Co_2Mo_{10}Co_3$	$Co_5Co_2Mo_{10}O_{38}H_4$	16.0	4.2	38.0
Ref16CoMo	AHM, Co nitrate	16.0	4.2	22.0

The results show unambiguously that the solids 8 $CoMo_6C_{3/2}$ and $16Co_2Mo_{10}(Co)$ are more active than the reference ones. Moreover, the improvement is more important with the use as starting material of the dimeric HPA, which has a higher Co/Mo ratio.

Thus, the use of such compounds as starting materials appears very promising for the preparation of HDS oxidic precursors. The physical characterisations allowed us to conclude that the catalytic improvement is due to a better interaction between the promoter and the molybdenum atoms in their oxidic state. The optimisation of the interaction is assigned to the complexation of the Co atoms in the HPA structure.

Conclusion

This study confirms that the use of Co (or Ni) salts of heteropolyoxomolybdates is a promising way to improve the efficiency of HDS catalysts. The use of these complexes allows to impregnate alumina with stable anions in which Co is included. This permits to improve the interaction between the Co or Ni counterions with the HPA. Both lead to an improvement of the promoting effect of the Co or Ni as shown by the catalytic performances.

Références

[1] N.-Y. Topsoe and H. Topsoe, *J. Catal.*, 75 (1982) 354-374.
[2] P. Blanchard et al., *Studies in Surf. Sc. and Catal.*, 106 (1995) 211-223.
[3] V. Harle et al., *Patent n°02/09 840*, France (2002).
[4] K. Nomiya, T. Takahashi, T. Shirai and M. Miwa, *Polyhedron*, 6 (1987) 213-218.
[5] G. Tsigdinos, *Thesis*, Boston university graduate school (1961).
[6] N. V. Kosova et al., *J. Solid State Chem.*, 165 (2002), 56-64.

CATALYTIC DEEP HDS OF MODEL FCC FEED OVER A CoMo/Al₂O₃ CATALYST MODIFIED BY POTASSIUM

D. MEY[1), S. BRUNET[1), G. PEROT[1), F. DIEHL[2]

1) UMR CNRS 6503, Catalyse en Chimie Organique, Université de Poitiers, 40 avenue du Recteur Pineau, 86022 Poitiers Cedex, France
Email : sylvette.brunet@univ-poitiers.fr
2) IFP, 1 et 4 avenue de Bois Préau, BP 311, 92850 Rueil Malmaison Cedex, France

Introduction

It is well known that the gas emission (NO$_x$ and SO$_x$) from motor vehicles contribute widely to air pollution. To address this environmental problem, new restrictive regulations were adopted by the European Community (Directive 98/70/EC). For instance, the sulfur level in Diesel fuel and gasoline will have to be lowered down to 50 ppm [1] by 2005.

Consequently, it is essential to modify conventionnal hydrotreating catalysts in order to achieve deep HDS with a minimum of alkene saturation. Several catalytic processes are commercialized by licensors to help the refiners to meet the future stringent regulations on FCC gasoline (Scan-fining® from ExxonMobil, Prime® G+ from Axens-IFP). Moreover, several authors have proposed new catalysts with reduced acidity of the alumina carrier [2-6] or the use of less acidic or basic supports such as TiO₂, SiO₂ or MgO. It was also reported recently that the selectivity for HDS could be increased with CoMo catalysts supported on Mg-Al oxide supports [7-10]. For the HDS of gasoline, hydrotalcite supported catalysts showed a decrease in the total activity (HDS and hydrogenation) but an increase in the HDS selectivity.

In this paper we report the activity of a CoMo/Al₂O₃ commercial catalyst modified by potassium, for the transformation of a model feed made of compounds (2-methylthiophene –2MT-, 2,3-dimethylbut-2-ene –23DMB2N and orthoxylene in n-heptane) which are considered as representative of the sulfur containing molecules and olefins found in FCC gasoline [11].
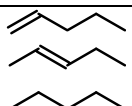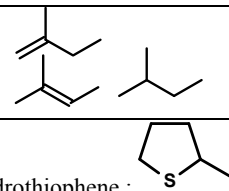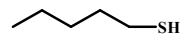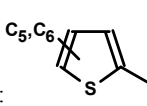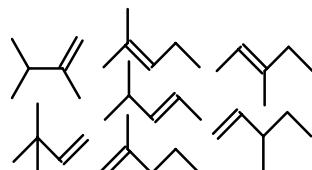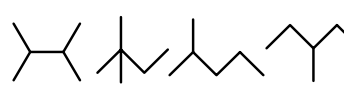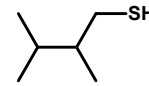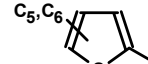
Experimental

Catalyst. The reference hydrotreating catalyst was a commercial CoMo/Al₂O₃ catalyst, containing 3 wt% CoO, and 14 wt% MoO₃. The catalyst modified by potassium (CoMoK/Al₂O₃) was prepared by incipient wetness impregnation of the reference catalyst with an aqueous solution of potassium carbonate (3 wt. %). The impregnated catalyst was dried at 100 °C and calcined at 500°C under air flow during 10 hours. The catalyst samples were presulfided at 400°C for 10 hours with a mixture of 10 mol% H₂S in H₂ under atmospheric pressure and then cooled down to 200°C.

Activity measurements. Catalytic activity measurements were carried out in a dynamic fixed-bed reactor at 200°C under a total pressure of 20 bar. The model feed made of 2-methylthiophene (10000ppm S), 2,3-dimethylbut-2-ene (20 wt. %) and orthoxylene (30 wt. %) in n-heptane was injected into the reactor with a syringe pump and the reaction products were analyzed on-line by means of a Varian gas chromatograph equipped with an automatic sampling valve, a PONA capillary column, a flame ionization detector and a cryogenic system. The identification of the products was made possible by GC-MS coupling (Table 1).

No significant transformation of orthoxylene was observed, whatever the experimental conditions.

Table 1. Products resulting from the transformation of model compounds

The major products of 2-methylthiophene (2MT) transformation were pentane and pentenes. The main by-products were alkylthiophenes obtained through the alkylation by alkenes (2,3-dimethylbut-2-ene and pentenes) of 2-methylthiophene. Thiols were also observed in small amounts.
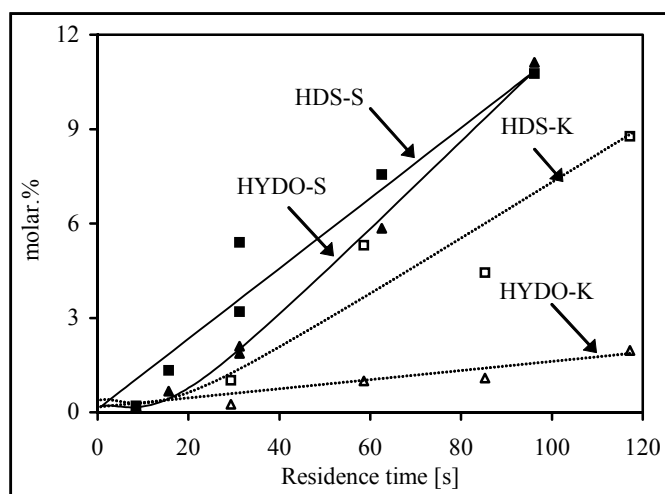
The transformation of the 2,3-dimethylbut-2-ene (23DMB2N) led to the formation of hydrogenation products (mainly 2,3-dimethylbutane) and isomerization products (mainly 2,3-dimethylbut-1-ene).

Desulfurized products resulting from the transformation of 2-methylthiophene were designated as HDS products. The selectivity of the reaction was given by the ratio "hydrodesulfurization conversion of 2MT/hydrogenation conversion of 23DMB2N" (HDS/HYDO).
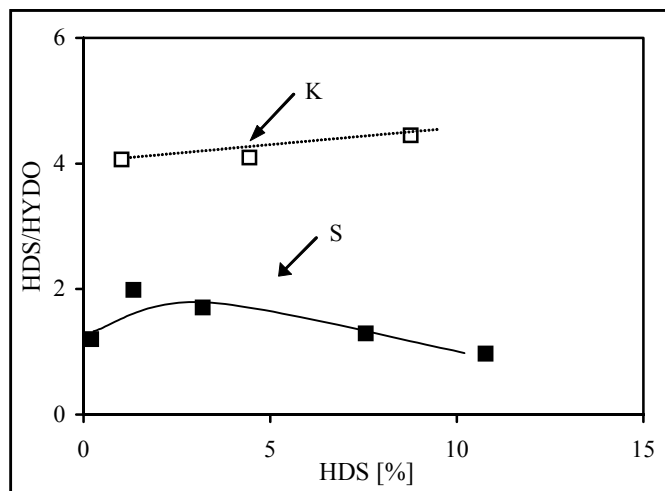
Results and Discussion

The transformation of the model FCC gasoline was carried out over the reference CoMo/Al$_2$O$_3$ and over the same catalyst modified by 3 wt.% of potassuim (CoMoK/Al$_2$O$_3$).

First of all we could notice a decrease in the total activity for the transformation of both molecules corresponding mainly to a lower conversion of 2MT into of alkylthiophenes and of 23DMB2N into 2,3-dimethylbutane. However, the decrease in hydrogenation conversion was more significant than the decrease in the HDS of 2MT (figure 1).

Figure 1. Transformation of the synthetic model gasoline over CoMo/Al$_2$O$_3$ (S) and CoMoK/Al$_2$O$_3$ (K). 20 bar; H$_2$/Feed = 200 l/l; 200°C; 500 mg. Hydrodesulfurization (HDS) of 2MT and hydrogenation (HYDO) of 23DMB2N.

The transformation of the pentenes resulting of the HDS of 2MT into pentane was also less significant with the potassium-modified catalyst, which was also a consequence of the decrease in its hydrogenation activity.

Figure 2. Transformation of the synthetic model gasoline.over CoMo/Al$_2$O$_3$ (S) and CoMoK/Al$_2$O$_3$ (K). 20 bar; H$_2$/Feed = 200 l/l; 200°C; 500 mg. Effect of the presence of potassium on the selectivity HDS/HYDO.

The selectivity HDS/HYDO measured by the ratio of the HDS reactivity of 2MT to the hydrogenation reactivity of 23DMB2N was improved by the presence of potassuim (figure 2). It was multiplied by 2 and was nearly constant in the range of HDS conversion which was obtained. These results can be explained both by a modification of the electronic properties of the catalyst because of the presence of potassium and by a decrease of the activity of the potassium-modified catalyst in the isomerization of 23DMB2N into 2,3-dimethylbut-1-ene. Actually it was found that on the unmodified catalyst, this reaction was very fast [11] and that the hydrogenation of 2,3-dimethylbut-1-ene was much faster than the hydrogenation of 23DMB2N. Consequently any inhibition of the isomerization activity is likely to decrease the hydrogenation activity of the catalyst.

The characterization of these materials (by the adsorption of probe molecules followed by infra-red and by electron microscopy) showed that the presence of potassium decreased the number and the strength of the acid sites without modification of the promoted active phase. The formation of the by-products (isomerization and alkylation) which involves the acid properties of the catalyst is therefore inhibited in the presence of potassium.

Conclusions

The modification by potassium of a commercial catalyst makes it possible to improve its selectivity in HDS of a synthetic FCC gasoline with respect to the hydrogenation of the olefins. In fact, the addition of potassium decreases the hydrogenation activity more than the HDS activity. This is considered to be the consequence of both a modification of the electronic properties of the sulfide phase and of the isomerization properties of the support.

References
(1) *Off. J. Eur. Commun.* L350 (28 december 1998) 58.
(2) Hatanaka, S.; Yamada, M.; Sadakane, O. *Ind. Eng. Chem. Res* **1997**, 36, 1519-1523.
(3) Hatanaka, S.; Yamada, M.; Sadakane, O. *Ind. Eng. Chem. Res* **1997**, 36, 5110-5117.
(4) Hatanaka, S.; Yamada, M.; Sadakane, O. *Ind. Eng. Chem. Res* **1998**, 37, 1519-1523.
(5) Hillerova, E.; Vir, Z.; Zdrazil, M. *Appl. Catal.* **1994**, 118, 111.
(6) Bertolacini, R.J.; Sue-A-Quan, T.A. U.S. Patent 4,140,626.
(7) Sherwood, D.E. Jr; Dai, E.P.; **1995** AIChE Spring National Meeting.
(8) Klimova, T. Casados, D.S., Ramirez, J. *Catalysis Today*, **1998**, 43, 135.
(9) Zhao, R.; Yin, C.; Liu, C. *Prepr. Pap.- Am.Chem.Soc., Div. Pet.Chem.* **2001**, 46 (1), 30-32.
(10) Zhao, R.; Yin, C.; Liu, C. *Prepr. Pap.- Am.Chem.Soc., Div. Pet.Chem.* **2002**, 47 (3), 309-311
(11) Mey, D., Brunet, S., Perot, G., Diehl, F., Kasztelan, S. *Prepr. Pap.-Am.Chem.Soc., Div. Pet.Chem.* **2002**, 47, 69-72

VERSATILES CLUES FROM *AB INITIO* MODELING TO IMPROVED METAL SULFIDES CATALYSTS

P. Raybaud and H. Toulhoat

Institut Français du Pétrole
1&4 avenue de Bois-Preau
92852 Rueil-Malmaison Cedex, FRANCE

Introduction

The production of ever cleaner fuels by hydrotreating processes can vastly be improved if a rational understanding of the nano-structure of γ-alumina supported Co(Ni)MoS catalysts is established. Modern density functional simulation techniques have been proven to be well suited for providing new clues to challenging issues such as active sites characterization, role of promoters, morphology effects, influence of sulfo-reductive conditions, poisoning effects of inhibitors, role of the support. The goal of the present paper is to give an overview of recent IFP's achievements obtained through *ab initio* molecular modeling: we show that it provided rational interpretations for many experimental results. Moreover, we outline how molecular modeling may open exploratory routes for the pre-screening of new potential active phases.

Methods

The results presented here are the outcome of simulations based on density functional theory (DFT) within the generalized gradient approximation, and employing a plane wave basis set together with periodic boundary conditions. To solve the Kohn-Sham equations, we used the Vienna *Ab initio* Simulation Package (VASP) (1). For all details on calculation hypothesis (electronic convergence criteria, energy cut-off...), the reader may refer to the papers cited herein.

Results and Discussion

Nano-structures of Co(Ni)MoS. As well-established by TEM and XPS, the active phase of HDT catalysts consists of nano-sized MoS_2 layers promoted by Co or Ni. Under HDT conditions, this highly active mixed phase exhibits two competing edges : the (10-10) metal edge and the (-1010) sulfur edge. DFT simulations revealed the electronic and structural properties of these edges in *vacuum* (2), and in typical sulfo-reductive conditions (3,4,5). Using a simple thermodynamic model to describe the equilibrium state of the Co(Ni)MoS nano-phase in contact with the gas phase, the edge energy, σ_{edge}, can be expressed as a function of the H_2S and H_2 partial pressures, and temperature:
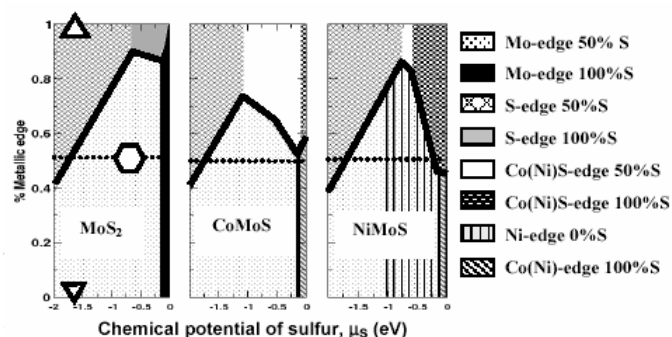
$$\sigma_{edge} = \sigma_0 - \alpha\mu_S \quad [1]$$

$$\text{where } S\sigma_0 = E_{cluster} - E_{bulk} \quad [2]$$

$$\text{and } \mu_S = g_{H_2S}(T) - g_{H_2}(T) + RT\ln\left(p_{H_2S}/p_{H_2}\right) \quad [3]$$
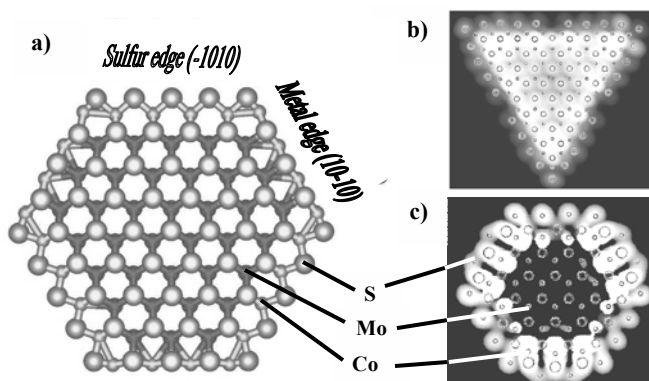
μ_S stands for the chemical potential of sulfur and α for a constant depending on the cluster's stoichiometry. σ_0 is calculated using the size dependent energies of model triangular clusters, $E_{cluster}$, per surface unit, S.

By injecting the σ_{edge} values in the Gibbs-Curie-Wulff law, the morphologies of nano-particles were deduced, as depicted in **Figure 1.** The calculated morphology varies from a triangle to an hexagon via a deformed hexagon, which is compatible with the geometrical model of Kasztelan (6). At the same time, the edge structures (**Figure 2a**) were consistent with EXAFS distances ($d_{Co(Ni)-Mo}$=2.75-2.90 Å and $d_{Co(Ni)-S}$ =2.10-2.20 Å), and revealed typical electronic properties (**Figures 2b and c**). Thus, total energy calculations demonstrated unambiguously the stable localization of Co and Ni in substitution for Mo at the edges.

Figure 1. Equilibrium morphologies (thick broken lines) and edge compositions of the nano-particles as a function of μ_S. The ordinate represents the percentage of (10-10) metal edge exposed for the corresponding equilibrium morphology.
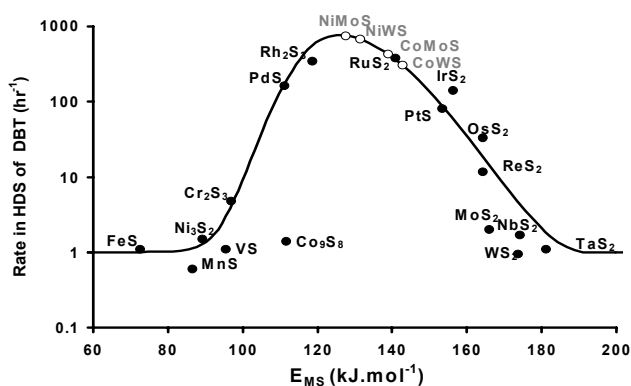
Moreover, as shown by the thick lines in **Figure 1**, and according to the preferential affinity of Co or Ni for one type of edge, the promoter acts as a morphology modifier (5). The sulfiding conditions have an impact on the stable shape of the nano-particles (4,5), whereas for very high reductive conditions ($\mu_S < -1.1$ eV), the mixed phase becomes unstable, leading to the catalyst's deactivation.

Figure 2. a) Ball and stick representations of the local structures of a Co(Ni)MoS cluster and simulated STM images of **b)** a MoS_x triangle (4) and **c)** a CoMoS cluster with Co on the sulfur edge (5).

Prediction of new active phases. The former modeling aims at two main objectives: improving industrially used active phases, and establishing robust basis for exploring new phases. Indeed, DFT calculations of relevant energy descriptors are well suited for providing a predictive approach. For HDT reactions, it was shown that the sulfur-metal bond energy, E_{MS}, as defined in (7,8,9), correlates well with the activity via a volcano master curve.

Actually, combining adapted Bronsted-Evans-Polanyi relationships with fitted Langmuir-Hinshelwood rate expressions, allows to recover HDS activity pattern exhibiting a volcano, when plotted against the E_{MS} descriptor (**Figure 3**). Since this approach also correctly predicted HDS activity of mixed sulfides, we are convinced that micro-kinetic modeling is improved when integrating *ab initio* descriptors. This approach, has been recently extended to various reactions by calculating carbon-metal bond energy descriptors in carbides (11).
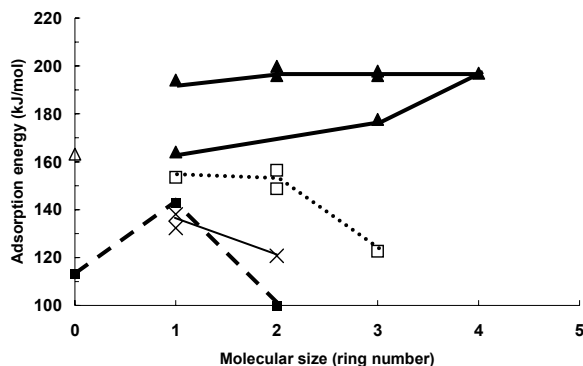
Figure 3. Pattern of experimental activity (particle size corrected) for the HDS of DBT ((10) •) plotted against the computed E_{MS}. ——— : theoretical relationship that best fits the data. Predictions for mixed M'Mo(W)S sulfides (o) are superimposed. The "bulk" averages of E_{MS} computed for binaries are used to locate mixed sulfides.

Inhibitors effects. HDT feedstocks contain nitrogen compounds, that may compete with sulfur or aromatic compounds for the active sites. Using a similar approach as for the thiophene adsorption on MoS_2 (12,13), we calculated adsorption energies of various nitrogen compounds on the (10-10) edge of a NiMoS model catalyst, supposed to contain 50% of Ni atoms in substitution for Mo at the edge. The adsorption energy is defined as:

$$E_{ads} = E(catalyst + molecule) - E(catalyst) - E(molecule) \quad [4]$$

For a given species, we first observe a clear dependency of the adsorption energy with the type of adsorption site. Almost all compounds exhibit higher adsorption energies on Mo-CUS sites than on Ni-CUS, due to the stronger Lewis acidity of the Mo-CUS. Azaarenes are also adsorbed on Mo-SH sites with an intermediate adsorption level. Furthermore, as shown in **Figure 4**, nitrogen compounds (including ammonia) are more strongly bonded than sulfur compounds and aromatics. Thus, by displacing sulfur and aromatic compounds on the CUS, and by poisoning SH groups required for HDS reaction, nitrogen compounds inhibit HDS and HYD reactions. Moreover, our simulations reveal that azaarenes are more strongly adsorbed on CUS than pyrrole and derivatives, pointing out crucial differences between the two nitrogen compound families regarding the NiMo active site.

Figure 4. Adsorption energies as a function of the molecular size: azaarenes (▲), pyrrole derivatives (□), sulfur compounds (■), aromatics (✗), ammonia (△).

Role of the support. DFT simulations on the active phase cannot overlook support effects. Significant progresses have been made in the description of relevant aluminum oxide surfaces (14,15,16). In particular, a recent work on γ-alumina models (16) investigated the variations of surface hydroxylation rate as a function of temperature and a subsequent vibrational analysis led to a precise assignment of bands in the high frequency IR spectrum to surface hydroxyl groups (**Table 1**). This revisited interpretation of Knözinger's assignments establishes a fresh and robust basis for further DFT investigations on active phase-support interactions.

Table 1. Calculated Vibrational Stretching Frequencies of γ-Alumina Surface Hydroxyl Groups

Site	Surface	ω_{calc} (cm^{-1})	ω_{exp} (cm^{-1})
HO-μ_1-Al$_{IV}$	(110)	3842	3785-3800
HO-μ_1-Al$_{VI}$	(100)	3777	3760-3780
HO-μ_1-Al$_V$	(110)	3736	3730-3735
HO-μ_2-Al$_V$	(110)	3707	3690-3710
HO-μ_3-Al$_{VI}$	(100)	3589	3590-3650

Conclusions

Ab initio modeling asserted itself as a versatile tool to investigate complex issues raised by HDT catalysis. In line with the long story of experimentation on sulfides, it may go beyond when traditional techniques are reaching their limits. Finally, in the spirit of high throughput screening, *ab initio* bond energy activity descriptors such as volcano curves are very promising as a first screening tool.

References
(1) Kresse, G.; and Hafner, J., *Phys. Rev B.*, **1993**, *47 (588)*, 14251. Kresse, G.; and Furthmüller, J., *Comput. Mat. Sci.*, **1996**, *15*, 6.
(2) Raybaud, P.; Hafner, J.; Kresse, G.; and Kasztelan, S; and Toulhoat, H., *Surf. Sci.*, **1998**, *407 (1-3)*, 237.
(3) Raybaud, P.; Hafner, J.; Kresse, G.; Kasztelan, S; and Toulhoat, H., *J. Catal.*, **2000**, *189*, 129; ibid. **2000**, *190*, 128.
(4) Schweiger, H.; Raybaud, P.; Kresse, G.; and Toulhoat, H., *J. Catal.*, **2002**, *207*, 76.
(5) Schweiger, H.; Raybaud, P.; and Toulhoat, H., *J. Catal.*, **2002**, *212*, 33.
(6) Kasztelan, S.; Grimblot, J.; Bonelle, J.P.; Payen, E.; Toulhoat, H.; and Jaquin, Y., *Appl. Catal.*, **1983**, *7*, 91.
(7) Raybaud, P.; Hafner, J.; Kresse, G.; and Toulhoat, H., *J. Phys.: Condens. Matt.*, **1997**, *9*, 11085; ibid. **1997**, *9*, 11107.
(8) Toulhoat, H.; Raybaud, P.; Kasztelan, S.; and Hafner, J., *Catal. Today*, **1999**, *50*, 629.
(9) Chianelli, R.R.; Berhault, G.; Raybaud, P.; Kasztelan, S.; Hafner, J.; and Toulhoat, H., *Appl. Catal. A : General*, **2002**, *227*, 83.
(10) Pecoraro, T.A.; and Chianelli, R.R., *J. Catal.*, **1981**, *67*, 430.
(11) Toulhoat, H.; and Raybaud, P., *J. Catal.* (in press).
(12) Raybaud, P.; Hafner, J.; Kresse, G.; Kasztelan, S.; and Toulhoat, H., *Phys. Rev. Lett.*, **1998**, *80*, 1481.
(13) Raybaud, P.; Hafner, J.; Kresse, G.; Kasztelan, S.; and Toulhoat, H., *Stud. Surf. Sci. Catal.*, **1999**, *127*, 309.
(14) Raybaud, P.; Digne, M.; Iftimie, R.; Wellens, W.; Euzen, P.; and Toulhoat, H., *J. Catal.*, **2001**, *201*, 236.
(15) Krokidis, X.; Raybaud, P.; Gobichon, A-E.; Rebours, B.; Euzen, P.; and Toulhoat, H., *J. Phys. Chem. B*, **2001**, *105*, 5121.
(16) Digne, M.; Sautet, P.; Raybaud, P.; Euzen, P.; and Toulhoat, H., *J. Catal.*, **2002**, *211*, 1.

AN APPROACH TO DESIGN THE CATALYST FOR DEEP HYDRODESULFURIZATION TO ACHIEVE 10PPM SULFUR LEVEL

Naoyuki Kunisada, Ki-Hyouk Choi, Yozo Korai, Isao Mochida[*], and K. Nakano[+]

[*]Institute of Advanced Material Study, Kyushu University,
Kasuga-Koen, Kasuga Fukuoka 816-8580, JAPAN
[+]Catalysts & Chemicals Ind. Co. Ltd, JAPAN

*e-mail: mochida@cm.kyushu-u.ac.jp

INTRODUCTION

NOx, SOx and particulate matters exhausted from diesel engine which combusts gas oil as fuel has provided a sincere social problem all over the world. The drastic reduction of sulfur in gas oil is expected to reduce those environmental pollutants and burden for diesel engines. Removing sulfur species deeply from gas oil has two difficulties; the first one is very low reactivity of some refractory sulfur species in gas oil such as 4,6-dimethyldibenzothiophene (4,6-DMDBT), 4,6,x-trimethyldibenzothiophene (4,6,x-TMDBT) having methyl group at 4 and 6 positions, the second is the strong inhibitors in feed oil and the products such as H_2S, NH_3, nitrogen species and aromatic compounds[1,2]. Hence deep HDS of these refractory sulfur species in gas oil can be achieved rather easily by the first and second stages of the catalysts when H_2S removal is performed between stages. Another approach is to develop catalysts of higher activity. Larger amount or better dispersion of sulfides have potential possibility for higher activity. Nevertheless severe condition appeared necessary.

In this present study, several NiMo and CoMo sulfide catalysts were examined in first and second layers with or without H_2S and NH_3 reduction between the layers. The functions of the catalysts in the two layers are defined as follows. 1st layer : complete removal of reactive sulfur species and 95% removal of refractory sulfur species. 2nd layers : remaining refractory sulfur species (around 400-500ppm) must be removed to less than 10ppm in the presence of H_2S and NH_3.

EXPERIMENTALS

a, Gas oil samples

Straight Run Gas Oil (SRGO) and Hydrodesulfurized Straight Run Gas Oil (HSRGO) were used as typical feedstocks for the first and second layer catalysts, respectively in this study. The SRGO contains 11780ppm while the HSRGO contains 340ppm of sulfur. Furthermore, the SRGO contains 155ppm while the HSRGO contains 20ppm of nitrogen.

b, Catalysts

The catalysts used in this study were CoMo and NiMo supported on alumina(-A), silica-alumina(-SA) and alumina-zeolite composite(-AZ), which were manufactured by a commercial catalyst vendor. **Table 1** shows their surface area, average pore size measured by BET and NH_3 desorbed amount measured by NH_3-TPD. **Figure 1** shows the pore size distribution of the several catalysts.
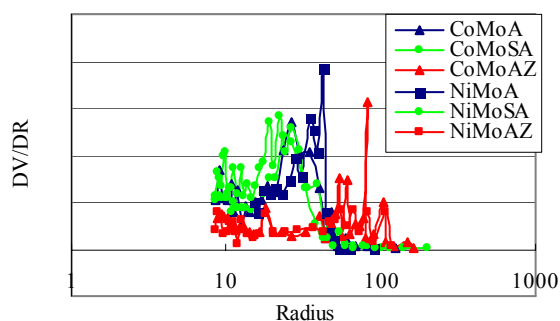
c, Hydrotreatment

SRGO and HSRGO were hydrotreated over the catalyst at 340°C under 50kg/cm² of H_2 for first layer, 50 kg/cm² H_2 with H_2S (1.67%) and 50 kg/cm² H_2 with H_2S (1.67%) added ethylenediamine (15ul) for second layer in a 100ml autoclave.

The ratio of catalyst to feed was 1g/10g. Catalyst was presulfided at 360°C under the stream of $H_2S(5\%)/H_2$ mixture for 2hr before the catalytic reaction.

Table 1. Catalysts properties

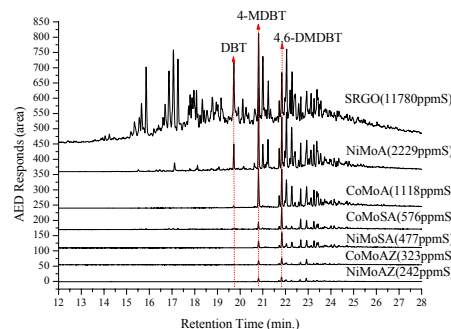|	Surface area (m²/g)	Pore volume (cm³/g)	NH₃-Desorbed area (Arb. Unit)
CoMoA	191	0.41	0.48
NiMoA	175	0.34	0.62
CoMoSA	221	0.41	0.56
NiMoSA	242	0.39	0.49
CoMoAZ	265	0.34	0.81
NiMoAZ	262	0.30	0.66

Figure 1. pore size distribution of several catalysts

RESULTS

a, HDS of SRGO

Figure 2 shows remaining sulfur chromatograms of SRGO after HDS over NiMo- and CoMo-A, NiMo- and CoMo-SA NiMo- and CoMo-AZ catalysts at 340°C under 50 kg/cm² H_2. NiMo-AZ shows the highest activity among six catalysts, and its remaining sulfur content is less than 300ppmS. Zeolite containing catalysts tend to show higher activity than SA- and A-series catalysts for HDS of SRGO that contained major reactive sulfur species. The HDS at this stage removed all reactive sulfur species and about 95% of refractory sulfur species to achieve sulfur level of 500ppm.

Remaining nitrogen compounds of SRGO after HDS over six catalysts were as follows. Three of NiMo catalysts showed higher activity than themselves couples of CoMo. NiMo-A, NiMo-SA, NiMo-AZ and CoMo-AZ achieved less than 20ppm of nitrogen content. From this result and the last time, NiMo-SA, NiMo-AZ and CoMo-AZ catalyst were the suitable catalyst for the first layer.

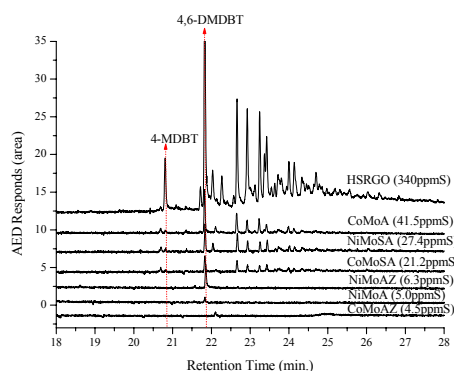**Figure 2.** HDS of SRGO over several NiMo and CoMo catalysts

b, HDS of HSRGO without H₂S and NH₃

Hydrodesulfurization of H-SRGO without H_2S or NH_3 over several NiMo or CoMo catalysts was assumed to simulate the two stage with separation of produced inhibitors (see **Figure 5**). Many of the catalysts achieved sulfur level less than 10ppm.

c, HDS of HSRGO in the presence of H₂S

Figure 3 shows GC-AED sulfur chromatograms on HDS of H-SRGO with H_2S. For HDS of refractory species, H_2S has been believed as the major inhibitor[3]. In directly connected two layer HDS, the second layer catalyst must stand with H_2S.
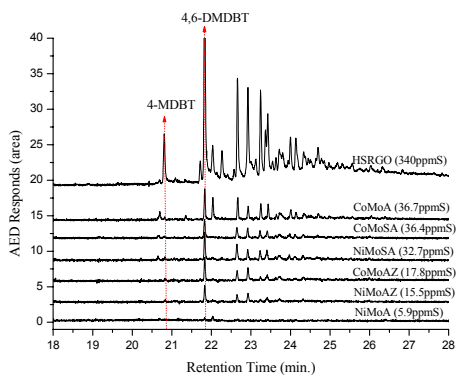
CoMo-AZ, NiMo-AZ, and NiMo-A of more acidic sites showed higher activity than any other catalysts. In contrast, CoMo-A or NiMo-SA which was less acidic showed lower activity. The acidity of the catalyst provides the tolerance to H_2S to show high HDS activity. HDS product oil over CoMo-AZ contains not 4,6-DMDBT but unidentical peak was observed near 4,6-DMDBT.

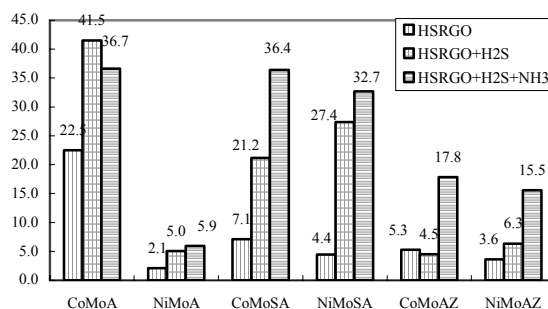**Figure 3**. GC-AED sulfur chromatograms on HDS of H-SRGO in the presence of H_2S

d, HDS of HSRGO in the presence of H₂S and NH₃

Figure 4 shows HDS of H-SRGO in the presence of both H_2S and NH_3. **Figure 5** summarizes the inhibition effects of H_2S and NH_3 on the HDS of H-SRGO. NiMo-A of large pore was found very active for HDS of refractory sulfur species in the presence of H_2S and NH_3 to achieve less than 6ppmS. In contrast, CoMo-A, NiMo-SA and CoMoSA were less active. NiMo-AZ and CoMo-AZ were much inhibited by addition NH_3.

Figure 4. GC-AED sulfur chromatograms on HDS of H-SRGO in the presence of H_2S and NH_3

AZ and NiMo-A with a number of acidic sites received little inhibition of H_2S. In contrast, SA and CoMo-A with less acidity received much inhibition of H_2S. NiMo-A and CoMo-A suffers little inhibition effects of NH_3 while NiMo-AZ and CoMo-AZ suffers marked inhibitions of both inhibitors.

Figure 5. Inhibition effect of H_2S and NH_3 on HDS of HSRGO

DISCUSSIONS

The present study revealed that the two layers of the best HDS catalysts with appropriate activity under respective conditions can be a logical approach to achieve deep HDS of gas oil.

The first layer catalyst must eliminate 100% of reactive sulfur species, first of all. Hence, the catalyst must have larger surface area, slightly smaller pore being allowed for the larger surface area. Acidity helps higher activity. 95% of refractory sulfur species must be also eliminated. Its content is still in relatively large range, being less influenced by inhibitors. Moderate acidity is helpful for the hydrogenative HDS. Another important function of the first layer catalyst appears the activity for HDN to send less nitrogen inhibitor for the second layer.

The second layer catalyst eliminates the refractory sulfur species of 100-500ppm to less than 10ppm in the presence of H_2S and NH_3. Least nitrogen species is required. The present HSRGO contains 20ppmN. The catalyst must have larger pores to accept the refractory sulfur species of tri aromatic rings with methyl groups more than di aromatic rings. Acidity is important to enhance HDS of the refractory sulfur species in the hydrogenation route by moderate H_2S inhibition. However too strong acid may suffer inhibition of NH_3 which is more basic than carbazoles. Zeolite containing CoMo and NiMo showed higher activity in SRGO, HSRGO and HSRGO+H_2S. On the other hand, as you know, zeolite having strong acidity is easily deactivated. Hence, AZ catalyst need larger the life time. Appropriate sets of two catalysts with successive layers are very active to achieve regulated Sulfur level of gas oil. It is always discussed whether CoMo or NiMo is better catalyst for the first and second layers. The support and supporting procedure appear very influential and hence we can not tell which is better at this stage. Nevertheless high dispersion in designed shape of the sulfides must be practiced in any supports.

REFERENCES
1. Isoda, T.; Ma, X.; Mochida, I. *Sekiyu Gakkaishi*, **1994**, *37*, 506.
2. Whitehurst, D. D.; Isoda, T.; Mochida. I, *Adv. Catal.*, **1998**, *42*, 345.
3. Isoda, T.; Ma, X.; Mochida, I. *Sekiyu Gakkaishi*, **1995**, *25*, 38.

QUANTUM CHEMICAL MOLECULAR DYNAMICS SIMULATION ON CATALYTIC REACTION DYNAMICS OF METHANOL SYNTHESIS PROCESS

Momoji Kubo[1], Minako Ando[1], Satoshi Sakahara[1], Changho Jung[1], Kotaro Seki[1], Tomonori Kusagaya[1], Akira Endou[1], Seiichi Takami[1], Akira Imamura[2], and Akira Miyamoto[1],[3]

[1] Department of Materials Chemistry,
Graduate School of Engineering, Tohoku University,
Aoba-yama 07, Sendai 980-8579, Japan.
[2] Department of Mathematics,
Faculty of Engineering, Hiroshima Kokusai Gakuin University,
6-20-1, Nakano, Aki-ku, Hiroshima 739-0312, Japan.
[3] New Industry Creation Hatchery Center, Tohoku University,
Aoba-yama 04, Sendai 980-8579, Japan.

Introduction

Recently, computational chemistry made great impacts on catalysts design. First-principles method is mainly employed in order to elucidate the catalytic reaction mechanism, catalyst activity, catalyst selectivity, and other important information. However, since the first-principles calculation can investigate only the static states at 0 K, this approach is not enough for theoretical catalyst design and research. For example, catalytic reaction dynamics depending on temperatures cannot be investigated by the first-principles calculation. Moreover, many reaction paths should be assumed in order to clarify the catalytic reaction mechanism and a lot of experimental information is essential to assume the reaction paths. Since a lot of experimental information is essential before the first-principles calculation, the present first-principles approach cannot contribute to the proposal of completely new catalysts. In addition to the understanding of the well-known catalytic properties at atomic and electronic levels, computational chemistry is expected to have an important role to predict new catalysts, which have high activity, selectivity, and tolerance to poisons.

In order to solve the above problem, the simulation on the catalytic reaction dynamics at reaction temperatures is strongly demanded. The products can be proposed directory from the reactants and catalysts by the reaction dynamics simulation, and any assumption of the reaction paths is not needed. Moreover, by-products and selectivity depending on the temperature can be clarified. First-principles molecular dynamics method is one of the most promising methodologies to realize the reaction dynamics simulation. However, it requests large computational costs, and then only a small model can be employed by the first-principles molecular dynamics method. Hence, the realistic catalysts model including active metals, supports and additives cannot be simulated by the first-principles molecular dynamics method.

Recently, we have succeeded in the development of an accelerated quantum chemical molecular dynamics program "Colors", which is more than 5,000 times faster than the regular first-principles molecular dynamics method [1,2]. This program was developed based on our original tight-binding theory, which enables us to simulate the catalytic reaction dynamics on large catalyst model at reaction temperatures. We have already applied the above tight-binding quantum chemical molecular dynamics simulator to various systems, such as Si semiconductor, GaN light emitting materials, ionics materials, and so on [1-5]. We have confirmed that the above tight-binding quantum chemical molecular dynamics simulator is very effective to simulate the chemical reactions and electron transfer dynamics at finite temperatures.

On the other hand, recently the synthesis of the high-quality transportation fuels is strongly demanded in terms of high-efficient utilization of energy and low environmental impact. In order to advance the synthesis of high-quality transportation fuels, the development of highly active and highly selective methanol synthesis catalysts with high-tolerance to the sulfur is essential and expected. Cu/ZnO is a most famous catalyst for the methanol synthesis reaction, and a large amount of experimental results for the Cu/ZnO catalyst were accumulated [6-8]. Moreover, recently Pd/SiO_2 gained much attention as a new methanol synthesis catalyst.

Hence, in the present study, we applied our original tight-binding quantum chemical molecular dynamics program to the methanol synthesis reaction on various catalysts and the applicability of our new simulator was demonstrated.

Methods

Our accelerated quantum chemical molecular dynamics program was based on our original tight-binding theory. The equations to be solved in this simulator are shown in Eqs. (1) and (2).

$$HC = SC\varepsilon \quad (1)$$

$$C^T SC = I \quad (2)$$

where, H is the Hamiltonian matrix, S is the overlap matrix, C is the eigenvector matrix, ε is the eigenvalue matrix, and C^T is the transformation matrix of C. The total energy in the system is calculated employing Eqs. (3) and (4).

$$E = \sum_{i=1}^{n} \frac{1}{2} m_i v_i^2 + \sum_{k}^{occ} \varepsilon_k + \sum_{i=1}^{n}\sum_{j=i+1}^{n} \frac{Z_i Z_j e^2}{R_{ij}} + \sum_{i=1}^{n}\sum_{j=i+1}^{n} E_{ij}^{repul}(R_{ij}) \quad (3)$$

$$E_{ij}^{repul}(R_{ij}) = b_{ij} \times \exp\left(-\frac{R_{ij} - a_{ij}}{b_{ij}}\right) \quad (4)$$

In this formula, m_i is the atomic weight, v_i is the atomic velocity, e is the elementary electric charge, and R_{ij} is the interatomic distance. The parameters a_{ij} and b_{ij} represent the size and stiffness of each atom, respectively. Z_i is the atomic charge obtained by the tight-binding electronic states calculation. Here, Mulliken analysis is employed to evaluate the above atomic charge. The first term refers to the kinetic energy of the atoms, the second term is the summation of the eigenvalues of all the occupied orbitals calculated by the tight-binding electronic states calculation, and the third term represents the Coulombic interaction. The last term corresponds to the short-range exchange repulsion energy.

Results and Discussion

In addition to the acceleration of the calculation speed, the realization of high accuracy, similarly to the first-principles molecular dynamics method, is essential. In order to accelerate the calculation speed, we employed some parameters in the Hamiltonian. If the parameters are determined as to fit the experimental results, our simulator will be lack of the predictability. Hence, in our program all the parameters were determined by the first-principles calculation results. In order to realize it, we developed a new parameter-fitting program. Here, we demonstrate the applicability and effectiveness of our new parameterization procedure.

Fig. 1 shows the CO adsorption structure on the Pd_3 cluster. Some distances and atomic charges calculated by our new simulator were compared with those obtained by the static first-principles calculation (Table 1). Our simulator results are in good agreement with the first-principles results. It indicates that our simulator has high accuracy, similarly to the first-principles calculation. After the validity of our parameterization procedure was

confirmed, we performed a quantum chemical molecular dynamics simulation of the CO adsorption on Pd surface model (Fig.2). Here, Pd(111) surface was employed as the catalyst, and the calculation was performed under three-dimensional periodic boundary condition. Vibrational frequency of CO molecule adsorbed on the Pd surface was calculated (Table 2). Here, we compared the simulation results with the experimental results. As shown in Table 2, our simulation results are in significantly good agreement with the experimental results. Moreover, we applied our quantum chemical molecular dynamics simulation to the H_2 adsorption and the methanol synthesis reaction dynamics on the large Pd catalyst model.

We also applied our tight-binding quantum chemical molecular dynamics simulator to the Cu/ZnO methanol synthesis catalyst. We constructed a significantly large Cu/ZnO catalyst model for the reaction dynamics simulation as shown in Fig. 3. Fig. 3 includes more than 1,000 atoms and some Al additives are incorporated in the ZnO support in order to clarify the effect of the additives. Moreover, formate intermediate is also placed on the Cu particle. Calculation results show that the average charge of the Cu atoms on the ZnO support is +0.1, which indicates that the ZnO support strongly influences the electronic states of the Cu ultrafine particle. The regular first-principles molecular dynamics simulator cannot obtain the above information, since it requests large computational costs and cannot be applied to the huge catalyst model as shown in Fig. 3. After we constructed an appropriate model for Cu/ZnO catalyst, we simulated a catalytic reaction dynamics of the methanol synthesis process on the above huge Cu/ZnO model.

Conclusions

In the present study, we confirmed that our tight-binding quantum chemical molecular dynamics simulator is very effective to simulate the catalytic reaction dynamics on large catalyst model at reaction temperatures, which cannot be performed by the regular first-principles molecular dynamics.
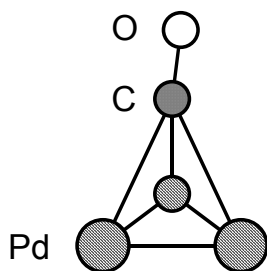
References
(1) Yamada, A.; Endou, A.; Takaba, H.; Teraishi, K.; Ammal, S. S. C.; Kubo, M.; Nakamura, K. G.; Kitajima, M.; Miyamoto, A. *Jpn. J. Appl. Phys.* **1999**, *38*, 2434.
(2) Takaba, H.; Endou, A.; Yamada, A.; Kubo, M.; Teraishi, K.; Nakamura, K. G.; Ishioka, K.; Kitajima, M.; Miyamoto, A. *Jpn. J. Appl. Phys.* **2000**, *39*, 2744.
(3) Inaba, Y.; Onozu, T.; Takami, S.; Kubo, M.; Miyamoto, A.; Imamura, A. *Jpn. J. Appl. Phys.* **2001**, *40*, 2991.
(4) Yokosuka, T.; Kurokawa, H.; Takami, S.; Kubo, M.; Miyamoto, A.; Imamura, A. *Jpn. J. Appl. Phys.* **2002**, *41*, 2410.
(5) Suzuki, K.; Kuroiwa, Y.; Takami, S.; Kubo, M.; Miyamoto, A.; Imamura, A. *Solid State Ionics*, in press.
(6) Sun, Q.; Liu., C.-W.; Pan, W.; Zhu, Q.-M.; Deng, J.-F. *Appl. Catal. A* **1998**, *171*, 301.
(7) Peppley, B. A.; Amphlett, J. C.; Kearns, L. M.; Mann, R. F. *Appl. Catal. A* **1998**, *179***, 31.
(8) Fujita, S.; Kanamori, Y.; Satriyo, A. M.; Takezawa, N. *Catal. Today*, **1998**, *45***, 241.
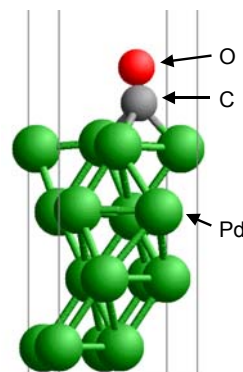
Figure 2 Adsorption structure of CO molecule on Pd(111) surface

Table 2 Vibrational frequency of CO molecule on Pd(111) surface

CO Molecule in Vapor Phase		
	Frequency [cm⁻¹]	Bond Distance [Å]
Experiments	2143	1.13
Our Program	2163	1.13

CO Molecule on Pd（111）Surface		
	Frequency [cm⁻¹]	Bond Distance [Å]
Experiments	1825	1.15
Our Program	1836	1.15

Fig. 1 CO adsorption structure on Pd₃ cluster

Table 1 Bond distances and atomic charges of Pd₃ cluster with CO molecule

Bond Distances [Å]

	C-O	Pd-Pd	Pd-C
First-principles	1.19	2.64	2.01
Our program	1.20	2.67	2.00

Atomic Charges

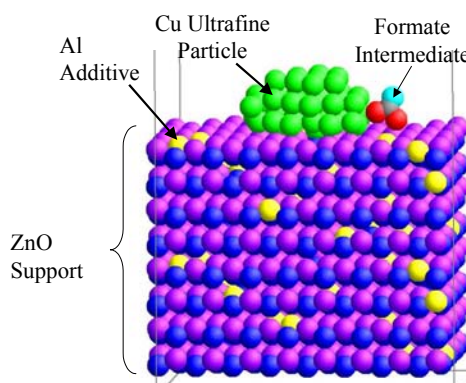|	Pd	C	O
First-principles	0.11	-0.01	-0.32
Our program	0.11	-0.02	-0.31

Figure 3 Structure of huge Cu/ZnO catalyst model including Al additives and formate intermediate

Atomic-scale study of hydrodesulfurization model catalysts

Jeppe V. Lauritsen [1], Bjerne S. Clausen [2], Henrik Topsøe [2], Jens K. Nørskov [3], Flemming Besenbacher [1,].*

[1]Center for Atomic-Scale Materials Physics (CAMP) and Interdisciplinary Nanoscience Center (iNANO)
Department of Physics and Astronomy, University of Aarhus,
Ny Munkegade
DK-8000 Aarhus C
Denmark.

[2]Haldor Topsøe A/S,
Nymøllevej 55
DK-2800 Lyngby
Denmark.

[3]Center for Atomic-Scale Materials Physics (CAMP),
Department of Physics
Technical University of Denmark
DK-2800 Lyngby
Denmark.

Introduction

The production of clean transport fuels by hydrotreating and especially hydrodesulfurization (HDS) has recently attracted increased attention due to the introduction of new environmental legislation regarding fuel specifications and technological requirements of high-purity fuels . In order to meet the new stringent demands there is a need to understand and improve HDS catalysts. It is generally accepted, that the HDS activity is related to the presence of so-called Co-Mo-S structures which consist of small MoS_2 nanoclusters with promoter atoms located near the edges[1]. Controversy prevails, however, since the traditional spectroscopy-based techniques for catalyst characterization provide no conclusive information regarding the cluster morphology, catalytically relevant edge structures, active sites or the promotional effect of Co.

To aid the understanding of the industrial catalyst, new insight has been gained from studies of catalyst model systems by applying surface science techniques. In a series of studies, we have successfully used high-resolution Scanning Tunneling Microscopy (STM) to study the real space atomic structure of single-layer MoS_2 nanoclusters synthesized on an inert Au(111) substrate as a model system for the HDS catalysts. The insight gained from the STM studies gives a hitherto unprecedented view of the atomic details of the MoS_2 nanoclusters[1].

Experimental

The experiments are performed in an ultra-high vacuum chamber equipped with the unique home-built high-resolution Aarhus STM, which has demonstrated the capability of providing atom-resolved images of a large variety of systems on a routine basis[2]. The Au(111) surface is chosen as a model substrate for two reasons. Gold is chemically rather inert, and furthermore gold belongs to the class of metal the surface of which reconstructs in its clean state. Specifically the Au(111) has a characteristic "herringbone" reconstruction pattern, which is ideal for providing nucleation sites for the deposited metal atoms and thereby dispersing submonolayer amounts of material into Mo or Co nanoclusters[3,6]. En ensemble of ~30 Å wide crystalline MoS_2 nanoclusters were formed by initially depositing Mo (10% coverage) in an background H_2S (10^{-6} mbar) followed by high-temperature annealing (673K) for 15 min while maintaining the sulfiding atmosphere.
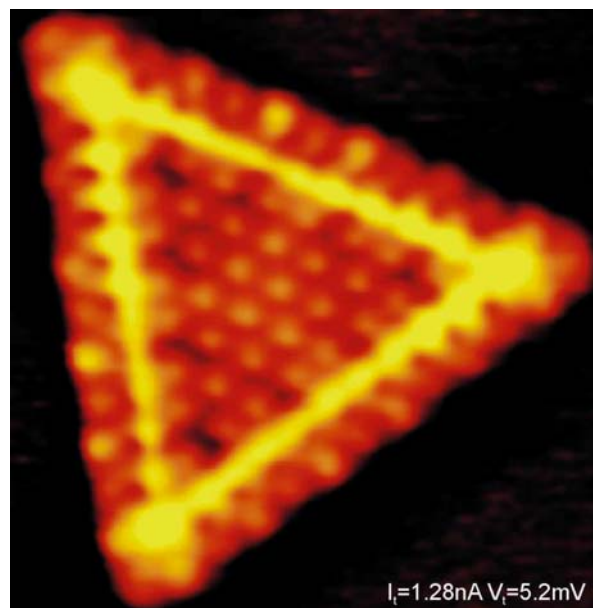
Figure 1: Atom-resolved (41x42Å^2) STM image of an unpromoted single-layer MoS_2 nanocluster synthesized on a Au(111) template[3].

Results and Discussion

High resolution STM images reveal new insight into the atomic details of the MoS_2 nanostructures (**Figure 1**). Contrary to our expectations based on the structure of bulk MoS_2, the majority of the nanoclusters are found to exhibit a pronounced triangular morphology. The shape of a single-layer MoS_2 cluster is in principle governed by the relative stability of two low-index types of edge terminations, an S-edge and a Mo-edge. Equal stability between these would produce a perfectly hexagonal cluster. The observed triangular morphology implies, however, that one type of edge termination is considerably more stable than the other.

It is important to point out that STM to a first approximation measures contours of constant local density of states (LDOS) in the surface projected onto the apex of the STM tip, and that STM images therefore reflect a rather complicated convolution of both geometric and electronic structure. This is especially true for adsorbates on surfaces, oxide or sulfide materials and in the STM images of the MoS_2 nanoclusters we indeed observe two examples of this. First of all, we observed the protrusions at the edge of the MoS_2 triangle to be out of registry with the basal plane S atoms. Second, a pronounced bright brim extending all the way around the perimeter of the triangular MoS_2 nanoclusters is identified in the STM image. Rather than geometrical effects pertaining to the triangular MoS_2 cluster (Figure 1), these features reflect subtle electronic changes at the edges, and are therefore attributed to distinct electronic features existing only near the edges, i.e. one-dimensional electronic edge states. The brim is seen in the STM image to be highly localized in the direction perpendicular to the edge and furthermore exhibits a very high electronic conductivity. It can thus be associated with a one-dimensional nanosized, metallic wire[2].

In density functional theory (DFT) calculations of the band structure of the MoS_2 edges we indeed find the existence of several

localized electronic edge states pertaining to the Mo edge. By comparing the detailed atomic-scale structure observed in the experimental images with STM simulations resulting from the DFT calculations (**Figure 2**) we have confirmed that electronic edge states are responsible for the features observed at the edges of the MoS$_2$ triangles and we have identified the edge termination as the Mo edge fully saturated with S dimers.[3,4]
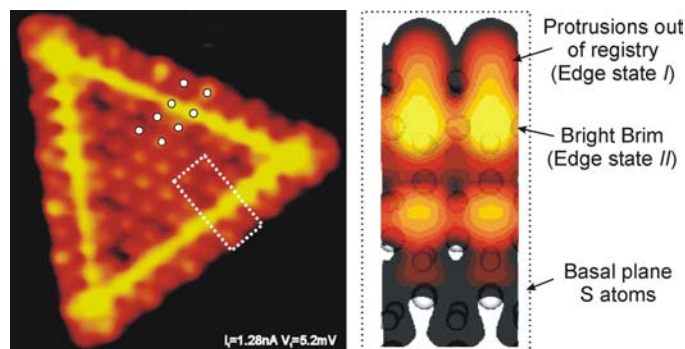

Figure 2: Left: Experimental STM image. White dots denote the position of protrusions on the MoS$_2$ nanocluster. Right: STM simulation (Tersoff-Hamann) of part of the Mo edge fully saturated with S dimers.

By means of the STM we have recently investigated the interaction of the MoS$_2$ clusters with thiophene (C$_4$H$_4$S) - a typical sulfur containing molecule widely used to test HDS reactivity. Upon adsorption of thiophene molecules we find in STM images that relatively inert molecules like thiophene preferentially interact with unusual sites located near the edges. Interestingly, we find that this interaction is modified by the presence of hydrogen species, and that the adsorption serves as an initial activation of thiophene molecules during catalytic hydrotreating reactions. This is followed by extrusion of sulfur at, for instance, edge vacancies, provided by reaction with gaseous hydrogen. We have exploited the capability of the STM to image in real-space these active sites on the atomic-scale with STM and investigated the energetics of the reaction with DFT calculations. The results thus provide new detailed insight into the reaction mechanism resulting in the extrusion of sulfur in the HDS process[5].

The industrial MoS$_2$-based HDS catalysts are typically promoted with Co which enhances the catalytic activity by more than an order of magnitude. By applying an approach similar to the unpromoted MoS$_2$ experiments described above we have also obtained the first atomic-scale images of the structure of Co-Mo-S nanocrystals[6]. The idea behind our synthesis of Co-Mo-S is first to form MoS$_2$ embryos on the Au(111) surface followed by capping of these nanoclusters to facilitate the addition of Co to the edges of MoS$_2$ nanocrystals.

High resolution STM images of the resulting CoMoS structures reveal that the presence of the Co atoms has a dramatic influence on the morphology of the single-layer MoS$_2$ clusters (**Figure 3**). This surprising morphological transition, from triangular to hexagonally truncated, appears to be driven by a preference for Co to be located at only one type of MoS$_2$ edges - the S edge. The STM results also provide direct information on changes in the local electronic environment neighboring the Co edge atoms. This novel insight into the atomic and electronic structure may be important for understanding the promoting role of Co.
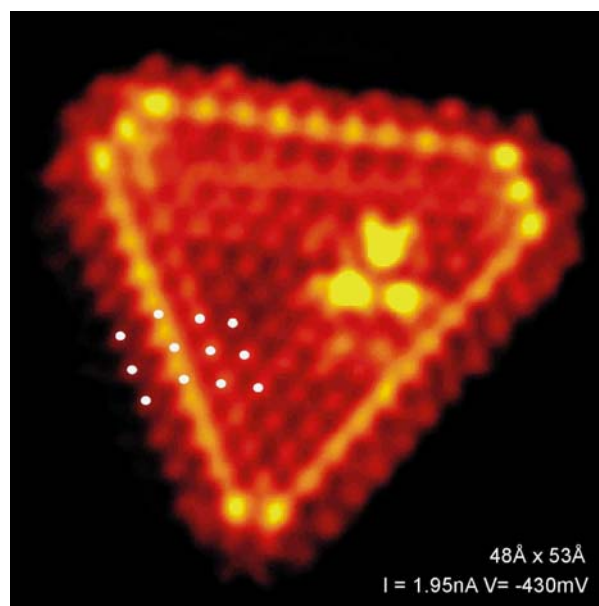
Figure 3: Atom-resolved STM image (48x53Å^2) of a promoted Co-Mo-S nanocluster[6] supported on Au(111).

References
(1) Topsøe, H., Clausen, B. S. & Massoth, F. E. *Hydrotreating Catalysis, Science and Technology* (ed. M. Boudart, J. R. Anderson.) (Springer Verlag, Berlin, 1996).
(2) Besenbacher, F., Reports on Progress in Physics **59**, 1737-1802 (1996).
(3) S. Helveg, J. V. Lauritsen, E. Lægsgaard, I. Stensgaard, J. K. Nørskov, B. S. Clausen, H. Topsøe, F. Besenbacher, Phys. Rev. Lett. **84**, 951 (2000).
(4) M. Bollinger, J. V. Lauritsen, K. W. Jakobsen, J. K. Nørskov, F. Besenbacher, Phys. Rev. Lett. **87**, 196803 (2001).
(5) J. V. Lauritsen, R. T. Vang, M. Nyberg, M. Bollinger, K.W. Jacobsen, B. S. Clausen, H. Topsøe, J. K. Nørskov, E. Lægsgaard, F. Besenbacher, Submitted (2002).
(6) J. V. Lauritsen, S. Helveg, E. Lægsgaard, I. Stensgaard, B. S. Clausen, H. Topsøe, F. Besenbacher, Journal of Catalysis **197**, 1-5 (2001).

Development of highly active hydrodesulfurization catalysts - Effect of the Addition of CyDTA and Boria -

*Hideyuki Itou, Masahiro Shingu, Yosuke Kikuchi, Naoto Koizumi,
and Muneyoshi Yamada*

Department of Applied Chemistry, Graduate School of Engineering,
Tohoku University
07 Aoba, Aramaki, Aoba-ku, Sendai 980-8579, JAPAN

Introduction

To meet the severe regulation for reductions of SOx, NOx, and SPM contained in the exhaust gases from diesel vehicles, the improvement of catalyst performances especially for hydro-desulfurization (HDS) is one of the most important subjects. van Veen *et al.*[1] reported that CoMo catalysts modified with nitric tri-acetic acid (NTA) show higher activities for HDS of thiophene at atmospheric pressure. We have investigated effects of other chelating reagents such as ethylenediamine-N, N, N', N'-tetra-acetic acid (EDTA) and *trans*-1, 2-Cyclohexanediamine-N, N, N', N'-tetraacetic acid (CyDTA) and found that CyDTA improves the activity of CoMo/Al$_2$O$_3$ catalyst for HDS of dibenzothiophene (DBT) at high pressure more more effectively than NTA.[2] Besides, CyDTA is found to be effective for hydrogenation of *o*-xylene[3] and tetralin over NiW/Al$_2$O$_3$ catalyst. Since CyDTA forms stable complexes with Co or Ni in the impregnating solution, it is suggested that CyDTA retards the sulfidation of Ni species, leading to the effective formation of active phases, namely Co(Ni)-Mo-S or Ni-W-S phases.

On the other hand, the addition of boric acid to NiMo/Al$_2$O$_3$ catalyst has been reported to improve the activities for HDS of DBT[4]. From EXAFS analysis of NiMo/B$_2$O$_3$/Al$_2$O$_3$ catalyst, the addition of boric acid improves the sulfidation degree of Mo sulfide species. Since Decanio *et al.*[5] showed that the addition of boric acid to γ-Al$_2$O$_3$ affects the distribution of hydroxyl groups on γ-Al$_2$O$_3$ surface by means of IR spectroscopy, it is suggested that boria weakens the interaction between Mo sulfide species and γ-Al$_2$O$_3$.

Since the additions of CyDTA and boric acid affects the structure of sulfide phases in different ways, it is expected that the simultaneous addition of both CyDTA and boric acid improves the HDS activities of hydrotreating catalysts than CyDTA and boric acid alone. Thus, in the present study, we have prepared the catalysts modified with both CyDTA and boric acid and investigated their activities for HDS of 4, 6-dimethyldibenzothiophene (4,6-DMDBT) and their surface fine structures.

Experimental

Catalyst Preparation. Catalysts were prepared by an incipient wetness method. γ-Al$_2$O$_3$ was impregnated with an aqueous H$_3$BO$_3$ solutions followed by drying and calcination. B$_2$O$_3$/Al$_2$O$_3$ thus prepared was then impregnated with an aqueous solution containing ammonium heptamolybdate (or ammonium metatungstate), cobalt nitrate (or nickel nitrate) and CyDTA followed by the drying at 393 K. MoO$_3$ (WO$_3$) loading of the prepared catalyst was 10 (or 14) mass% with Co(Ni)/Mo(W) molar ratio of 0.32.

Activity Measurement. The catalyst was packed in a fixed bed flow reactor and sulfided *in-situ* in a stream of 5% H$_2$S/H$_2$ at 673 K and 1.1 MPa. After the sulfidation, the catalyst was cooled down to 573 K and the feed composed of 0.3 mass% 4, 6-DMDBT and decalin. was flown into the catalyst bed under the flow of H$_2$ at 5.1 MPa.

Characterization. SO$_2$ Uptake Measurement. The catalyst was pretreated in a stream of He 673 K and 0.1 MPa. Then, SO$_2$ was introduced into the catalyst bed by pulse method. SO$_2$ uptake was determined with GC-TCD. NO Uptake Measurement. The catalyst was sulfided in the same manner as employed for the activity measurements, and then NO was introduced into the catalyst bed by pulse method. NO uptake was detected with GC-TCD. EXAFS Measurement. The catalyst was pressed into a self-supporting wafer and set in the high-pressure EXAFS cell. The catalyst wafer was sulfided in the same manner as employed for the activity measurements. X-ray absorption spectra near W L$_{III}$ edge were measured in a transmittance mode at room temperature using EXAFS 2000 spectrometer (RIGAKU).

Results and Discussion

The effect of CyDTA and boria on HDS activities for 4,6-DMDBT. In HDS of 4,6-DMDBT, dimethylbicyclohexane (DMBiCH) , bimethylcyclohexylbenzene (DMCHB) and dimethyl-biphenyl (DMBiPh) and their isomers were observed to be produced. We have investigated the effects of CyDTA and boria on HDS activity for 4,6-DMDBT. Here, HDS activity is defined by the sum of product yields per the loading amount of Co(Ni) and Mo(W).
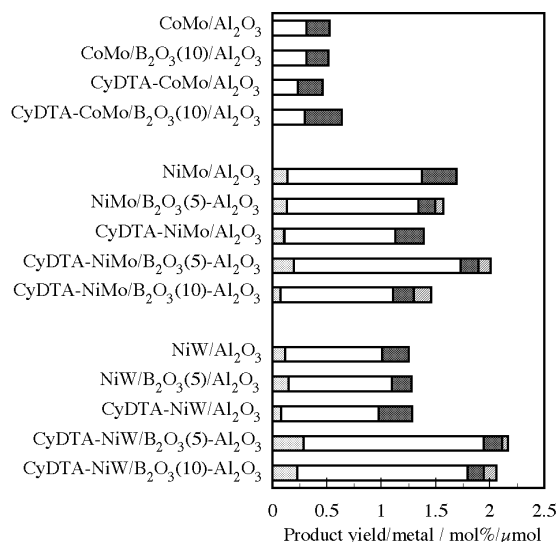

Figure 1. Effect of CyDTA and boria on HDS activities of Co(Ni)Mo/Al$_2$O$_3$ and NiW/Al$_2$O$_3$ for 4,6-DMDBT. (▨); DMBiCH, (▢); DMCHB, (▩); DMBiPh, (▨); iso-DMBiCH or iso-DMCHB. Numbers in parentheses indicate boria loading.

Figure 1 shows HDS activities of Co(Ni)Mo/Al$_2$O$_3$ and NiW/Al$_2$O$_3$. The main product is DMCHB over every catalysts. Comparing HDS activities of the catalysts without additives, the order of HDS activity is as follows: CoMo/Al$_2$O$_3$ < NiW/Al$_2$O$_3$ < NiMo/Al$_2$O$_3$. By the addition of CyDTA, no positive effects appears on HDS activities for 4,6-DMDBT while HDS activity of CyDTA-NiW/Al$_2$O$_3$ for DBT was about 1.6 times higher than NiW/Al$_2$O$_3$[2]. From this result, it is suggested that the active phase which is selectively formed by CyDTA isn't efficient for HDS of 4,6-DMDBT. As with CyDTA, HDS activities were not improved by the addition of boria. Contrary to these results, catalysts modified with both CyDTA and boria shows much higher HDS activity than non-modified catalysts. In other word, we found the synergetic effect between CyDTA and boria on HDS activity of 4,6-DMDBT. The effect of both CyDTA and boria on HDS activity of NiW catalyst is more remarkable than those of Co(Ni)Mo/Al$_2$O$_3$. Perhaps, it is related to the fact that sulfidation of W species is more difficult than that of Mo species.
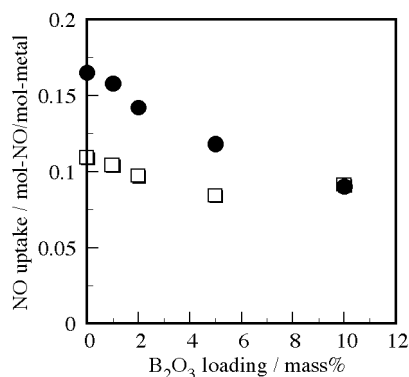
The effect of CyDTA and boria on the surface structure of NiW/Al$_2$O$_3$. Sulfur dioxide (SO$_2$) is known to adsorb on the basic

OH groups on Al_2O_3 surface. Therefore it is expected to investigate the effect of boria on Al_2O_3 surface by using SO_2 as probe molecules. **Figure 2** shows SO_2 uptake on B_2O_3/Al_2O_3. As B_2O_3 loading increases, SO_2 uptake sharply decreases and it reaches almost zero at above $60 * 10^{13}$ B atoms/cm^2-Al_2O_3 (10 mass% B_2O_3). This indicates that boria interacts with basic OH groups of Al_2O_3. Considering the fact that WO_3 species interact with basic OH groups of Al_2O_3, it is expected that boria induces the change of the structure of WS_2 after sulfidation.
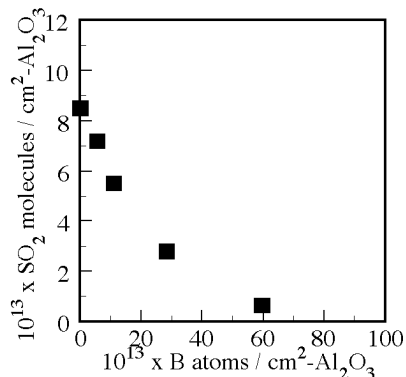
Figure 2. SO_2 uptake on B_2O_3/Al_2O_3.

It is well-known that nitric oxide (NO) adsorbs on the coordinatively unsaturated sites (CUS) on active metals, where the reaction is considered to take place. We have measured NO uptake on (CyDTA-)NiW/B_2O_3/Al_2O_3 (**Figure 3**). Regardless of whether CyDTA is present or not, NO uptake decreases with the increase in boria loading. This is due to the relaxation of the interaction between W and Al_2O_3. The change of NO uptake on CyDTA-NiW/B_2O_3/Al_2O_3 is more notable rather than that on NiW/B_2O_3/Al_2O_3. This result indicates that the number of CUS decreases while HDS activity is improved by the addition of CyDTA and boria. Therefore, the effect of CyDTA and boria can't be explained in terms of the number of CUS. Therefore, it is assumed that boria improves the HDS activity of CUS and it causes the higher HDS activity for 4,6-DMDBT.

Figure 3. Effect of CyDTA and boria on NO uptake on NiW catalysts. (   ); NiW/B_2O_3/Al_2O_3, (   ); CyDTA-NiW/B_2O_3/Al_2O_3.

We have investigated that the effect of CyDTA and boria on the structure of WS_2 on CyDTA-NiW/B_2O_3/Al_2O_3 by EXAFS analysis (**Table 1**). Table 1 presents W-W and W-S coordination numbers of CyDTA-NiW/B_2O_3/Al_2O_3 which contained different amount of boria. It is found that the W-W coordination number hardly changes by the addition of boria to CyDTA-NiW/Al_2O_3. The dispersion of WS_2 is

considered to be almost constant on each catalyst. This is the opposite result to that obtained from NO uptake measurements (see **Figure 3**). In contrast to this, W-S coordination number increases with the increase in boria loading. This result suggests that the sulfidation degree of WS_2 is improved by the addition of boria. Therefore, the decrease of the number of CUS by the addition of boria is due to the increase in the crystallinity of WS_2. Since there is a good correlation between HDS activity and the sulfidation degree of WS_2, the improvement of HDS activity by the addition of boria to CyDTA-NiW/Al_2O_3 is explained in terms of the sulfidation degree of WS_2. This means that boria induces the improvement of the quality of CUS. To sum up, the addition of boria causes the opposite effects on the surface structure of CyDTA-NiW/Al_2O_3, in other words, the improvement of the HDS activity of CUS and the decrease in the number of CUS.

Table 1. Structural Parameter of W-S, W-W Coordination

sample[a]	W-S		W-W	
	N[b]	R (nm)[c]	N	R (nm)
WS_2 powder	6.0[d]	0.24	6.0[d]	0.32
CyDTA-NiW/Al_2O_3	4.9	0.24	3.5	0.32
CyDTA-NiW/B_2O_3(1)/Al_2O_3	5.0	0.24	2.9	0.32
CyDTA-NiW/B_2O_3(2)/Al_2O_3	5.3	0.24	3.0	0.32
CyDTA-NiW/B_2O_3(5)/Al_2O_3	5.7	0.24	3.0	0.32
CyDTA-NiW/B_2O_3(10)/Al_2O_3	5.7	0.24	2.9	0.32

a) Numbers in parentheses indicate boria loading.
b) Coordination number. c) Interatmic distance.
d) Both coordination numbers are fixed for 6.

Conclusion

It is considered that the addition of boria enhances the formation of highly sulfided and highly crystallized WS_2. It causes the two opposite effects, in other words, the improvement of the HDS activity of CUS and the decrease in the number of CUS. Moreover, it is considered that CyDTA enhances the coordination of Ni to the edge sites of the WS_2 and it promotes the positive effect of boria. Consequently, it is suggested that highly active site is selectively formed by the simultaneous addition of both CyDTA and boria, and it leads to the improvement of HDS activity for 4,6-DMDBT.

References
(1) van Veen, J. A. R.; Gerkema, E.; van der Kraan, A. M.; and Knoester, A., *J. Chem. Soc. Chem. Commun.*, **1987**, 1684.
(2) Shimizu, T.; Hiroshima, K.; Honma, T.; Mochizuki, T.; Yamada, M., *Catal. Today*, **1998**, *45*, 271.
(3) Ohta, Y.; Shimizu T.; Honma, T.; Yamada, M., *Hydrotreatment and Hydrocracking of Oil Fractions*, **1999**, 161.
(4) Li, D.; Sato, T.; Imamura, M.; Shimada, H.; Nishijima. A., J. Catal., **1997**, *170*, 357.
(5) DeCanio, E. C.; Weissman, J. G., *Colloids and Surface A*, **1995**, *105*, 123.

NOVEL PREPARATION OF TITANIA (TiO$_2$) CATALYST SUPPORT BY APPLYING THE MULTI-GELATION METHOD FOR ULTRA-DEEP HDS OF DIESEL OIL

*Shinichi Inoue[*1], Hidehiko Kudou[*1], Akihiro Muto[*1], Takeo Ono[*2]*

*1: Research & Development Center, Chiyoda Corporation,
1-1 Minamiwatarida-cho, Kawasaki-ku, Kawasaki, 221-0022, Japan
E-mail : sinoue@ykh.chiyoda.co.jp
*2 : Ono Professional Engineer Office
1-38 Furuichiba, Saiwai-ku, Kawasaki 211-0952, Japan

Introduction

It is widely accepted that specific activity of titania (TiO$_2$) catalyst is superior to alumina catalyst. But, TiO$_2$ supported metal catalyst has not been employed, so far, for industrial use in hydrodesulfurization (HDS) or hydrotreating processes, because TiO$_2$ is regarded having a small specific surface area less than 50-60m^2/g and poor thermal stability.

In this study, a novel synthesis method of multi-gelation of TiO$_2$ as catalyst carriers or catalysts has been proposed [1]. The physical properties of TiO$_2$ can be controlled to enhance some catalytic activity. Since the physical properties of well controlled TiO$_2$ have superior characteristics to the conventional TiO$_2$, we tried to apply TiO$_2$ as the catalytic materials to the fields of petroleum refining for ultra-deep HDS of diesel oil.

Multi-Gelation Method

Multi-gelation method, originally developed for Alumina [2], is the procedure to produce the inorganic oxides gel by swinging of pH of solution dexterously several times. This method can be employed in preparation of hydrous titanium. It can control a particle size of TiO$_2$ uniformly with a designed pore size.

Experimental

Preparation Method of TiO$_2$ Support

Figure 1 shows the principle of the multi-gelation method to synthesize TiO$_2$. The raw materials are acidic TiCl$_4$ and basic ammonia solutions. Hydroxyl gel of TiO$_2$ was synthesized by swinging pH from TiCl$_4$ and ammonia solutions. TiCl$_4$ and ammonia solutions were supplied to the gelation vessel alternately, and hydrous titanium was synthesized. Particles of hydrous titanium were controlled in desirable particle size by alternately supplying TiCl$_4$ or ammonia solution. And hydrous titanium was washed by water to remove ammonium chloride. After filtration, TiO$_2$ as a catalyst or a catalyst carrier was molded to cylindrical shapes by the extruder, for example. And it was dried at 120 ^{o}C and is calcined at 500 ^{o}C in the standard procedure.

Catalyst

TiO$_2$ supports properties used in this study are as follows: Specific surface area is 162m^2/g, average pore diameter is 9nm whose pH swing number is 3 times. The CoMo/TiO$_2$ catalysts were prepared by gel impregnation method: TiO$_2$ gel was impregnated with ammonium heptamolybdate and Cobalt nitride as required. This was followed by drying at 120°C for 3h and calcination in air at 500°C for 3h.
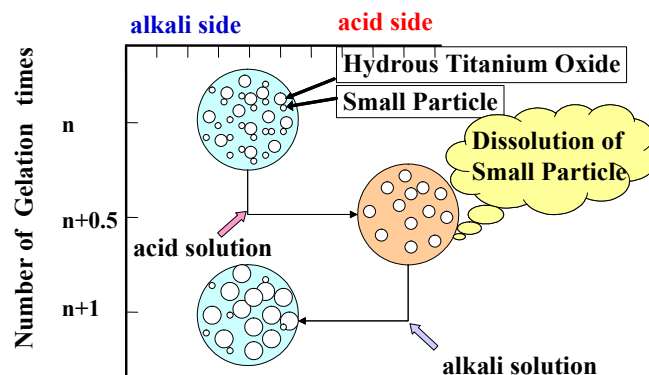

Figure 1   Principle of Multi-Gelation Method

Measurement of HDS activity

The HDS experiments were carried out with a fixed-bed reactor. The catalyst was presulfided with the feed oil spiked by DMDS. Typical reaction conditions were as follows: H$_2$/Oil ratio 250, LHSV 2 h^{-1}, reaction pressure 5 MPa, Reaction temperature 330 - 350°C. The Middle-East straight run gas oil with 1.3wt% sulfur was used as feed stock.

Results and Discussion

Specific surface area, particle size and crystal form are summarized in Table 1.

Table 1   Properties of TiO$_2$

Preparation Method	No. of Geration (−)	Surface Area (m2/g) by BET	Crystallite Size (nm) by XRD	Crystalline Form by XRD
Multi-geration	1	175	5.9	anatase
	2	170	6.3	anatase
	3	162	6.7	anatase
	4	151	7.1	anatase
	5	138	8.5	anatase
	6	133	9	anatase
Convensional(CS-300)	−	61	19	anatase

Particle Size, Pore Distributions and Crystal Structures

Photo 1 shows TEM image of the primary particles of TiO$_2$ obtained by multi-gelation method. It was found that the particle size varies according to the number of gelation times. Namely as shown in Table 1, for example, two times of gelation gives ca. 6.3 nm, while five times of gelation gives ca.8.5 nm size of the particle. In addition, it was observed that each particle size becomes more uniform with times of gelation.
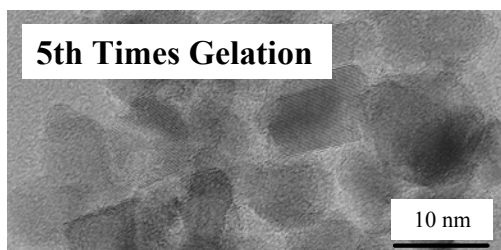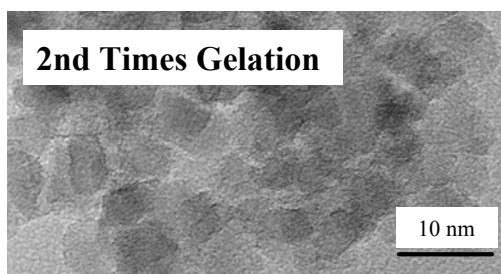
2nd Times Gelation

10 nm

5th Times Gelation

10 nm

Photo 1 TEM Image of Multi-gelation TiO$_2$

The multi-gelation method has a good performance for controlling pore structures, i.e., pore size distributions as shown in Figure 2. The figure shows the pore diameter versus differential value of pore volume on various numbers of gelation times. This method gives well controlled nano-porous structures of TiO$_2$. The pore size distribution, which can be controlled sharply in accordance with numbers of gelation times, reflects that of particle size. In other words, it shows that this synthesis method can materialize the TiO$_2$ of arbitrary and uniform particles. This is an important point to evaluate the catalytic performance in relation to the physical properties, especially the particle size, of TiO$_2$.
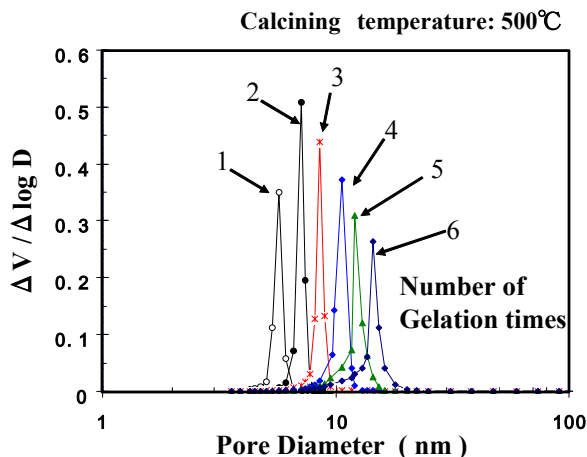

Calcining temperature: 500℃

Number of Gelation times

Figure 2   Pore Distributions of TiO$_2$ Controlled by Multi-gelation Method

Specific Surface Area

TiO$_2$ obtained by this method has higher specific surface area even after the calcinations at 500 ℃ than the conventional TiO$_2$, shown in Table 1. It decreases from 175m^2/g to 133m^2/g by increasing gelation times from one to six times. This may be due to the growth of crystal particle with gelation times.

Hydrodesulfurization Activity

The activity of the proprietary TiO$_2$ catalyst compared with the conventional CoMo/alumina catalyst for 500 ppm HDS are shown in Figure 3. This Figure also shows the reactivity of CoMo/TiO$_2$ catalyst prepared using conventional TiO$_2$ carrier with 60 m^2/g of surface area. It is important to mention that the catalytic activity of the TiO$_2$ supported prepared by multi-gelation method with high surface area and good pore distribution is much higher than that of the catalyst using conventional TiO$_2$ support with low surface area. Furthermore, it also shows that the new TiO$_2$ catalyst has 2 times higher hydrodesulfurization activity than that of the commercial alumina catalyst.
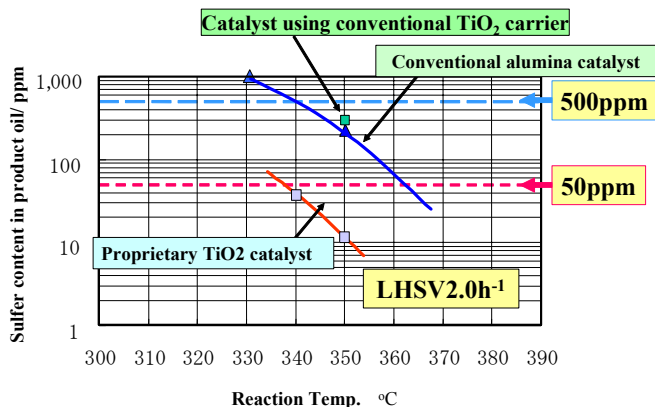

Figure 3   HDS Performance of Proprietary TiO$_2$ Catalyst

Conclusions

It was confirmed that TiO$_2$ with high specific surface area by the novel multi-gelation method showed good performance of catalytic activity in ultra-deep HDS reaction. Since the multi-gelation method can control the physical properties of TiO$_2$, it expected to be widely employed in various application fields. The proprietary TiO$_2$ catalyst prepared by the multi-gelation method is good candidates for the hydrodesulfurization or hydrotreating processes.

References
[1] Kudou, H., Inoue, S., Takatsuka, T., Ono, T., Nakata, S., Kato, S., The 6th International Conference on TiO$_2$ Photocatalytic Purification and Treatment of Water and Air, Abstracts, p.63, Ontario, Canada, June25-29, 2001.
[2] Shiroto, Y., Ono, T., Asaoka, S., Nakamura, M., USP:4,422.960

ULTRASOUND ASSITED SYNTHESIS AND HYDRODESULPHURIZATION ACTIVITY OF Ru-Al-PILLARED CLAYS

M. Josefina Pérez-Zurita*, Gabriela Pérez Quintana, José Gregorio Biomorgi and Carlos Eduardo Scott

Universidad Central de Venezuela, Facultad de Ciencias, Escuela de Química, Centro de Catálisis, Petróleo y Petroquímica. Apartado Postal 47102, Caracas, Venezuela

Introduction

The need for more active catalysts for hydrotreatment reactions has lead researchers to work on non conventional systems capable of meet the continuously increasing demands of the environmental national agencies for cleaner fuels. An alternative for the afore mentioned non conventional systems could well be Pillared Interlayer Clays (PILC) as catalysts, supports or precursors of highly disperse catalysts. The synthesis of PILC has been carried out for many research groups and many applications have been found for these type of materials. However, their use in a commercial scale is not yet a reality mainly because, on their synthesis, a great amount of water has to be used. In the past five years some efforts has been done to overcome this problem and good advances has been achieved (1-4). Besides, Chianelli et al. (5) reported on the hydrodesulphurization of dibenzotiophene (DBT) on a series of transition metal sulfide catalysts and found that ruthenium shows the best catalytic performance, even better than Ni, Mo or Co sulfides. The synthesis of a ruthenium based PILC was reported by Lenarda et al.(6) who used two different preparation procedures and tested the resulting catalysts in the hydrogenation and isomerization of 1-butene. The aim of the present work was to synthesize and study the behavior of the Ru-Al-PILC system in the hydrodesulphurization of tiophene.

Experimental

Ru-Al-PILC catalyst was prepared following the method reported by Lenarda et al.(6) but using ultrasound radiation on the exchange step in order to diminish exchange time. A Ru/Al-PILC catalyst was also prepared as a reference by conventional wet impregnation of an aqueous solution of $RuCl_3.xH_2O$ (Aldrich) on an Al-PILC. The preparation method of the Al-PILC was reported elsewhere (3).

Ru-Al-PILC Synthesis. A commercial montmorillonite, KWK-200 from American Colloid Company, without further purification, was used during the study. The precursor solution of aluminium and ruthenium was prepared by adding, under continuous stirring, NaOH drop wise to a mix solution of $AlCl_3.6H_2O$ (Riedel-DeHaën) and $RuCl_3.xH_2O$ (Al/Ru ratio of 20). The resultant solution had a OH / (Al+Ru) ratio of 2.4 and was left to stand for 24 hours at room temperature. After this time, the solution was added to a 50% suspension of clay in acetone and the mixture was divided in 3 portions and placed immediately into the ultrasonic bath which was kept at 44 ºC. The portions were retired from the bath at various times (60, 75, 90 min). Once the exchange process was completed, the solids were centrifuged, washed 5 times with double distilled water and dried at 60 ºC overnight. This series of catalysts was named Al-Ru-PILC$_x$ where x represent the time of exchange. In some cases the samples were calcined in flowing air at 400 ºC for 4 hours. The catalysts were characterized by XRD (Philips, PW1830), Textural properties (MICROMERITICS, ASAP-2400) and Chemical analyses (GBC AVANTA).

HDS reaction. Prior to reaction, the catalysts were suphided with a 5:1 mixture of H_2/H_2S or N_2/H_2S at 400 ºC for 4 hours in an atmospheric flow system and using a specially designed reactor able to be transported sealed. The sample was then transferred to the catalytic system were the reaction was conducted at 280 ºC and atmospheric pressure. The flow of hydrogen was 0.1 cc/s and a solution of 10% tiophene in hexane was fed to the system through a syringe pump at a rate of 1 cc/h.

Results and Discussion

Synthesis results. Table 1 shows the Chemical Analyses, Specific Surface Area and the Basal Spacing of the studied samples.

Table 1. Chemical Analyses, Specific Surface Area and Basal Spacing results

Solid	% Ru	SSA (m^2/g)	d (001)
Original clay	-----	33	13
Al-Ru-PILC$_{60}$	-----	207	18
Al-Ru-PILC$_{75}$	1.02	229	18
Al-Ru-PILC$_{90}$	-----	228	18
Ru/Al-PILC	3.00*	175	-----

* Nominal

The pillaring process on the mix pillared clay was evidenced as the specific surface area and basal space increased substantially. The use of ultrasonic radiation resulted in an excellent tool to reduce time of exchange, as the optimal time of exchange was 75 minutes which represent a decrease of ≈ 90% in time, as compared with the conventional synthesis reported by Lenarda et al. (6). As reported by these authors, only around 1% ruthenium was incorporated on the Ru-Al-PILC.

A complete textural characterization was conducted on the Ru-Al-PILC catalysts and on the Al-PILC support. Both solids shown a type II isotherm (following BET classification) with a type B hysteresis, characteristic of laminar solids. Detailed results are shown in table 2.

Figure 1 shows the pore distribution plot.
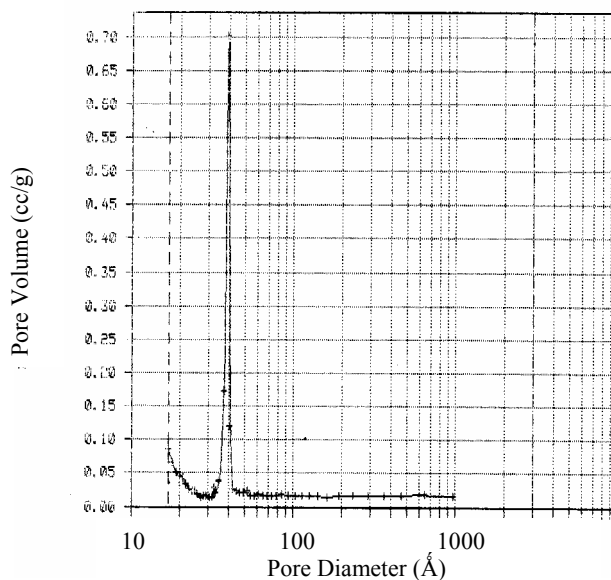
Figure 1. BJH average pore diameter of Ru-Al-PILC

A narrow pore distribution at around 40 Å is observed providing evidence of a great homogeneity of the Ru-Al-PILC sample

Table 2. Textural properties

Solid	SSA (m^2/g)	D$_p$ (Å)	Vp (cc/g)	Vμ (cc/g)	SSAμ (m^2/g)
Al-Ru-PILC$_{75}$	229	46	0.123	0.077	195
Al-PILC	300	50	0.180	0.097	255

As expected, ruthenium impregnation leads to a decrease on surface area, porous volume and pore diameter.

Catalytic results. The catalytic results are shown in table 3.

Table 3. Catalytic results on the HDS of tiophene

Catalyst	Sulphiding mixture	Conv. (%)	Activity * 10^7 (mol/s*g)
Ru/Al-PILC	H$_2$/H$_2$S	4	0.42
Ru-Al-PILC	H$_2$/H$_2$S	14	1.42
Ru-Al-PILC	N$_2$/H$_2$S	21	2.10
Ru-Al-PILC*	N$_2$/H$_2$S	3	0.33

* Calcined

It is expected that ruthenium on a PILC structure could be better dispersed as it would take defined positions in the pillar. Our results show that the Ru-Al-PILC catalyst is almost three times more active than the impregnated catalyst. This result seems to indicate that indeed the PILC structure lead to a better disperse ruthenium catalyst which in turn is more active. Further measurements are in progress in order to confirm this statement.

When the sulphiding mixture was changed from H$_2$/H$_2$S to N$_2$/H$_2$S, an increase in activity was observed. This result seems to point out that a high hydrogen concentration could lead to a loss of S atoms from the RuS$_2$ formed and, as a consequence, the active phase would be replaced by ruthenium completely reduced. A similar result was reported by De los Reyes et al.(7) and more recently by Castillo and Ramirez(8) in a 7% Ru/Al$_2$O$_3$ catalyst. These authors attributed the lost of activity to the fact that a high concentration of hydrogen in the sulphiding mixture, do not allow ruthenium atoms to complete its coordination sphere with S atoms but rather favors that part of ruthenium reduces completely to Ruº possibly segregated. These ruthenium atoms do not participate in the active phase RuS$_2$. Castillo and Ramirez(8) also reported that when the catalysts was pretreated with the H$_2$/H$_2$S mixture, the stability of the catalysts was very poor as compare with that of the N$_2$/H$_2$S pretreated catalysts. In their case, however, the lost of activity was more important. While their result show a lost of activity of up to 80% when the suphiding mixture was H$_2$/H$_2$S, we only observe a 33% lost of activity. This result seems to give evidence that ruthenium in our catalyst is more stable probably because it is in the PILC structure and as a consequence, its reduction is more difficult.

When the catalyst is calcined before sulphurization, the activity is lost probably because ruthenium is stabilized on the PILC structure hindering the formation of RuS$_2$ at the activation conditions.

Conclusions

By using ultrasonic radiation in the synthesis of a ruthenium based PILC, the time of exchange can be reduced in more than 90%.

The Ru-Al-PILC was a good precursor of a highly dispersed catalyst which showed higher hydrodesulphurization activity than ruthenium impregnated on Al-PILC.

The sulphiding mixture showed to have an important effect on the catalytic performance of the Ru-Al-PILC studied, the stability of the ruthenium species generated by the PILC structure minimized the reducibility of ruthenium when the sulphiding mixture was H$_2$/H$_2$S.

References
(1) Katdare S., Ramaswamy V. and Ramaswamy A. *Catal. Today*, **1999**, 49, 313.
(2) Katdare S., Ramaswamy V. and Ramaswamy A *Micro & Meso Porous Mat.* **2000**, 37, 329
(3) Pérez Zurita M.J., Pérez Quintana G., Maldonado A., Biomorgi J.G. and Scott C.E., *Prepr. Pap TOCAT IV*, **2001**, 279
(4) Pérez Zurita M.J., Pérez Quintana G., Maldonado A., Biomorgi J.G. and Scott C.E*., to be published*
(5) Chianelli R.R, **1984,** Catal. Rev- Sci. Eng., 26, 361
(6) Lenarda M., Storaro l., Ganzerla R., Rinaldi A., *J. Mol. Catal. A* **1999**, 144, 151.
(7) De los Reyes A., Vrinat M., Geantet C., Breysse M., Catal. Today, **1991,** 10, 645
(8) Castillo Villalón P. and Ramírez Solis J., Prepr. Pap*. – XVIII Simposio Iberoamericano de Catálisis* **2002***, 1068.*

ACTIVATION OF HYDROGEN OVER SULFIDE CATALYSTS. RELEVANCE TO KINETICS AND MECHANISMS OF HYDROTREATING REACTIONS.

Guy Pérot

Laboratoire de Catalyse en Chimie Organique
Département de chimie
Faculté des Sciences Fondamentales et Appliquées de l'Université de Poitiers
40, Avenue du Recteur Pineau, 86022 Poitiers, France

Introduction

The regulations on transportation fuels regarding sulfur content in particular are more and more severe. This forces the refiners to achieve what is commonly called deep desulfurization. One of the consequences of this requirement is that the demand in the refinery regarding hydrogen is increasing drastically. This is made all the more crucial as at the same time the tendency is to reduce the amount of aromatics in gasoline and consequently the capacity of the reforming units which provide hydrogen in the refinery.

Another reason why it is essential to better understand hydrogen activation on hydrotreating catalysts and the hydrogenation properties of these catalysts is related to the HDS of FCC gasoline in which the objective is to obtain high sulfur removal with a minimum of olefin hydrogenation.

Twenty years ago, Barbour and Campbell [1] reported the results of the hydrogenation of buta-1,3-diene on a D_2S-treated MoS_2 catalyst. They concluded that hydrogen present as SH groups on the surface was involved in the hydrogenation of the diene, which could suggest that the dissociation of H_2 was heterolytic. Later on, in their theoretical approach of the homolytic and heterolytic dissociation of H_2, Anderson et al. [2] concluded that the most stable chemisorption form of hydrogen was heterolytic at edges of MoS_2 crystals. Since then the authors of numerous studies have assumed that the dissociation of hydrogen on sulfides was heterolytic [3-8].

In a recent review, Furimsky et al. [9] examined in detail the reaction of sulfide surfaces with hydrogen and in particular the mechanism of creation of vacancies as well as the nature of the species resulting from the chemisorption of hydrogen. The purpose of this contribution is not to cover all the aspects of the interaction of hydrogen with sulfides, it will focus mainly on the dissociation of H_2. We will review a number of experimental results which are in favor of the heterolytic dissociation of hydrogen and show its relevance to mechanisms and kinetics of hydrotreating reactions. We will also report examples of promoter effects related to hydrogen activation and to the hydrogenation of olefins.

Tracer experiments on the dissotiation of hydrogen on sulfides

To our knowledge no direct proof of the heterolytic dissociation of H_2 over MoS_2 catalysts has been reported yet. However quite a number of experimental facts obtained by various authors are clearly in favor of such a dissociation mode.

Isotopic exchange experiments between H_2 and D_2S. The experiments were carried out at 80°C on $NiMo/Al_2O_3$ catalyst samples which were presulfided with a H_2/H_2S mixture (10 vol.% of H_2S) at 400°C [10].

The formation of HD indicated that isotopic exchange occurred between H_2 and D_2S. Similar results were obtained by Hensen et al. on carbon supported catalysts [11]. Hence,we can suppose that both reactants dissociate in the same maner on the same kind of catalytic centers. If we assume as it is generally accepted that the dissociation of H_2S (D_2S) on sulfides is heterolytic [2,4,12-18], we can suppose that the chimisorption of hydrogen also is heterolytic.

Involvement of support hydrogen in the isotopic exchange between gas phase H_2 and D_2. By carrying out H_2-D_2 exchange experiments on a H_2/H_2S presulfided $NiMo/Al_2O_3$ catalyst or by reacting D_2 on such a catalyst sample, it was shown through isotopic delution that gaseous D_2 could incorporate H-atoms coming from the support [10,19,20]. On a typical commercial catalyst, the amount of support hydrogen which could be incorporated into the deuterium of the gas phase varied depending on the pretreating conditions and could be as high as 90% of the hydrogen held by the solid after sulfidation. It was also shown that the latter resulted mostly from the adsorption of H_2S [20]. Since the isotope exchange between H_2 and D_2 is extremely slow under the same conditions with the pure alumina support, it was concluded that the hydrogen held by the support could only exchange with gas phase hydrogen via the sulfide through a spillover-like process. This was confirmed by FTIR experiments [19,20] which showed that OD bands (2640 cm^{-1}) appeared readily on the alumina support of a presulfided $NiMo/Al_2O_3$ catalyst during its exposure to D_2 while OH bands (3580 cm^{-1}) desappeared. This process barely existed on the pure presulfided support under the same conditions.

Since the H atoms of the hydroxyl groups of the alumina support have undoubtedly an ionic character, this is also good evidence in favor of the heterolytic splitting of D_2 (H_2).

Incorporation of deuterium from D_2S in propane via propene hydrogenation. The hydrogenation of propene over a D_2S-treated $NiMo/Al_2O_3$ catalyst showed that D-atoms from D_2S were involved in the reaction [21]. This is in accordance with the results reported previously by Barbour and Campbell [1] regarding the hydrogenation of buta-1,3-diene over a D_2S-treated MoS_2 catalyst although it is difficult at the moment for us to conclude, as these authors did for butadiene, that D-atoms were incorporated directly from D_2S to propene.

Relevance of the heterolytic dissociation of hydrogen to reaction mechanisms and kinetics

The heterolytic dissociation of H_2 on a catalytic center composed of a sulfur vacancy located on a molybenum atom and of a neighbouring sulfur anion leads to the H-atom having a hydride character adsorbed on the metal ion and the H-atom with a protonic character adsorbed on the sulfur anion [3-6]. However, as shown recently by DFT calculations [22], the hydride bound to the metal seems to be highly unstable with Molybdenum-based catalysts, especially with nickel-molybdenum. Contrary to what was obtained with ruthenium catalysts [18], metal-hydrogen species have not been observed yet. H_2S is supposed to dissociate in the same manner with its proton adsorbed on a sulfide anion and the sulfhydril group on the metal; this leads to two SH groups.

The first step of the hydrogenation of unsaturated substrates can be either the addition of H^+ or of H^-. Kinetic modeling studies bring some information on this point [6,7,23].

In their study of the effect of H_2S on the hydrogenation of toluene over a Mo/Al_2O_3 catalyst, Kasztelan and Guillaume [6] compared various kinetic models supposing molecular, homolytic and heterolytic dissociative adsorption of H_2 and H_2S. By computing the rate laws according to the classical Langmuir-Hinshelwood-Hougen-Watson method, they came to the conclusion that the model which fitted at best the kinetic orders of the reaction with respect to the various reactants, especially H_2S, was the one supposing the heterolytic dissociation of H_2 and H_2S on a vacancy and a sulfur anion. The hydrogenation was found to proceed via addition of a hydride followed by the addition of a proton to the aromatic molecule. The changes in kinetic order with respect to H_2S was

explained by supposing that the rate-limiting step of the reaction was changing from one of these two elementary steps to the other as the H_2S partial pressure increased.

More recently, Blanchin et al. [23] have used the Chemkin/Surface Chemkin II tool to investigate the effect of H_2S and of NH_3 on the same reaction catalysed by a $NiMo/Al_2O_3$ catalyst. They found also that the model involving the heterolytic dissociation of H_2 and H_2S on centers composed of an unsaturated molybdenum ion and of a sulfur anion fitted at best with the experimental data. They confirmed that the hydrogenation of the aromatic molecule started with the addition of a hydride followed by the addition of a proton, the latter being the rate-limiting step of the reaction in the range of H_2S partial pressures investigated. However the rate-limiting character of this step depended very much on the partial pressure of H_2S which in addition to H_2 provides protons to the system.

Orozco and Vrinat used the same approach as Kasztelan and Guillaume to investigate the effect of H_2S on the hydrodesulfurization of dibenzothiophene through kinetic modeling [7]. Like Kasztelan and Guillaume, they concluded that the reaction involved the heterolytic dissociation of H_2 and H_2S and that depending on the   partial pressure the rate-limiting step of the reaction could be the addition of a hydride ion to the adsorbed substrate or the attack of a dihydrointermediate by a sulfur anion to achieve carbon-sulfur bond cleavage.

Promoter effects in hydrogen activation and in the hydrogenation of olefins.

The role of the promoters in the hydrogenation process on sulfides was investigated by measuring the effect of cobalt and nickel on the activities of MoS_2–based catalysts in the isotopic exchange between H_2 and D_2 and in the hydrogenation of cyclopentene in the absence of H_2S [24]. The catalyst samples containing the same amount of molybdenum and various quantities of cobalt or nickel were presulfided with a H_2/H_2S mixture (10 vol.% of H_2S) at 400°C then treated at 350°C under helium for 1 hour. Under these conditions, the catalysts containing cobalt were much more active than those containing nickel in the H_2-D_2 isotopic exchange reaction so that the experiments were carried out at 35°C with the former and 80°C with the latter [20]. It was verified that both series of catalysts exhibited the expected synergy effect in the hydrodesulfurization of dibenzothiophene at 340°C under 30 bar of hydrogen [25]. However no sinergy effect was obtained with nickel in the isotopic exchange between H_2 and D_2 while the catalyst containing cobalt with a Co/Co+Mo atomic ratio of 0.3 was found five times more active than the unpromoted catalyst. This is in accordance with other results reported in the litterature [11,26,27] and was interpreted by Travert et al. by a difference in the rate-limiting step of the process [22]. Surprisingly, the reverse was obtained regarding the promoting effect in the hydrogenation of cyclopentene. The promoting effect of cobalt (2 only for a Co/Co+Mo atomic ratio of 0.3) was much weaker than the effect of nickel (about 10 for the same atomic ratio).

While both promoters have similar effects in hydrotreating reactions as well as in the thioreduction of ketones [25], their effect on hydrogen activation and on the hydrogenation of olefins seem to be different. This might be a question of operating conditions but also of kinetics [22] regarding hydrogen activation and hydrogenation or of sulfur coverage connected to the intrinsic properties of the solids.

Conclusions

Various observations (the isotopic exchange between H_2 and D_2S, the contribution of the support to the isotopic exchange between H_2 and D_2) as well as theoretical calculations are definitely in favour of the heterolytic dissociation of hydrogen on sulfides.The best

fittings regarding the kinetic modeling of hydrotreating reactions is also obtained when supposing such a dissociation process.

However certain observations like differences in promoting effects with cobalt and nickel in hydrogen activation and hydrogenation have to be rationalize and further experiments are needed.

References
(1) Barbour, J.; Campbell, K.C., *J. Chem. Soc., Chem. Commun.* **1982**, 1371.
(2) Anderson, A. B., Al-Saigh, Z. Y., and Hall, W. K., *J. Phys. Chem.*, **1988**, *92*, 803.
(3) Kasztelan, S., *Ind. Eng. Chem. Res.*, **1992**, *31*, 2497.
(4) Kasztelan, S., Prepr. Pap. - *Am. Chem. Soc., Div. Petrol. Chem.*, **1993**, *38*, 642.
(5) Kasztelan, S., In *Hydrotreating Technology for Pollution Control Catalysts, Catalysis, and Processes,* Occelli M. L., Chianelli, R. Eds., Marcel Dekker, Inc., New York, Basel, Hong Kong, 1995, pp 29-45.
(6) Kasztelan, S., and Guillaume D., *Ind. Eng. Chem. Res.*, **1994**, *33*, 2497.
(7) Orozco, O., and Vrinat, M., *Appl. Catal.*, **1998**, *170*, 195.
(8) Mijoin, J., Pérot, G., Bataille, F., Lemberton, J.-L., Breysse, M., Kasztelan, S., *Catalysis Letters,* **2001**, *71*, 139.
(9) Furimsky, E., Breysse, M., Kasztelan, S., Lacroix, M. and Pérot, G., *Catal. Rev.-Sci. Eng.,* in the press.
(10) Thomas, C.; Vivier, L.; Lemberton, J.L.; Kasztelan, S.; Pérot, G. *J. Catal.* **1997**, *167*, 1.
(11) Hensen, E.J.M.; Lardinois, G.M.H.J.; de Beer, V.H.J.; van Veen, J.A.R.; van Santen, R.A. *J. Catal.* **1999**, *187*, 95-108.
(12) Schuit, G. C. A., *Int. J. Quantum Chem.,* **1977**, *12*, 43.
(13) Wright, C. J., Sampson, C. Fraser, D., Moyes, R. B., Wells, P. B., and Riekel, C., *J. Chem. Soc. Faraday Trans. I.,* **1980**, *76*, 1585.
(14) Yang, S. H., and Satterfield, C. N., *J. Catal.* **1983**, *81*, 168.
(15) Yang, S. H., and Satterfield, C. N., *Ind. Eng. Chem. Process Des. Dev.*, **1984**, *23*, 20.
(16) Olalde, A., and Pérot, *Appl. Catal.,* **1985**, *13*, 373.
(17) Lacroix, M., Yuan, S., Breysse, M., Dorémieux-Morin, C., and Faissard, J., *J. Catal.* **1992**, *138*, 409.
(18) Jobic, H., Clugnet, C., Lacroix, M., Yuan, S., Mirodatos, C., and Breysse, M., *J. Am. Chem. Soc.* **1993**, *115*, 3654.
(19) Thomas, C.; Vivier, L.; Travert, A.; Maugé, F.; Kasztelan, S.; Pérot, G., *J. Catal.* **1998**, *179*, 95-502.
(20) Scaffidi, A.; Vivier, L.; Travert, A.; Maugé, F.; Kasztelan, S.; Scott, C.; Pérot, G., *Stud. Surf. Sci. Catal.* **2001**, *138*, 31-38.
(21) Brémaud, M., Vivier, L., Pérot, G., and Harlé, V., *This meeting,* Submitted.
(22) Travert, A., Nakamura, H., van Santen, R. A., Cristol, S., Paul, J.-F., and Payen, E., *J. Am. Chem. Soc.* **2002**, *124*, 7084.
(23) Blanchin, S., Galtier, P., Kasztelan, S., Kressmann, S., Penet, H., and Pérot, G., *J. Phys. Chem.*, **2001**, *105*, 10860.
(24) Vivier, L., Mijoin, J., Schneider, S., Lemberton, J.-L., Kasztelan, S., Scott, S., and Pérot,G., to be published.
(25) Mijoin, J., Thévenin, V., Garcia-Aguirre, N., Yuze, H., Wang, J., Li, W. Z., Pérot, G., and Lemberton, J.-L., *Appl. Catal.,* **1999**, *180*, 95.
(26) Thomas, C.; Vivier, L.; Lescanne, M., Kasztelan, S.; and Pérot, G., *Catalysis Letters,* **1999**, *58*, 33.
(27) Lacroix, Dumonteil, C., Breysse, M., and Kasztelan, S.; *J. Catal.* **1999**, *185*, 219.

HYDROGENATION OF PROPENE ON SULFIDE CATALYSTS - H-D ISOTOPIC STUDY

M. Brémaud[a], L. Vivier[a*], G. Pérot[a] and V. Harlé[b]

[a]Laboratoire de Catalyse en Chimie Organique UMR CNRS 6503
Faculté des Sciences – Université de Poitiers
40, avenue du Recteur Pineau, 86022 Poitiers Cedex, France
*e-mail : laurence.vivier@univ-poitiers.fr
[b]Institut Français du Pétrole
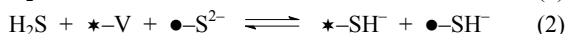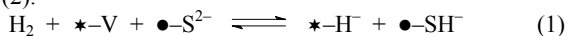1 et 4, avenue de Bois Préau, 92852 Rueil-Malmaison Cedex, France

Introduction

Because of increasing environmental constraints hydrotreating becomes more and more important in refineries for the removal of sulfur and nitrogen impurities from petroleum.

The catalysts have to be more and more efficient in hydrodesulfurization whereas the consumption of hydrogen has to be limited. Moreover, in the case of gasoline hydrotreating, the selectivity in hydrodesulfurization in comparison with the hydrogenation of olefins has to be controlled and has to be improved in order to limit the octane loss.

In order to better understand the factors which influence this selectivity, the hydrogenation of propene in parallel with the isotopic exchange between H_2 and D_2 has been studied on sulfided $NiMo/Al_2O_3$ and the interaction of H_2 with H_2S during the hydrogenation reaction was also examined.

It was shown previously that an exchange of hydrogen atoms between H_2 and D_2S occurred on sulfided hydrotreating catalyst [1-4]. The existence of this exchange reactions seems to indicate that there is a common mode of dissociation, presumably heterolytic, for both reactants on the same catalytic centers as described in Eqs (1) and (2).

$$H_2 + {*}{-}V + {\bullet}{-}S^{2-} \rightleftharpoons {*}{-}H^- + {\bullet}{-}SH^- \qquad (1)$$

$$H_2S + {*}{-}V + {\bullet}{-}S^{2-} \rightleftharpoons {*}{-}SH^- + {\bullet}{-}SH^- \qquad (2)$$

FTIR studies have confirmed that hydrogen from the gas phase can be exchanged with the hydrogen atoms of hydroxyl groups of the support by the intermediate of the sulfide phase. Under our experimental conditions the amount of exchangeable hydrogen preadsorbed on the support was very significant compared to the amount on the active phase, which represented less than 10% of the total amount [2]. The hydrogen present on the support was essentially due to adsorbed H_2S [5].

The aim of this study is to examine the influence of H_2S on the hydrogenation of propene and to see if the hydrogen present at the surface of the catalyst as preadsorbed H_2S can be involved and incorporated in propene during the hydrogenation.

Experimental

Catalysts. The $NiMo/Al_2O_3$ commercial catalyst contained 2.9 wt% NiO and 12.5 wt% MoO_3 deposited on alumina (230 $m^2.g^{-1}$). The catalyst was presulfided *in situ* with a flow of H_2 (90%) and H_2S (10%) at 400°C for 15 hours. After sulfidation, and before the hydrogenation reaction, the catalyst underwent two different pretreatments : it was either cooled down to 80°C in the presence of the sulfidation mixture and treated for 1h under He at 80°C (pretreatment **1**) or treated for 1h at 350°C and cooled down to 80°C under He (pretreatment **2**). After both pretreatments, the catalyst was treated at 80°C for 1h under a flow of Ar. The treatment under Ar was necessary to remove He which has the same mass as D_2.

Hydrogenation of Propene. The hydrogenation of propene by H_2 or D_2 was carried out at 80°C in a 72 cm^3 recycling reactor. The reactants (H_2 or D_2 plus propene ; 0.5 bar of each) were introduced into the reactor and the recycling pump was started. The apparatus which was described elsewhere [1], was fitted with a gas chromatograph with a FID detector and with a mass spectrometer in order to analyze H_2, HD, D_2, propene and propane, deuterated or not.

Preadsorption of D_2S. After sulfidation and pretreatment **2**, D_2S was introduced in the closed reactor and recycled at 80°C (0.5 bar with 1.5 bar of He) for 1h. The catalyst was then treated under a flow of He at diverse temperatures for 1h, cooled down to 80°C, and then treated under a flow of Ar. The hydrogenation of propene was carried out in the presence of H_2 at 80°C.

Results and Discussion

The rate of the hydrogenation of propene hydrogenation in the presence of sulfided $NiMo/Al_2O_3$ after pretreatment **2** increased when the partial pressure of H_2 and the partial pressure of propene increased from 0.1 bar to 0.5 bar. The kinetic orders deduced from these results are about 1 with respect to H_2 and propene.

In subsequent experiments , the partial pressures of H_2 (or D_2) and of propene were of 0.5 bar each. Table 1 shows the influence of the pretreatment procedure of the sulfided $NiMo/Al_2O_3$ catalyst on the initial rate of hydrogenation of propene by H_2 and by D_2. The rate of propene hydrogenation or deuteration was in the average 100 times greater after pretreatment **2** than after pretreatment **1**. Indeed, pretreatment **2** allows the desorption of a large amount of H_2S present on the catalyst after sulfidation. Table 2 shows the influence of H_2S in the gas phase on the hydrogenation of propene. The reaction was carried out with 0.4 bar of each reactant in the absence or in the presence (0.04 bar) of H_2S. Helium was added to reach a total pressure of 2 bar. H_2S had an important inhibiting effect on the hydrogenation of propene since in its presence the reaction was about two orders of magnitude slower then in its absence.

Table 1. Effect of the Pretreatment Procedure on the Initial Rate of Propene Hydrogenation.

|	Hydrogenation r° (10^{-7} mol.s^{-1}.g^{-1})	Deuteration r° (10^{-7} mol.s^{-1}.g^{-1})
Pretreatment **1**	0.20	0.12
Pretreatment **2**	14.2	14.6

Table 2. Influence of the Presence of H_2S on the Initial Rate of Propene Hydrogenation.

Composition of the gas phase (plus He to reach a total pressure of 2 bar)	Hydrogenation r° (10^{-7} mol.s^{-1}.g^{-1})
H_2 (0.4 bar) + propene (0.4 bar)	19.7
H_2 (0.4 bar) + propene (0.4 bar) + H_2S (0.04 bar)	0.23

Table 1 shows also that there was no significant difference between the hydrogenation by H_2 or by D_2 especially after pretreatment **2**. For the experiments with D_2, the incorporation of deuterium atoms in the different products was followed by mass spectrometry. After pretreatment **1**, the hydrogenation was very slow. Nevertheless, HD was formed with an initial rate of 8.6 10^{-7} mol.s^{-1}.g^{-1}. Previous experiments, carried out on the same catalyst treated under the same conditions, showed that D_2, introduced alone, was exchanged with hydrogen adsorbed on the catalyst to produce HD with a rate of 8.4 10^{-7} mol.s^{-1}.g^{-1} [1]. The formation of HD occurred with a very similar rate in these two experiments. Mono- and di-deuterated propenes were also formed but since the reaction was very slow (initial rate of about 0.2 10^{-7} mol.s^{-1}.g^{-1}) we can conclude that the formation of HD was essentially due to a direct exchange between D_2 and the "H" preadsorbed on the catalyst.

After pretreatment **2**, the major reaction was the deuteration of propene to yield di-deuterated propane (d2) (Figure 1). The

consumption of D_2 was greater than the consumption of propene, which was a consequence of the H-D exchange of D_2 with the hydrogen adsorbed on the catalyst. HD and H_2 formed by isotopic exchange were added to propene to form mono-deuterated and non-deuterated propane (d1 and d0). The existence of tri- and tetra-deuterated propane (not reported in Figure 1) reveals the exchange reaction between D_2 and propene prior to hydrogenation. Actually it was shown that there was no exchange between propane and D_2 under the same conditions.
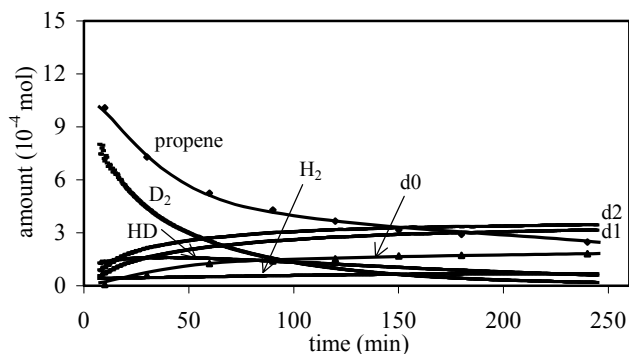
Figure 1. Products present in the gas phase during the reaction of propene with D_2 on sulfided NiMo/Al$_2$O$_3$ catalyst after pretreatment **2**. (d0 ; d1 ; d2 : non-, mono- and di-deuterated propanes, respectively).

As it was shown above, under our conditions, H_2S inhibited the hydrogenation reaction very much. In order to study the involvement of hydrogen sulfide in the hydrogenation of propene, experiments were carried out on a sulfided NiMo/Al$_2$O$_3$ catalyst which was pretreated with D_2S at 80°C then treated at various temperatures in order to desorb part of the D_2S. Table 4 shows the influence of the temperature of D_2S desorption on the initial rate of hydrogenation and on the incorporation of deuterium atoms in propane and hydrogen after 2 hours of reaction.

Table 4. Influence of the Temperature of D_2S Desorption on the Hydrogenation of Propene

Temperature of D_2S desorption (°C)	200	280	350
Initial rate of formation of :			
non-deuterated propane (10^{-7} mol.s^{-1}.g^{-1})	4.3	15.2	25.6
mono-deuterated propane (10^{-7} mol.s^{-1}.g^{-1})	0.7	0.8	1.4
Amount of incorporated deuterium atoms into propane and hydrogen after 2 h :			
total amount (10^{-5} mol)	13.2	9.5	7.4

The rate of hydrogenation increased when the temperature of D_2S desorption increased while the amount of incorporated deuterium atoms decreased (Table 4). The formation of mono-deuterated propane was not significantly influenced by the temperature of D_2S desorption and it was very slow compared to the formation of the non-deuterated propane. This is the result of a compensation phenomenon between, on the one hand the increase of the overall rate of hydrogenation of propene following the elimination of D_2S as its desorption temperature increased and, on the other hand, the decrease in concentration of D-atoms (as D_2S) present in the medium.

Nevertheless, it is clear that deuterium atoms adsorbed on the catalyst as D_2S were incorporated into propane via propene hydrogenation. This is in accordance with the results reported by

Barbour and Campbell [4] who carried out similar experiment with 1,3-butadiene. However, contrary to what they did, it is difficult to tell at the moment from our experiments whether D-atoms from D_2S are added to propene directly or not. Actually, if one excepts the point at low conversion, the isotopic distribution in dihydrogen and in propane were quite similar (Figure 2), which would not be the case if D-atoms would add directly from D_2S to propene. This means that under our conditions D-atoms from D_2S could exchange with H-atoms of H_2 of the gas phase prior to the addition to propene. Complementary experiments at very low conversion with higher concentration of adsorbed D_2S are necessary to make this point clearer.
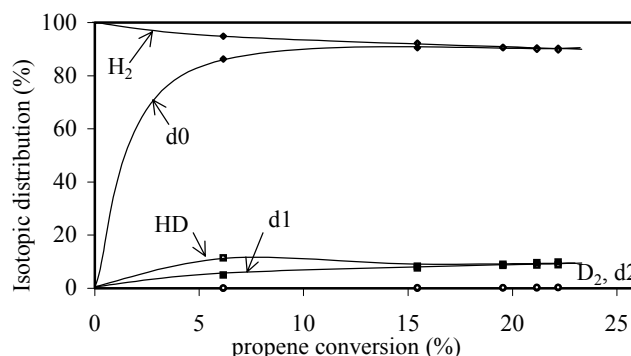
Figure 2. Isotopic distribution in propane and in dihydrogen in the gas phase during the hydrogenation of propene on sulfided NiMo/Al$_2$O$_3$ catalyst treated with D_2S desorbed at 200°C. (d0 ; d1 ; d2 : non-, mono- and di-deuterated propanes, respectively).

As was the case with the experiments of Barbour and Campbell [4] the presence of H_2 in the gas phase was necessary for the hydrogenation to proceed and for D-atoms to be incorporated in propane. They concluded that hydrogen gas was necessary to replenish the SH groups involved in the hydrogenation. However, if we assume that the dissociation of H_2 and H_2S is heterolytic, another explanation is possible, i.e. that preadsorbed H_2S (D_2S) can only provide H^+ (D^+) to the reaction and that hydrogen gas is necessary to provide H^- via dissociation on the sulfide.

Conclusion

The hydrogenation of propene was very sensitive to the presence of H_2S in the gas phase or to H_2S previously adsorbed on sulfided NiMo/Al$_2$O$_3$. It was also shown that D-atoms from preadsorbed D_2S were incorporated in propane via propene hydrogenation in the presence of gas phase hydrogen. This is in agreement with the hypothesis that the dissociation of H_2 and H_2S on sulfide catalysts is heterolytic. The presence of gas phase hydrogen is thought to be necessary to provide H^- to the reaction medium.

References
(1) Thomas, C.; Vivier, L.; Lemberton, J.L.; Kasztelan, S.; Pérot, G. *J. Catal.* **1997**, *167*, 1-11.
(2) Thomas, C.; Vivier, L.; Travert, A.; Maugé, F.; Kasztelan, S.; Pérot, G., *J. Catal.* **1998***, 179*, 95-502.
(3) Hensen, E.J.M.; Lardinois, G.M.H.J.; de Beer, V.H.J.; van Veen, J.A.R.; van Santen, R.A. *J. Catal.* **1999**, *187*, 95-108.
(4) Barbour, J.; Campbell, K.C., *J. Chem. Soc., Chem. Commun.* **1982**, 1371-1372
(5) Scaffidi, A.; Vivier, L.; Travert, A.; Maugé, F.; Kasztelan, S.; Scott, C.; Pérot, G., *Stud. Surf. Sci. Catal.* **2001**, *138*, 31-38.

Influence of the Support Acidity on the Sulfided Phase Properties

Françoise Maugé[a], Gérald Crépeau[a],
Arnaud Travert[a] and Tivadar Cseri[b]

[a] Catalysis and Spectrochemistry Laboratory, CNRS - EnsiCaen - University, 14050 CAEN cedex, France
[b] IFP, Kinetics and Catalysis Department, 1-4 av. de Bois Préau, 92852 Rueil Malmaison cedex, France
email : francoise.mauge@ismra.fr

Introduction

High pressure hydrocracking is a key catalytic refining process used to upgrade low quality feedstocks into high quality middle distillates (kerosene and gasoil). In addition to the cracking of the molecules the ability of the hydrocracking process to ensure the elimination of sulfur and nitrogen compounds and a deep saturation of aromatics, allows to produce high quality diesel fuels that will match the future and more stringent specifications (1). The catalysts used in hydrocracking are bifunctional, associating a hydro-dehydrogenating function (generally a sulfided phase) with an acidic function. The acidity of the catalyst is a key parameter to control the activity and the selectivity of the hydrocracking catalysts. Generally, hydrocracking catalysts are supported on zeolites or amorphous silica-alumina (ASA).

This study concerns sulfided NiW catalysts supported on ASA presenting various Si/Al ratio. Our aim was to describe precisely the acidity of the ASA, the sulfided phase sites and to establish the influence of the acidity of the support on the sulfided phase properties.

Experimental

The ASA used as support are denoted SiXAlY where X and Y represent the weight % in SiO_2 and in Al_2O_3 respectively. Mo and NiW catalysts were prepared by incipient wetness impregnation of salt precursors, dried at 393 K and calcined at 773 K under air.

For IR characterization, the samples were pressed under the form of a disc and activated in situ in the cell. Surface properties of pure ASA were studied after evacuation at various temperatures. Catalysts were characterized after sulfidation under a flow of H_2S(15%vol)/H_2 at 623 K (for Mo catalysts) or 723 K (for W-based catalysts) followed by an evacuation at the same temperature. After activation, acidity of surface sites of the support and of the sulfided phase was characterized by CO adsorption at 100 K. IR spectra are recorded on a Magna Nicolet using a MCT/A detector.

Activity of sulfided NiW catalysts supported on ASA and alumina were tested for the transformation of a feed composed of 74% cyclohexane, 20% toluène and 6% DMDS. The reaction was performed at 623 K under 60 bars with a VVH of 2 h^{-1}.

Results and Discussion

On ASA, CO adsorption shows the presence of two types of Lewis acid sites which present a very strong and a weak acidity (Figure 1). They are attributed to vacancies situated on surface Al(IV) or on surface Al(IV)Al(VI) respectively. Silanol groups are also present on ASA surface. These SiOH groups exhibit mainly a very weak acidity equivalent to that detected on pure silica (type C). However, a small amount of these silanol groups show an acidity as strong as that measured on Hβ zeolite (site A) and on partially exchanged NaY zeolite (site B). These specific OH groups should correspond to silanol groups situated close to an Al atom [2,3]. Results obtained on various ASA show that the Al situated in the vicinity of the silanol should be in a tetrahedral environment. Structures for sites A and B are proposed [4] taking into account the localisation of this Al (surface or bulk) and the number of Al(IV) in the neighbouring of the SiOH. These two types of sites are detected on all the studied ASA but their number increases with SiO_2 content.
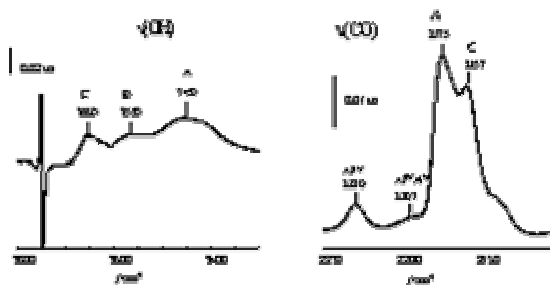
**Figure 1** : IR spectra of CO adsorbed (130μmol.g^{-1}) on Si88Al12 activated at 723 K (difference spectra).

After sulfidation of the NiW catalyst, ν(CO) bands specific of coordinative unsaturated sites of the NiW phase are detected at 2135 and 2080(sh) cm^{-1} on the NiW/Si40Al60. The detection of a band at 2108 cm^{-1} indicates that part of the Ni is not in promotion. Similar features are observed for all the studied catalysts. As presented on Figure 2, the ν(CO/NiWS) values vary according to the ASA acidity i.e. the frequency increase with the number of strong acidic OH groups of the ASA. Extention to supports presenting various acidity confirms this sensitivity. Similar trends are also observed in the case of Mo-based catalysts. These results provide evidence for the influence of the acidity of the support on the adsorptive properties of the sulfided phase.
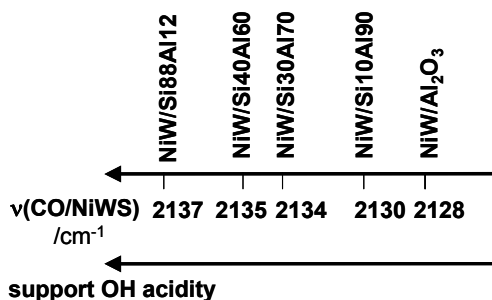
Figure 2 : Variation of the ν(CO/NiWS) frequency for NiW sulfided catalysts supported on oxides presenting various acidity.

On NiW catalysts, catalytic tests show that cyclohexane isomerisation and toluene hydrogenation activities are higher for catalysts supported on ASA than on alumina (Figure 3). Comparison with IR results show that isomerisation activity depends on the number of the most acidic OH groups. Moreover, a linear relationship between CO wavenumber in interaction with the NiW phase and activity for cyclohexane isomerisation is observed (Figure 3). It is concluded that the wavenumber of CO in interaction with the sulfided phase is a good indicator of the global acidity of the support.

Parallel between IR spectroscopy and toluene hydrogenation points out that the catalyst activity depends both on the number of CUS sites of the sulfided phase and also on the "quality" of these sites which is modified by the support acidity.
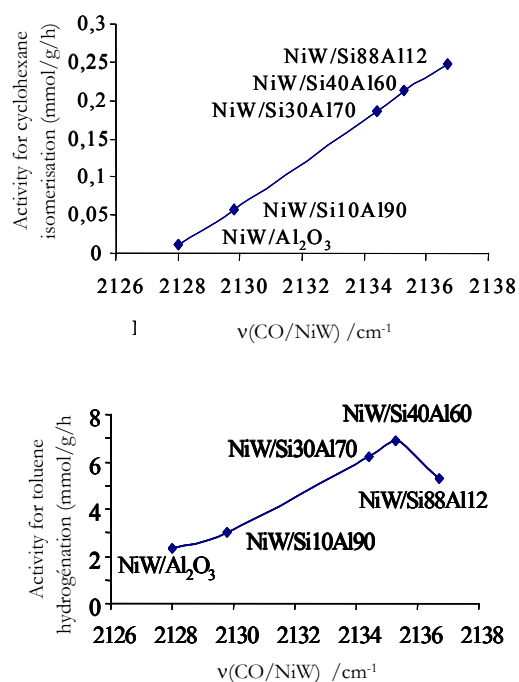
Figure 3 : Activity for cyclohexane isomerisation and toluene hydrogenation versus the wavenumber of CO in interaction NiW sulfided phase deposited on various supports.

Conclusion

This study provides evidence for the influence of the acidity of the support on the adsorptive properties as well as on the reactivity of the sulfided phase.

References

1 P. Marion, D. Duee and E. Benazzi, *Petroleum Technology Quaterly*, summer 2001, page 23.
2 O. Cairon, Th. Chevreau, J.C. Lavalley, *J. Chem. Soc., Faraday Trans.*, 94, 3039 (1998).
3 M. Trombetta, G. Busca, S. Rossini, V. Piccoli, U. Cornaro, A. Guercio, R. Catani, R.J. Willey, *J.Catal.*, 179, 581 (1998).
4 G. Crepeau, PhD Thesis, University of Caen, 2002.

Effect of Methyl Groups on the HDN Activities of Indole and Quinoline

F.E. Massoth and Jack Simons*

Department of Chemical and Fuels Engineering and
*Department of Chemistry
University of Utah, Salt Lake City, UT 84112

Introduction

Catalytic hydrotreating has become an important process for removal of sulfur and nitrogen from petroleum due to increasing environmental constraints. Heterocyclic compounds containing sulfur and nitrogen are relatively stable structures requiring high temperatures and high hydrogen pressures for removal of sulfur and nitrogen.

A number of studies have shown that methyl groups on C-atoms adjacent to the S-atom resulted in lower HDS activity, although only limited studies have been reported on the effect of alkyl substituents on HDN reactivity of N-heteroatom compounds (1).

The HDN of heterocyclic nitrogen compounds generally involves the following reactions: (1) hydrogenation of nitrogen heterorings, (2) hydrogenation of adjacent aromatic rings, and (3) C-N bond cleavage. The aim of the present study was to determine the effect of methyl substituents on the above reactions for indole and quinoline. The numbering systems for these compounds are shown below.
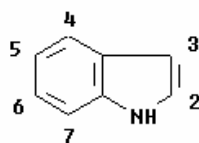
indole
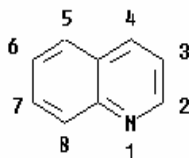
quinoline

Experimental

The catalysts used was Topsøe TK-555, which consisted of 3.8% NiO, and 24% MoO_3 supported on alumina containing 2% phosphorous ($160 m^2/g$). Reactions were carried out in a fixed-bed reactor under vapor-phase conditions at 613 K and 3.1 MPa H_2. Liquid feeds consisted of 0.5 wt% of indole or quinoline or their methyl-substituted analogs.Further details are given elsewhere (2,3).

Results and Discussion

Figures 1 and 2 display reaction pathways for the HDN of indole and quinoline. We assume the same apply to the methyl analogs. For all reactants, equilibrium between the parent and its N-ring hydrogenated structure was rapidly achieved. For indole, the equilibrium lies heavily to the left and thus favors the parent compound, while for quinoline, the opposite is true. This equilibrium was also significantly affected by the position of the substituent methyl group, generally suppressing the ratio when methyl groups are on the N-ring (Figure 3).

Subsequent reaction of equilibrium mixtures to intermediate and final products (overall conversion) was also affected by the position of the substituent methyl group. Methyl groups on the N-ring substantially lowered this conversion (except for 2-methylquinoline, which was higher). On the other hand, methyl groups on the aromatic ring had little effect. Similar trends were obtained for HDN.

The reaction of equilibrium mixtures followed two pathways, viz a CNH path (C-N bond cleavage) and a HYD path (aromatic and N-ring hydrogenation). The relative ratios of the HYD/CNH paths were also affected by the methyl group position. The CNH path leading to OEA or OPA was suppressed by methyl groups on the N-ring, and slightly augmented with methyl groups on the aromatic ring; whereas the HYD path to indole hydrogenated products or DHQ was hardly affected by methyl groups.

The quinoline network has an additional important pathway not found for indole, that is, hydrogenation of the aromatic ring in quinoline to THQ5. Compared to hydrogenation to THQ1, this contribution is small. However, it becomes more significant in quinolines in which methyls are in N-ring positions. Since the latter also result in lower equilibrium ratios (THQ1/Q), the lower reactivities appear to be a manifestation of the equilibrium properties, rather than differences in intrinsic rates due to methyl position.

Structural (computational) chemistry calculations of ionization potentials of the methyl-substituted HIND's and THQ1's performed made in order to compare to their respective equilibrium ratios. Reasonably good correlations were obtained in both cases, suggesting that the transition state complex is in the hydrogenated form.

Calculations were also performed relating initial CNH rates (paths in Figs. 1 and 2) to electrostatic potentials on the N atom of the methyl-substituted HIND's and THQ1's, and relating initial HYD rates to ionization potentials. Again, reasonably good correlations were obtained in both cases.

These correlations are in line with the expected properties of the active catalytic sites responsible for hydrogenation and C-N bond cleavage reactions, namely hydrogenation is related to ionization potentials, while bond cleavage is related to the property of the N atom. This would seem to imply that adsorption of the molecule on the active site is via pi bonding during hydrogenation, and adsorption via the N atom for C-N bond cleavage.
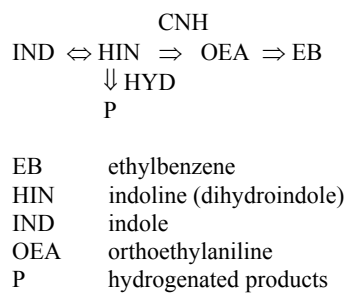
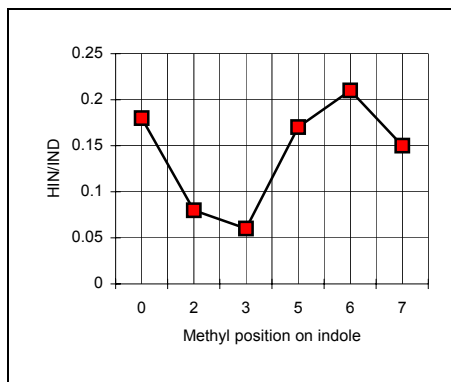Results will be compared to those obtained with a $CoMo/Al_2O_3$ catalyst.
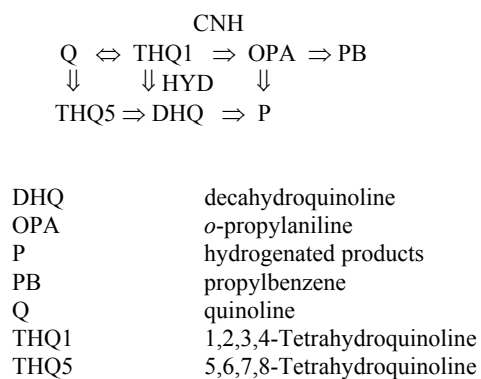
Acknowledgement

References

(1) Topsøe, H; .Clausen, B.S.; Massoth, F.E., Catalysis-Science and Technology, (J.R. Anderson and M. Boudart, eds.), Springer, New York, 1996.
(2) Kim, S.C.; Massoth, F.E., J. Catal. **2000**, *189*, 70.
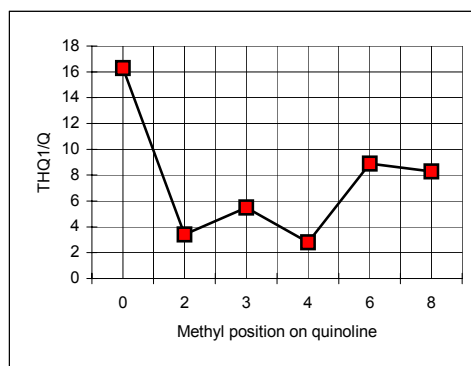(3) Kim, S.C.; Simons, Jack; Massoth, F.E., J. Catal. in press

```
              CNH
IND  ⇔ HIN   ⇒   OEA  ⇒ EB
         ⇓ HYD
         P
```

EB   ethylbenzene
HIN   indoline (dihydroindole)
IND   indole
OEA   orthoethylaniline
P   hydrogenated products

Figure 1. Indole reaction network

```
              CNH
   Q   ⇔ THQ1   ⇒  OPA  ⇒ PB
   ⇓        ⇓ HYD       ⇓
   THQ5 ⇒ DHQ   ⇒  P
```

DHQ   decahydroquinoline
OPA   *o*-propylaniline
P   hydrogenated products
PB   propylbenzene
Q   quinoline
THQ1   1,2,3,4-Tetrahydroquinoline
THQ5   5,6,7,8-Tetrahydroquinoline

Figure 2. Quinoline reaction network

Figure 3a. Equilibrium ratios for methylindoles.

Figure 3b. Equilibrium ratios for methylquinolines.

Effect of Methyl Groups at 4- and 6-Positions on Adsorption of Dibenzothiophenes over CoMo and NiMo Sulfide Catalysts

Xiaoliang Ma, Jae Hyung Kim, Chunshan Song

Clean Fuels and Catalysis Program, The Energy Institute, and Department of Energy & Geo-Environmental Engineering, Pennsylvania State University, 209 Academic Projects Building, University Park, PA 16802

Introduction

Ultra-deep hydrodesulfurization (HDS) of diesel fuel is becoming more and more important because the environmental regulations require producing ultra-low sulfur fuels (1). The major sulfur compounds existing in the current commercial diesel fuels are alkyl dibenzothiophenes (DBTs), especially those with one or two alkyl groups at the 4 and/or 6-positions, for example, 4-methyldibenzothiophene (4-MDBT) and 4,6-dimethyldibenzothiophene (4,6-DMDBT), which are difficult to remove by the conventional HDS processes (1-3).

The major challenge in ultra-deep HDS of diesel fuel is to remove such refractory sulfur compounds. In order to develop novel catalysts and to design more efficient HDS processes, it is necessary to fundamentally understand why and how the alkyl groups at the 4 and 6 positions decrease the HDS reactivity of DBTs. Some researchers attributed the refractory nature of 4,6-DMDBT to the steric hindrance towards the adsorption on the active sites (4,5). On the basis of the heats of adsorption for DBT, 4-MDBT and 4,6-DMDBT, which were obtained by measuring the parameters in a simplified Langmurir-Hinshelwood equation, Kabe and co-workers concluded that 4-MDBT or 4,6-DMDBT can be adsorbed on the catalyst through π-electrons in the aromatic rings more strongly than DBT, and the retarding effect of the methyl substitution on HDS rates of DBTs was not attributed to the inhibition of the adsorption of DBTs on the catalyst but to the steric hindrance in the C-S bond scission of the adsorbed DBTs (6,7). Recently, based on a study on the promoter effect of Co and Ni on HDS of DBTs, Bataille et al. proposed that the lower reactivity of 4,6-DMDBT compared to that of DBT measured on the promoted catalysts could not be attributed to difference in the adsorption strength of the reactants, but to a steric hindrance by the methyl groups to the adsorption of the dihydrointermediates and/or others (8). However, many explanations regarding the adsorption of DBTs are deficient in direct experimental evidence.

In the present study, we directly examined the adsorption of DBT, 4-MDBT and 4,6-DMDBT on two sulfided commercial catalysts, CoMo/alumina and NiMo/alumina, by using a liquid-phase adsorption device. The adsorption capacity and selectivity of DBTs over the two catalysts were measured and compared. We believe that such adsorption information is important for our fundamental understanding of the retarding effect of the alkyl groups at the 4 and 6-positions of DBTs on HDS.

Experimental

Two commercial catalysts, Cr344 (CoMo/Al$_2$O$_3$, CoO: 3wt%, MoO$_3$: 14wt% Suface area: 190 m^2/g) and Cr424 (NiMo/Al$_2$O$_3$, NiO: 3.0wt%, MoO$_3$: 13wt%, Surface area: 155 m^2/g,), used in the present study, were from Criterion Catalysts and Technologies. A model diesel fuel, which contains the same molar concentration of DBT, 4-MDBT and 4,6-DMDBT, was used in the adsorption experiments. 2-Methylnaphalene (2-MNaph) with the same molar concentration as the sulfur compounds was also added into the fuel for comparing adsorption selectivity. The detailed composition of the model diesel fuel with their purity is listed in Table 1. The sulfur compounds and hydrocarbons contained in the fuel were purchased from Aldrich without further treatment before use.

After presulfidation at 350 ˚C with 10 vol % H$_2$S in H$_2$ at a flow rate of 200 ml/min for 4 h, the catalysts were cooled to room temperature under the same atmosphere, and then, kept in hexane before use. The adsorption experiments were performed at ambient pressure using a liquid-phase adsorption device, including a gas control system, HPLC pump, adsorption column in a furnace and a sample collection system. The presulfided catalyst was packed into a stainless column with internal diameter of 4.6 mm and length of 150 mm. The adsorbent bed volume was 2.49 ml. Before feeding the model diesel fuel into the column, H$_2$ gas was passed through the column at 300 ˚C at a flow rate of 20 ml/min for 1.0 h, and then, the column temperature was reduced to the assigned temperature for adsorption experiment. The model diesel fuel was fed into the column and flow through the adsorption bed without using H$_2$ gas. The liquid flow rate was 0.2 ml/min. The effluent was collected for analysis using a GC-FID with a capillary column.

Results and Discussion

Figure 1 shows the molar concentration of sulfur compounds and 2-MNaph at the outlet as a function of the effluent amount for the adsorption on the NiMo catalyst at 50 ˚C and 150 ˚C, respectively. No detectable biphenyls and cyclohexylbenzenes were found in the effluent, indicating no HDS reaction takes place at such conditions. At 50 ˚C, the first break-through compound is 2-MNaph with a break-through point at ~0.2 g/g and a saturation point at ~1.6 g/g. The second one is 4,6-DMDBT with a break-through point at ~0.4 g/g. The concentration of 4,6-DMDBT kept below 0.2 mmol/l before the effluent volume reached 2.5 g/g, and then, increased to the saturation point at ~4.4 g/g. Break-through point of 4-MDBT is at 2.5 g/g with a saturation point at ~5.0 g/g. The last break-through compound is DBT with a break-through point at ~3.5 g/g and a saturation point at > 5.5 g/g. It is clear that DBTs exhibit much higher adsorption selectivity than 2-MNaph, indicating that the adsorption of DBTs on the NiMo catalyst not only depend on the interaction through π-electrons on aromatic ring but also depend on the interaction through the S atom in DBTs. As is well known, 2-MNAPH has higher π-electron

density on its aromatic ring than that of DBTs (9), although the aromatic ring size of the former is smaller than that of the latter. However, DBTs exhibit much higher adsorption selectivity, which indicates that interaction between the S atom and the adsorptive sites play an important role in the adsorption of DBTs. Furthermore, by comparing DBT, 4-MDBT and 4,6-DMDBT, the increases of adsorption selectivity in the order of 4,6-DMDBT < 4-MDBT < DBT implies that the methyl groups at the 4 and 6-positions inhibit the interaction between the S atom in DBTs and the active sites on the catalyst, which results in the decrease of adsorption capacities of 4,6-DMDBT and 4-MDBT on the catalyst.

The adsorption capacities corresponding to the saturation point of 4,6-DMDBT, 4-MDBT and DBT were calculated on the basis of data in Figure 1, being ~ 0.062, ~0.064, and ~0.068 mmol/g, respectively. It indicates that at least one tenth of the adsorptive sites on the catalyst are able to adsorb DBT, but fail to adsorb 4,6-DMDBT due to the steric hindrance of the methyl groups at the 4 and 6- positions.

When the column temperature was increased to 150 ˚C, the adsorption selectivity shows the same order: 2-MNAPH < 4,6-DMDBT < 4-MDBT < DBT, which confirms further the effect of the methyl groups on the adsorption of DBTs on the NiMo catalyst. Figure 1 also clearly shows that the adsorption capacity decreases at 150˚C in comparison with that at 50 ˚C. The saturated adsorption capacity for the total sulfur on the NiMo catalyst is 0.068 and 0.045 mmol/g, respectively, at 50 and 150 ˚C. This result confirms further that the low sulfur concentration in the effluent is because the surface adsorption instead of surface reaction. On the other hand, the effect of temperature on the adsorption capacity, observed in the present study, also implies that the adsorption might be weak and reversible.

Figure 2 shows the molar concentration of sulfur compounds and 2-MNaph at the outlet as a function of the effluent amount for the adsorption on the CoMo catalyst at 50 ˚C in comparison with the adsorption on the NiMo catalyst at the same temperature. It was found that the CoMo catalyst exhibits the break-through curves and selectivity similar to those of the NiMo catalyst. However, the CoMo catalyst has higher adsorption capacity than the NiMo catalyst for all examined species, probably because higher surface area of the former than that of the latter. The higher adsorption capacity of the CoMo catalyst indicates it has more adsorption sites on the surface.

In the HDS kinetic study (10), we found that the NiMo catalyst is more active than the CoMo catalyst for HDS of 4,6-DMDBT. If assuming that the HDS takes place at the same sites, the higher activity of the NiMo catalyst than the CoMo catalyst might not be attributed to the number of the active sites but the turnover frequency of the active sites. In general, HDS reactivity (rate constant) of 4,6-DMDBT over CoMo catalysts is lower than that of DBT by more than an order magnitude. However, the effect of the methyl groups at 4 and 6-positions on the adsorption of DBTs is weaker in comparison with their

effect on the HDS rate. It might indicate that 1) not all of the adsorptive sites are related to the active sites for HDS reaction, and/or 2) the effect of the steric hindrance by the methyl groups on the adsorption of DBTs is one of the factors but not the only factor that retard the HDS rate of 4,6-DMDBT.

References
1. Song, C. , Ma, X. Appl. Catal. B: Env. 2003, 40 (4) in press; Song, C. Am. Chem. Soc. Div. Fuel Chem. Prep., 47(2), 438-444 (2002).
2. Ma, X., Sakanishi, K,, Mochida, I. Ind. Eng. Chem, Res. 33, 218 (1994).
3. Gates, B.C., Topsoe, H. Polyhedron 16, 3213 (1997).
4. Ma, X., Schobert, H. H. Prepr., Div. Pet. Chem., Am. Chem. Soc. 42, 657-661 (1997).
5. Shafi, R., Hutchings, G. J. Catal. Today, 59, 423-442 (2000).
6. Kabe, T., Ishihara, A., Zhang, Q. Appl. Catal. A 97, L1-L9 (1993).
7. Zhang, Q., Ishihara, A., Kabe, T. Sekiyu Gakkaishi, 39, 410-417 (1996).
8. Batail, F., Lemberton, J., Michaud, P., Perot, G. Vrinat, M., Lemaire, M., Schulz, E. Breysse, M., Kasztelan, S. J. Catal. 191, 409-422 (2000).
9. Ma, X., Sakanishi, K,, Isoda, T., Mochida, I. Energy & Fuels 9, 33-37 (1995).
10. Kim, J. H., Ma, X., Song, C. Prepr., Div. Pet. Chem., Am. Chem. Soc. , 48 (1), in press (2003).

Table 1 Composition of Model Diesel Fuel

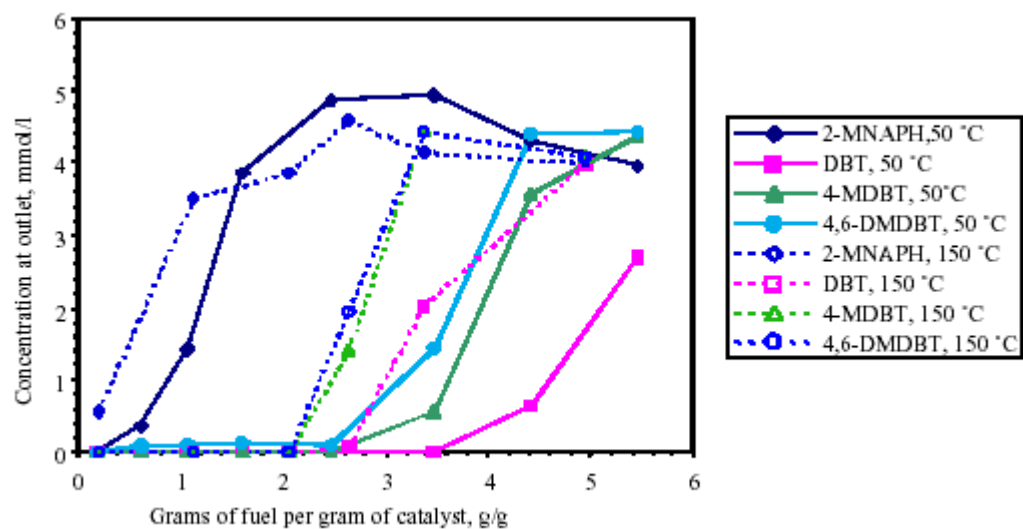| No.	name	concentration	
		wt %	mmol/l
1	DBT(99+%)	0.095	3.97
2	4-MDBT(96%)	0.102	3.97
3	4,6-DMDBT(97%)	0.109	3.97
4	Naphthalene (99%)	0.067	3.97
5	2-methylnaphthalene (98%)	0.074	3.97
6	n-Hexadecane(99+%)	39.965	
7	n-Dodecane(99+%)	39.500	
8	n-Tetradecane (99+%)	0.109	
9	Decalin(99+%)	9.988	
10	t-Butylbenzene(99%)	9.988	

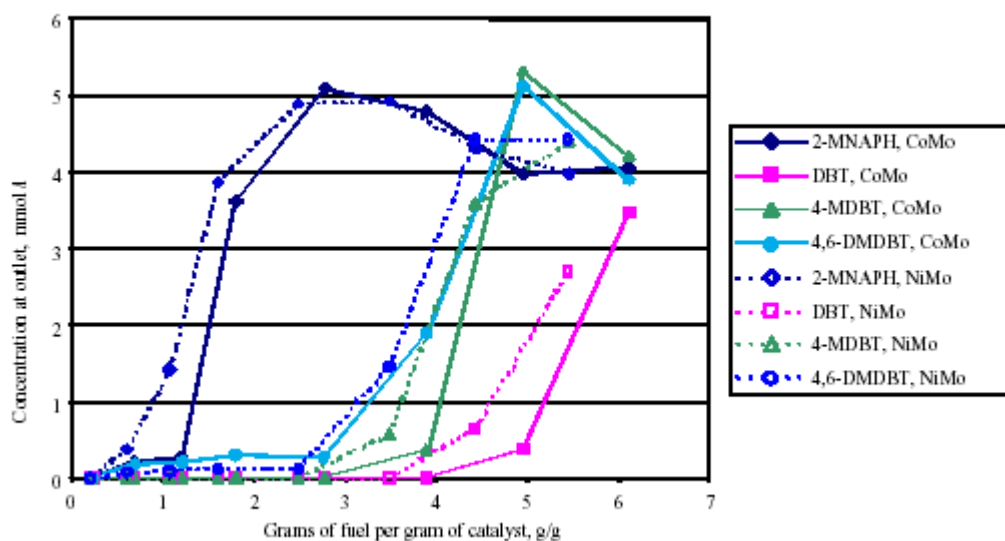Figure 1. Adsorption profile of DBTs on the NiMo catalyst.

Figure 2. Adsorption profile of DBTs on CoMo and NiMo catalysts at 50 °C.

ADSORPTIVE REMOVAL OF SULFUR AND NITROGEN SPECIES FROM A STRAIGHT RUN GAS OIL FOR ITS DEEP HYDRODESULFURIZATION

YOSUKE SANO, KI-HYOUK CHOI, YOZO KORAI

and ISAO MOCHIDA*

Institute of Advanced Material Study, Kyushu University,

Kasuga-koen, Kasuga, Fukuoka 816-8580 JAPAN

*mochida@cm.kyushu-u.ac.jp

INTRODUCTION

World refining industry is facing new and stricter challenges on the heteroatom content in their major products, such as diesel fuel and gasoline. The sulfur content of diesel fuel must be lowered to 15 ppmS from current 500 ppmS and even further regulations may be implemented with accelerated concerns on the atmospheric pollution[1]. Several kinds of new ideas have been proposed and some of them were practically examined to achieve the ultra deep desulfurization. However, more efficient and economic process is still being required in spite of various efforts. Critical barriers in achieving ultra deep desulfurization are refractory sulfur species, which have very low reactivity, and inhibitors such as H_2S, NH_3 and nitrogen species under conventional hydrotreating conditions. The inhibitors retard the desulfurization reaction, very markedly in ultra deep region [2, 3]. There are some suggestions on the pre-treatment of gas oil to remove nitrogen species prior to hydrodesulfurization [4,5]. However, detailed accomplishment of the suggestions has not been clarified yet

Activated carbon and activated carbon fiber have been known to be versatile absorbents of gaseous and liquid molecules. Its surface and properties can be easily controlled.

In this study, sulfur and nitrogen species were removed from straight run gas oil (SRGO) through adsorption by activated carbon materials and treated oil was examined in conventional hydrodesulfurization reaction to evaluate the effects of pre-treatment on the HDS activity.

EXPERIMENTAL

I. ASORPTION

Straight run gas oil (11,780 ppmS and 260 ppmN) used in this study was provided by a japanese commercial refinery. Carbon materials (activated carbons and activated carbon fibers), which were dried at 110 °C under vacuum oven prior to adsorption experiment, were packed into the stainless steel tube of 50 mm length and 6 mm diameter. Key properties of carbon materials were listed in Table 1. SRGO was fed into the tube by an HPLC pump at the rate of 0.1 ml/min and at the pressure of 20 psig. The temperature of the adsorption reactor was maintained at 10 - 40 °C by water bath. The eluted oil was sampled at every 10 min for 30 sec and analyzed by GC-AED (Atomic Emission Detector, HP5890P, and G2350A).

II. HDS REACTION

The eluted oil was hydrodesulfurized with commercial catalysts in autoclave-type reactor (100 ml internal volume). 10 g oil, 1 g catalyst, which was pre-sulfided by 5% H_2S/H_2 at 360 °C for 2 hours, and 50 kg/cm^2 hydrogen gas were charged into the reactor. The temperature of the reactor was raised to 340 °C by 50 min and maintained at that temperature for 2 hours. The HDS product was sampled through filter fitted in reactor. and analyzed by GC-AED.

RESULTS AND DISCUSSION

Fig. 1 showed carbon-, sulfur-, nitrogen-specific chromatograms of SRGO feed. Most of the sulfur species in SRGO were benzothiophenes (BT), dibenzothiophenes (DBT). Quinolines, indoles, and carbazoles were found in nitrogen-specific chromatogram of feed gas oil.

Sulfur and nitrogen species removal depended on the types of carbon materials as shown in Fig. 2. MAXSORB-II, which has the largest surface area and oxygen content, showed the largest capacity for sulfur and nitrogen species. Fig. 3 showed that breakthrough time for nitrogen species was much longer than that for sulfur species over MAXSORB-II. The other carbon materials exhibited the same trend with that of MAXSORB-II. Breakthrough points for sulfur and nitrogen contents were estimated to be around 40 and 240 ml-oil/g-absorbent, respectively over MAXSORB II. The calculated capacities of sulfur and nitrogen until breakthrough point were to be 0.095 g-sulfur and 0.029 g-nitrogen/g-absorbent, respectively. The relative affinity for adsorption of nitrogen and sulfur species depended on their size and molecular weight as indicated in Fig.4; DBT was eluted earlier than MDBT and DMDBT.

Carbon materials were regenerated by flowing toluene and drying it at 250 °C. As can be seen in Fig. 5, regenerated MAXSORB-II showed almost similar capability for nitrogen and sulfur removal to that of virgin MAXSORB- II. Small difference between them at the range of 20 - 80 ml-oil/g-absorbent could be suggested due to the change of surface area and surface functional group during heat treated at 250 °C.

Nitrogen species has been reported to be one of the strong inhibitors in deep range HDS due to its competition with sulfur species for the same active site. HDS products of nitrogen species removed SRGO showed much lower sulfur content. When 70% of nitrogen species was removed, attainable sulfur level was 11 ppmS while 180 ppmS for mother SRGO. Sulfur content of product oil was almost proportional to that of nitrogen in the feed, although the latter content of 39ppm allowed deep desulfurization less than 6ppm-sulfur. From this result, it is clear that partial removal of nitrogen species from SRGO is very effective to achieve sulfur content lower than 10 ppmS by using current catalyst and process conditions. Some of the activated carbon appears feasible on its capacity and rate of nitrogen removal for practical application.

CONCLUSIONS

Carbon material could be applied as an absorbent bed for the removal of sulfur and nitrogen species of gas oil. Adsorption capacity of carbon materials depended on the textural and surface properties of them. Nitrogen species removed gas oil showed significant enhancement of desulfurization.

REFERENCES

1. Halbert, T. R.; Brignac, G. B.; Demmin, R. A.; Roundtree, E. M. *Hydrocarbon Engineering*, June, **2000,** *2*.
2. Whitehurst, D. D.; Isoda, T.; Mochida, I. *Adv. Catal*., **1998,** *42***,** 345.
3. Whitehurst, D. D.; Farag, H.; Nagamatsu, T.; Sakanishi, K.; Mochida, I. *Catal. Today*, **1998,** *45***,** 299.
4. Zeuthen, P; Knudsen, K.G.; Whitehurst, D. D. *Catal. Today*, **2001**, *65,* 307.
5. Min, W-S et. al., U.S.patent 6,248,230, **2001**.

Table 1. The characteristics of carbon materials

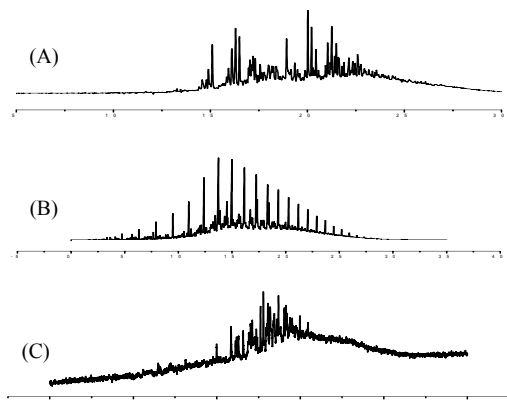| Carbon materials	C/H/N/O(%)	Surface area (cm^2/g)	Total pore volume (cm^3/g)
MAXSORB-II	85/0.49/0.14/14.16	2972	1.75
OG-20A	93.83/0.69/0.25/5.15	2000	1.1
MGC-B	80.11/0.6/3.23/7.27	683	0.59

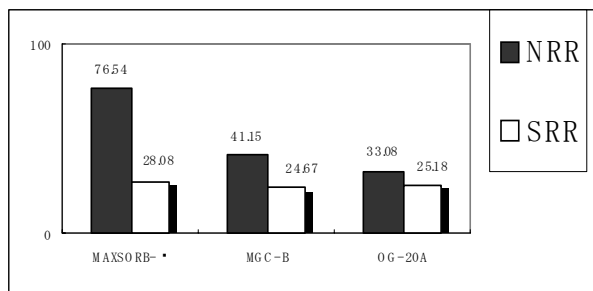Figure 1. (A) sulfur-, (B) carbon, and (C) nitrogen-specific chromatograms of SRGO

Figure 2. Nitrogen and sulfur removal ratio of carbon materials at 30 ^{o}C. Oil=72ml, adsorbent=0.3g
*NRR=Nitrogen removal Ratio (%)
*SRR=Sulfur Removal Ratio (%)
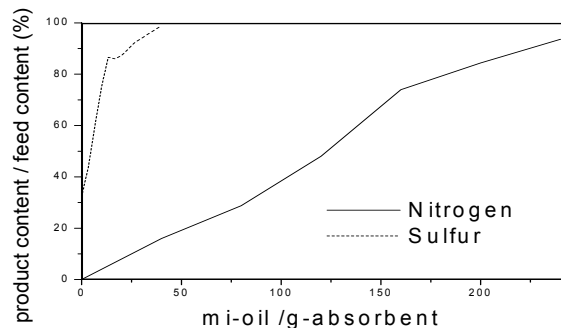
Figure 3. Sulfur and nitrogen breakthrough profile of SRGO on MAXSORB-II at 30 ^{o}C.
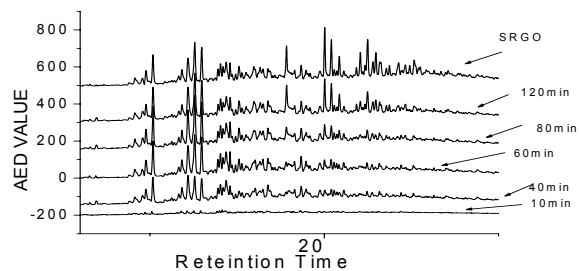
Figure 4. Sulfur-specific chromatograms of eluted SRGO from MAXSORB-II at 30 ^{o}C.
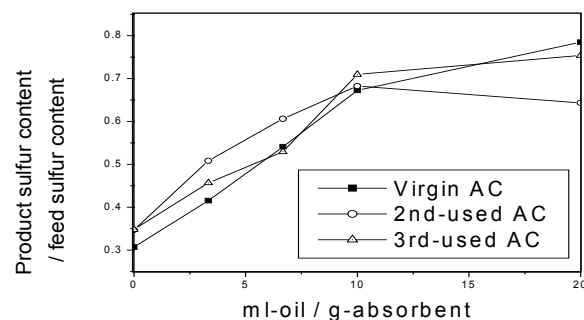
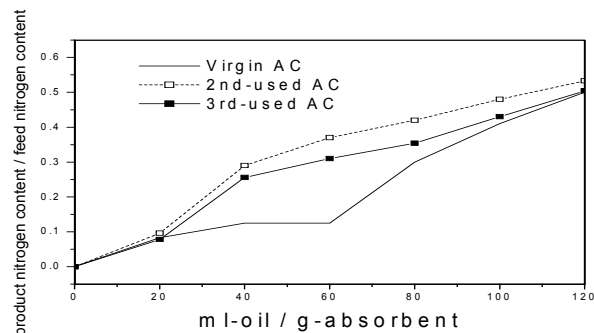Figure 5-A. Sulfur breakthrough profiles of virgin and regenerated MAXSORB-II at 30 ^{o}C.

Figure 5-B. Nitrogen breakthrough profiles of virgin and regenerated MAXSORB-II at 30 ^{o}C.
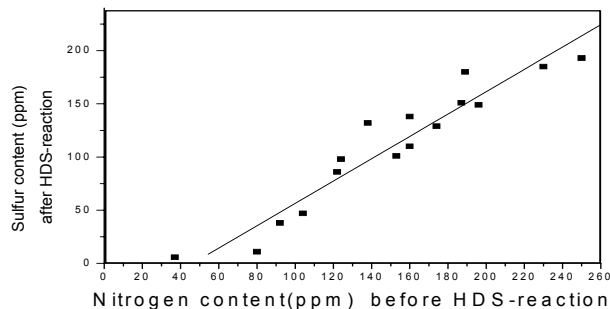

Figure 6. Plot of total sulfur content of HDS products and nitrogen content of feed gas oils.

NUCLEOPHILIC SUBSTITUTION RATHER THAN ELIMINATION IN THE HDN OF ALKYLAMINES

Y. Zhao and R. Prins

Laboratory for Technical Chemistry, Federal Institute of Technology (ETH), Zurich, Switzerland

The hydrodenitrogenation (HDN) of hexylamine, dihexylamine, and trihexylamine was studied at 300-340°C and 3-5 MPa total pressure over a sulfided $NiMo/Al_2O_3$ catalyst. The main products were hexanethiol, hexane, hexene, and disproportionation products of the alkylamines. Disproportionation occurred especially at low H_2S pressure and high alkylamine pressure. The conversions of the hexylamines increased with H_2 pressure and decreased with increasing partial pressure of the amines. The conversion of hexylamine and dihexylamine decreased slightly with H_2S pressure, but that of trihexylamine increased substantially.

The influence of the pressure of thiols, amines, and H_2S in the simultaneous HDN of alkylamines, hydrodesulfurization (HDS) of alkanethiols, and hydrogenation of alkenes was investigated as well. A high H_2S pressure promoted the substitution reaction of hexylamine to hexanethiol, but inhibited the decomposition of the resulting thiol to hexene and hexane. H_2S also strongly inhibited the hydrogenation of alkenes in the absence of amine, but less in its presence.

The simultaneous reactions of thiol and alkene in the presence of amine showed that the decomposition of thiol is much faster than the alkene hydrogenation. Therefore, alkenes, observed in the HDN of alkylamines, may not only be formed by elimination of the alkylamine, but also by substitution of the alkylamine by H_2S and decomposition of the resulting thiol.

The contributions of elimination and nucleophilic substitution to the HDN were determined from the product selectivities at short contact time. The initial alkene selectivities were low and accounted only for a minor part of the alkylamine conversion. A substantial part of this alkene even originated from the reaction of hexanethiol. These results demonstrate that the HDN of alkylamines proceeds mainly by nucleophilic substitution by H_2S and not by elimination. In accordance with this, the hexene/hexane ratio in the HDN of hexylamine was similar to the pentene/pentane ratio in the HDS of pentanethiol.

2-Methylpiperidine reacted by ring opening to 2-aminohexane rather than hexylamine. The same ring-opening pattern was observed for 2-ethylpiperidine, which demonstrates that the piperidine ring opens on the sterically less hindered side of the molecule and not on the side with the most H atoms.

This, and the small percentage of olefins formed, suggests that elimination does not play an important role in the HDN of piperidine either. In accordance with our HDN results for dihexylamine, we therefore assume that also piperidine undergoes HDN mainly by nucleophilic substitution by H_2S, followed by decomposition of the resulting alkanethiol.

TRANSITION METAL PHOSPHIDES: NEW CATALYSTS FOR HYDROPROCESSING

S. T. Oyama, Y.-K. Lee

Department of Chemical Engineering
Virginia Tech
Blacksburg, VA 24061

Introduction

Transition metal phosphides are a class of refractory metallic compounds formed from the alloying of metals and phosphorus. They have recently been shown to have excellent activity in hydroprocessing (1,2,3,4), with activity higher than sulfides for hydrodenitrogenation (HDN) and hydrodesulfurization (HDS). The materials can be prepared by the temperature-programmed reduction of phosphate precursors in bulk or supported form. A comparison of the activity of several phosphides indicates that the HDN and HDS activity at 3.1 MPa increases in the order: $Fe_2P < CoP < MoP < WP < Ni_2P$. Most of the work has been done on Ni_2P/SiO_2 because of its high activity. Analysis of the structure of the fresh catalyst by extended x-ray absorption fine structure (EXAFS) shows the presence of Ni-Ni and Ni-P distances corresponding to the bulk compound. The catalyst after reaction shows the appearance of a signal corresponding to a Ni-S distance, indicating that at high pressure the active phase is a phosphor-sulfide.

Experimental

The synthesis of the phosphide catalysts involved two steps. First, precursor phosphates were prepared by evaporating aqueous solutions of the metal nitrate, and ammonium orthophosphate $(NH_4)_2HPO_4$ (Aldrich, 99 %), followed by calcination at 773 K. Second, the precursors were reduced in a flow of hydrogen in a temperature-programmed manner using a heating rate of $\beta = 0.0167$ K s^{-1} (1 K min^{-1}), following which they were cooled in He, and passivated in 0.1% O_2/He. In the case of supported samples the phosphate precursors were prepared by impregnation of the metal nitrate and ammonium phosphate solutions onto a fumed silica (Cabosil, L90) followed by calcination. Sulfided Ni-Mo/Al$_2$O$_3$ (Shell 324) and Co-Mo/Al$_2$O$_3$ (Ketjenfine 756) were used as references. The catalysts were routinely characterized by x-ray diffraction, CO uptake, and BET surface area measurements. Irreversible CO uptake measurements, denoted here as *ex situ*, were obtained at room temperature after passivated samples were rereduced at 723 K. For the sulfide references, O_2 uptakes were measured at 195 K.

Hydrotreating activities of the samples were obtained in a three-phase trickle bed reactor for hydrodenitrogenation (HDN) and hydrodesulfurization (HDS) with a model petroleum liquid containing 2000 ppm nitrogen (quinoline), 3000 ppm sulfur (dibenzothiophene), 500 ppm oxygen (benzofuran), 20 wt.% aromatics (tetralin), and balance aliphatics (tetradecane). The operating conditions were close to industrial conditions, 3.1 MPa and 643 K, with a liquid flow rate of 5 cm^3/h and a hydrogen flow rate of 100 μmol s^{-1} (150 cm^3 min^{-1}) corresponding to a gas-liquid ratio of 9800 SCF H$_2$/barrel. The detailed description of the testing system is reported elsewhere (5). Quantities of catalysts loaded in the reactor correspond to the same amount of *ex situ* CO uptake (70 μmol). Prior to reactivity measurements, the catalyst samples were pretreated in exactly the same manner as before the *ex situ* CO uptake determinations. Hydrotreating samples were collected every two or three hours in sealed septum vials and were analyzed off-line with a gas chromatograph (Hewlett Packard, 5890A) equipped with a 0.32 mm i.d. x 50 m fused silica capillary column (CPSIL-5CB, Chrompack, Inc.) and a flame ionization detector.

The chemicals utilized in the reactivity study were dibenzothiophene (Aldrich, 99.5 %), quinoline (Aldrich, 99.9 %), benzofuran (Aldrich, 99.9 %), tetralin (Aldrich, 99.5 %) and tetradecane (Jansen Chimica, 99 %).

Results and Discussion

A more complete description of the content of this article is presented elsewhere (6). The general properties, structure, and preparation of transition metal phosphides have been described in a number of reviews (7,8). The materials have ceramic character, with high hardness and strength, but also possess metallic properties, such as conductivity. Their structure of phosphides is built up from trigonal prisms, with the phosphorus atoms surrounded by six metal atoms. Examples of structures are shown in Fig. 1. The phosphorus atoms may be isolated, or may interact to form chains or pairs (not shown).
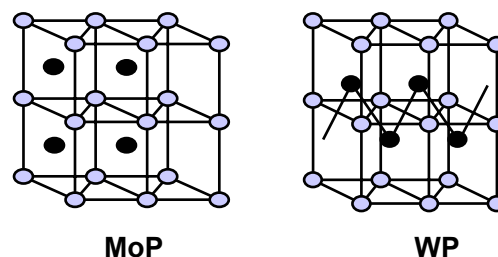

MoP   **WP**

Figure 1. Typical structures of transition metal phosphides.

Characterization of the samples by ^{31}P magic angle spinning nuclear magnetic resonance (9,10) and EXAFS (11) confirms the structural assignements. Results of characterization of the samples by surface area measurements and CO uptakes are shown in Table 1.

Table 1. Surface Area and CO Chemisorption

Catalyst	MoP	WP	Fe$_2$P/SiO$_2$ 14 wt.%[a]	CoP/SiO$_2$ 9 wt.%[b]	Ni$_2$P/SiO$_2$ 10 wt.%[b]
SA m^{2}g^{-1}	8	10	97	87	97
CO uptake μmol g^{-1}	15	10	16	16	28

[a] Metal loading = 2.31 mmol/g SiO$_2$ [b] Metal loading = 1.16 mmol/g SiO$_2$

The phosphides are stable and active catalysts for hydroprocessing (Table 2). The most active catalyst was nickel phosphide, with higher HDN and HDS than a commercial Ni-Mo catalyst sulfided *in situ*. The basis of comparison is equal sites loaded in the reactor, as measured by *ex situ* CO uptake for the phosphides and by O_2 uptake for the freshly sulfided Ni-Mo/Al$_2$O$_3$ catalyst.

Table 2. Activity in Hydroprocessing

Catalyst	MoP	WP	Fe$_2$P/SiO$_2$ 14 wt.%[b]	CoP/SiO$_2$ 9 wt.%[a]	Ni$_2$P/SiO$_2$ 10 wt.%[a]	Ni-Mo/ Al$_2$O$_3$
HDS	57	67	4.7	30	98	76
HDN	52	58	1.6	32	81	38

The Ni$_2$P/SiO$_2$ (Ni/P = 1/2) catalyst was studied with a real feed to test its performance at realistic conditions (12). The feed was a hydrotreated gas oil with low sulfur (440 ppm) and nitrogen (8 ppm) content, and moderate aromatics content (27 wt%), which mimics that which would be used in a second-stage hydrotreating process. In measurements in a trickle-flow system at 593 K and 3.9 MPa and a WHSV of 4 h^{-1}, the Ni$_2$P/SiO$_2$ compared well with a commercial Co-Mo-S/Al$_2$O$_3$, with HDS conversion of 85 % vs. 80 %.

The effect of P content on the Ni$_2$P/SiO$_2$ was studied (13) with samples prepared with initial Ni/P ratios of 2/1, 1/2, and 1/3. The best material had a Ni/P ratio of 1/2, with the other catalysts showing lower HDS and, especially, HDN. Elemental analysis showed that the actual Ni/P ratio after preparation was closer to the stoichiometric value of 2/1 due to volatilization of the P during reduction.
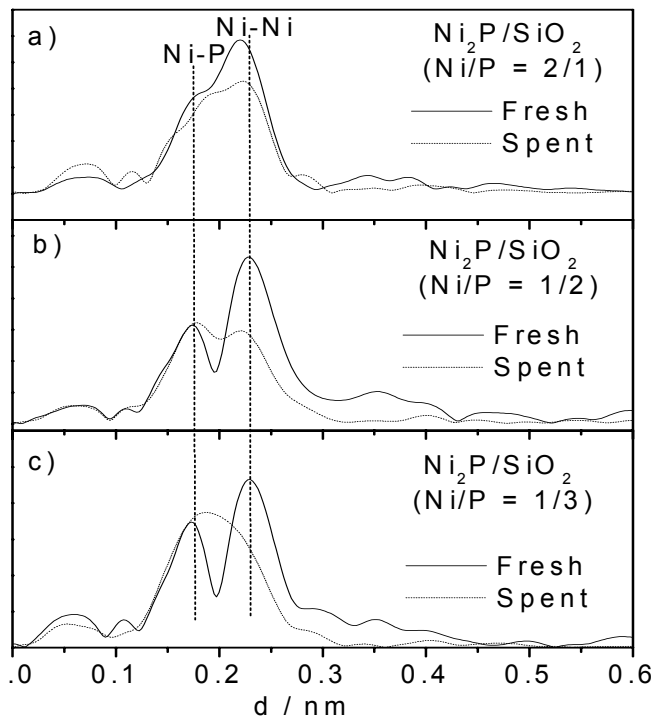
Figure 2. Nickel K-edge EXAFS of the fresh and spent samples with different Ni/P ratios: a) Ni/P = 2/1, b) Ni/P = 1/2, c) Ni/P = 1/3. The Ni/P ratios indicated are initial values. (Ref. 13)

Figure 2 compares the Ni K-edge EXAFS spectra of the fresh and spent samples. For the fresh materials, the sample with initial Ni/P = 2/1 (Fig. 2a) shows a main peak with a shoulder at lower interatomic distance. In contrast, the samples with initial Ni/P = 1/2 and 1/3 (Fig. 2b,c) display two distinct peaks. Comparison with a reference Ni$_2$P sample shows good agreement in the Ni-Ni and Ni-P distances. There is no such agreement with the features of NiO, Ni(OH)$_2$, and Ni metal, and this demonstrates that the predominant phase in these two supported catalysts is Ni$_2$P. For the sample with the initial Ni/P ratio of 2/1 (Fig. 2a) the Ni-P peak is reduced to a shoulder and the Ni-Ni peak shifts to the position of metallic Ni. Clearly, the amount of Ni$_2$P phase is smaller, as expected from the spreading of the metal and phosphorus components on the surface of the support, and this explains the low activity. With the Ni$_2$P/SiO$_2$ sample with the excess phosphorus (Initial Ni/P = 1/3), the EXAFS peak positions duly correspond to those of bulk Ni$_2$P. However, the intensity of the Ni-P relative to the Ni-Ni peak is now increased over that of bulk Ni$_2$P. The extra phosphorus probably resides on the surface of the highly dispersed particles, breaking up the catalytically active ensembles and again reducing activity.

For the spent catalysts, changes occurred after reaction. For the spent sample with initial Ni/P = 2/1, a small feature appears in between the main Ni-Ni peak and the Ni-P shoulder (Fig. 2a). For the spent sample with initial Ni/P = 1/2, the two-peak structure is retained, but there is a reduction in the Ni-Ni peak intensity (Fig. 2b). For the spent sample with initial Ni/P = 1/3, the Ni-Ni peak is almost entirely attenuated and a broad feature at lower interatomic distance appears (Fig. 2c). Clearly, in all cases there is disruption of the original Ni$_2$P phase, and this is likely due to the formation of sulfur compounds. The identification of the changes occurring in the spent samples was carried out by comparing their spectra to those of bulk sulfide references (13).

Conclusions

Transition metal phosphides constitute a new class of catalysts for hydrotreating that differ substantially from sulfide materials. The activity of the phosphides in HDS and HDN follows the order: Fe$_2$P < CoP < MoP < WP < Ni$_2$P. The most active material is Ni$_2$P/SiO$_2$, which compares favorably with commercial sulfided Ni-Mo/Al$_2$O$_3$ and Co-Mo/Al$_2$O$_3$ catalysts. Phosphorus content has a profound effect on the structure and activity of Ni$_2$P/SiO$_2$ catalysts. Samples prepared with initial ratios of Ni/P $\approx$ 1/2 result in a material with close to stoichiometric proportions of P (Ni/P = 1/0.5) with excellent activity in hydroprocessing. Characterization of the catalysts by EXAFS measurements before and after reaction indicates that the active phase in the catalysts is a phospho-sulfide. Overall results indicated that on these novel, high activity hydroprocessing catalysts, the HDS and HDN reactions are not promoted by nickel on its own, but that phosphorus plays an important role in the reaction.

References

(1) Robinson, W. R. A. M.; van Gastel, J. N. M.; Korányi, T. I.; Eijsbouts, S.; van Veen, J. A. R.; and de Beer, V. H. J., *J. Catal.* **1996**, 161, 539.
(2) Li, W.; Dhandapani, B.; Oyama, S. T., *Chem. Lett.* **1998**, 207.
(3) Stinner, C.; Prins, R.; Weber, T., *J. Catal.* **2000,** 191, 438.
(4) Phillips, D. C.; Sawhill, S. J.; Self, R.; Bussell, M. E., *J. Catal.* **2002,** 207, 266.
(5) Ramanathan, S.; Oyama, S. T., *J. Phys. Chem.*, **1995**, 99, 16365.
(6) Oyama, S. T., *J. Catal.* **2002**, In press.
(7) Aronsson, B., Lundström, T., Rundqvist, S., *Borides, Silicides and Phosphides*, Methuen, London and Wiley, New York, 1965.
(8) Corbridge, D. E. C., *Studies in Inorganic Chemistry*, Vol. 10, 4th Ed., Elsevier, Amsterdam, 1990.
(9) Clark, P.; Wang, X.; Oyama, S. T., *J. Catal.* 207, 256 (2002).
(10) Stinner, C.; Tang, Z.; Haouas, M.; Weber, Th.; Prins, R., *J. Catal.* **208**, 456 (2002).
(11) Oyama, S. T.; Clark, P.; Wang, X.; Shido, T.; Iwasawa, Y.; Hayashi, S.; Ramallo-López, J. M.; Requejo, F. G., *J. Phys. Chem.* 106, 1913 (2002).
(12) Oyama, S. T.; Wang, X.; Requejo, F. G.; Sato, T.; Yoshimura, Y., J. *Catal.* **209**, (2002).
(13) Oyama, S. T.; Wang, X.; Lee, Y.-K.; Requejo, F. G., *J. Catal.* **210**, 207 (2002).

NEW CATALYSTS FOR HYDRODESULFURIZATION: CARBIDES, NITRIDES AND PHOSPHIDES

Mark E. Bussell, Stephanie J. Sawhill,
Kathryn A. Layman, Autumn W. Burns

Dept. of Chemistry, MS-9150,
Western Washington University
Bellingham, WA 98225

Introduction

Concerns for the environment both in the United States and abroad have led to new regulations which will require dramatically lower sulfur levels in fuels. Considerable effort has been devoted to optimizing molybdenum sulfide-based hydrodesulfurization (HDS) catalysts and nearly a two-fold increase in catalyst activity has been achieved over the last thirty years.[1] When the requirement for lower sulfur levels in fuels is coupled with the need to process lower quality petroleum feedstocks, incremental improvement of the current sulfide-based HDS catalysts may not be sufficient to meet industry needs.

An approach to the development of new HDS catalysts we are exploring is to investigate how main group elements other than sulfur modify the catalytic properties of molybdenum (and other transition metals). Studies in a number of laboratories over the past few years have shown oxide-supported molybdenum carbide ($\exists$-Mo_2C)[2-4] and nitride (($-Mo_2N$)[3-7] to be more active HDS catalysts than conventional sulfided molybdenum catalysts. More recently, a few studies have appeared which show that silica-supported molybdenum phosphide (MoP)[8,9] and nickel phosphide (Ni_2P)[10-13] also demonstrate excellent potential for use as HDS catalysts.

In the current study, we describe the synthesis, characterization and HDS evaluation of a number of monometallic and bimetallic carbide, nitride and phosphide catalysts in oxide-supported form. Careful attention has been paid to the role of catalyst pretreatment in determining HDS activity, and the stability of the different catalytic materials under reaction conditions has been investigated.

Experimental

Catalyst Synthesis. Alumina-supported monometallic and bimetallic carbide and nitride catalysts were prepared as described elsewhere.[3,4,14] The syntheses involved carburization or nitridation of alumina-supported oxidic precursors in a CH_4/H_2 mixture or NH_3, respectively, using the temperature-programmed reduction (TPR) method. Silica-supported molybdenum carbide and nitride catalysts were prepared similarly.

Cobalt-promoted molybdenum carbide (Co-Mo_2C/Al_2O_3) catalysts, as well as oxidic precursors (Co-MoO_3/Al_2O_3) of sulfided Co-Mo/Al_2O_3 catalysts were prepared as follows. Promoted catalysts with theoretical molar ratios in the range $Co/Mo = 0.15$ - 1.5 were prepared by impregnation of MoO_3/Al_2O_3 and Mo_2C/Al_2O_3 catalysts with aqueous cobalt (II) nitrate ($Co(NO_3)_2 \bullet 6H_2O$). The Co-MoO_3/Al_2O_3 and Co-Mo_2C/Al_2O_3 catalysts were then transferred to a vacuum desiccator and vacuum dried overnight at room temperature. Following drying, the catalysts were passivated by back-filling the vacuum desiccator with 1 atm of a 1 mol% O_2/He mixture for 2 h. The Co-Mo_2C/Al_2O_3 catalysts were not calcined following Co promotion to avoid oxidation of the supported β-Mo_2C particles. So that the catalyst preparation procedures were the same, the Co-MoO_3/Al_2O_3 catalysts also were not calcined following addition of the cobalt nitrate.

Silica-supported molybdenum phosphide (MoP/SiO_2) and nickel phosphide (Ni_2P/SiO_2) catalysts were prepared as described elsewhere.[9,13] Briefly, silica-supported metal phosphate-like precursors were prepared by impregnation of the support with aqueous metal salts and diammonium hydrogen phosphate (($NH_4)_2HPO_4$ followed by calcination at 773 K in air. The oxidic precursors were reduced using TPR in flowing H_2 to give the phosphide catalysts.

The oxide-supported carbide, nitride and phosphide catalysts were characterized with a variety of techniques including X-ray diffraction (XRD), X-ray photoelectron spectroscopy (XPS), transmission electron microscopy (TEM) and chemisorption measurements. The details of these measurements have been described elsewhere.[3,9,13,14] Hydrodesulfurization activity measurements were carried out at 643 or 693 K using a feed consisting of 3.0 mol% thiophene (C_4H_4S) in H_2.[3,9]

Results and Discussion

The successful synthesis of the oxide-supported carbide, nitride and phosphide catalysts was verified using XRD and TEM. Shown in **Figures 1** and **2** are XRD patterns for a series of Ni_2P/SiO_2 catalysts with increasing Ni_2P loadings and a TEM image showing a Ni_2P particle on a 25 wt% of Ni_2P/SiO_2 catalyst, respectively.
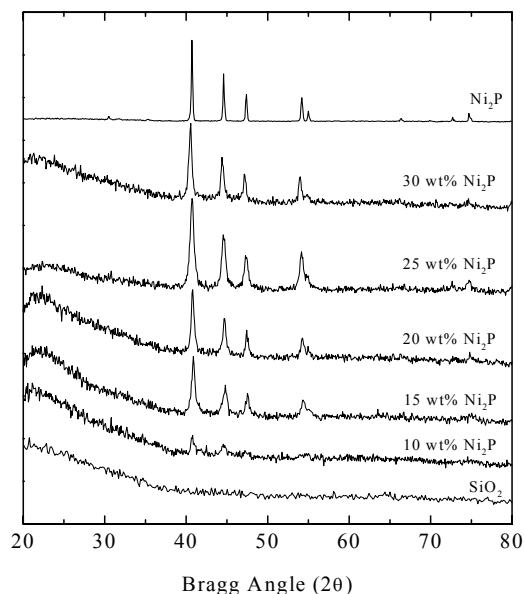

Figure 1. XRD patterns for Ni_2P/SiO_2 catalysts as well as the silica support and unsupported Ni_2P.
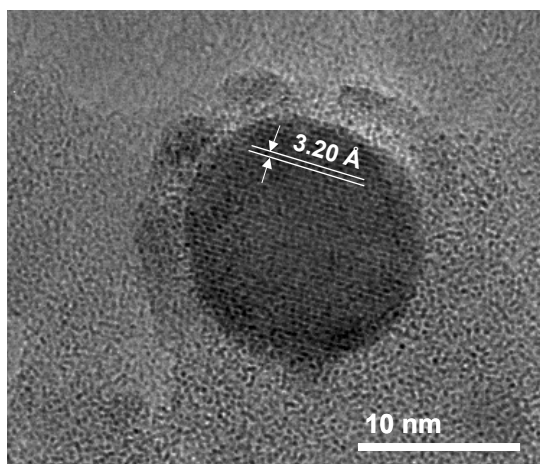
Figure 2. A TEM micrograph of a 25 wt% Ni_2P/SiO_2 catalyst.

The lattice spacing of 3.20 Å is assigned to the {001} crystallographic plane of Ni_2P which is consistent with the XRD patterns. The thiophene HDS activity of a 30 wt% Ni_2P/SiO_2 catalyst as well as of silica-supported molybdenum carbide (β-Mo_2C), molybdenum nitride (γ-Mo_2N), molybdenum phosphide (MoP) and a sulfided molybdenum catalyst are plotted versus time on-stream in **Figure 3**.
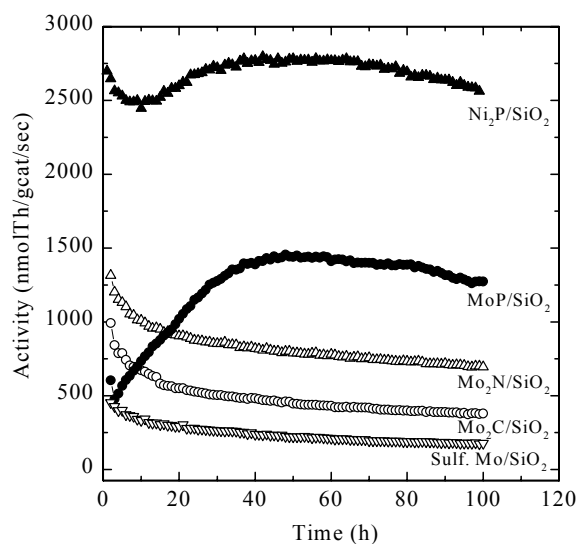
Figure 3. Comparison of thiophene HDS activity data for carbide, nitride and phosphide catalysts with similar data for a sulfided Mo catalyst.

The Mo-based catalysts have similar Mo loadings, corresponding to a 28.5 wt% MoO_3 loading in the oxidic precursor of the Mo carbide, nitride and sulfided Mo catalysts. The catalysts exhibit a wide range of thiophene HDS activities with the carbide, nitride and phosphide catalysts all having higher HDS activities than the sulfided Mo/SiO_2 catalyst. The Mo carbide, nitride and sulfided Mo catalysts display similar trends in HDS activity over time, decreasing over the entire time on-stream but achieving a relatively stable activity at 100 h. In contrast, the HDS activities of the MoP/SiO_2 and Ni_2P/SiO_2 catalysts show a different trend, increasing over approximately the first 50 h
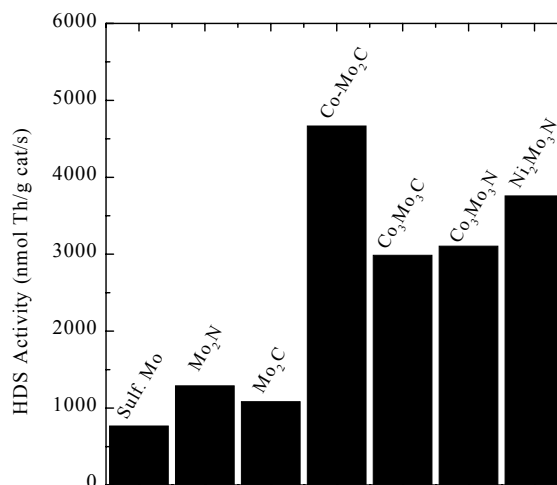
on-stream and then decreasing somewhat for the remaining 50 h of the testing period.

Similar to a model presented previously for alumina-supported catalysts,[3,4] the high HDS activities of the Mo_2C/SiO_2 and Mo_2N/SiO_2 catalysts are ascribed to a high density of active sites located on a thin, highly dispersed sulfided Mo layer formed at the surface of the supported carbide and nitride particles under reaction conditions. An understanding of the high HDS activities of the MoP/SiO_2 and Ni_2P/SiO_2 catalysts is less well developed at this time. Infrared spectroscopy studies of adsorbed CO and other probe molecules are currently under way to gain insight into the nature of the adsorption sites on the phosphide catalysts and their stability under reaction conditions.

In addition to our studies of monometallic carbide, nitride and phosphide catalysts, we have also investigated the HDS properties of bimetallic and promoted carbide and nitride catalysts. As recently described elsewhere,[14] the synthesis of alumina-supported bimetallic carbide (Co_3Mo_3C/Al_2O_3) and nitride (Co_3Mo_3N/Al_2O_3, Ni_2Mo_3N/Al_2O_3) catalysts requires care in order to avoid monometallic impurities. The preparation of promoted catalysts is far simpler, involving only impregnation of the carbide or nitride catalyst with the promoting metal salt followed by vacuum drying. The incorporation of a second metal (Co, Ni) to form bimetallic carbide and nitride phases (e.g. Co_3Mo_3C/Al_2O_3) or promoted materials (e.g. Co-Mo_2C/Al_2O_3) yields significantly more active HDS catalysts as summarized in **Figure 4.**

Conclusions

Oxide-supported metal carbide, nitride and phosphide catalysts can be prepared using the TPR method. These materials have high HDS activities and their catalytic properties warrant further investigation.

Figure 4. Thiophene HDS activities for alumina-supported carbide and nitride catalysts.

References
1. Kabe, T.; Ishihara, A.; Qian, W. *Hydrodesulfurization and Hydrodenitrogenation: Chemistry and Engineering*; Wiley-VCH: Weinheim, 1999.
2. Sajkowski, D. J.; Oyama, S. T. *Appl. Catal. A* **1996**, *134*, 339-349.
3. Aegerter, P. A.; Quigley, W. W. C.; Simpson, G. J.; Ziegler, D. D.; Logan, J. W.; McCrea, K. R.; Glazier, S.; Bussell, M. E. *J. Catal.* **1996**, *164*, 109-121.
4. McCrea, K. R.; Logan, J. W.; Tarbuck, T. L.; Heiser, J. L.; Bussell, M. E. *J. Catal.* **1997**, *171*, 255-267.
5. Nagai, M.; Miyao, T.; Tuboi, T. *Catal. Lett.* **1993**, *18*, 9-14.
6. Nagai, M.; Uchino, O.; Kusgaya, T.; Omi, S. In *Hydrotreatment and Hydrocracking of Oil Fractions*; Froment, G., Delmon, B., Grange, P., Eds.; Elsevier: New York, 1997; p 541.
7. Nagai, M.; Kiyoshi, M.; Tominaga, H.; Omi, S. *Chem. Lett.* **2000**, 702-703.
8. Oyama, S. T.; Clark, P.; Teixiera da Silva, V. L. S.; Lede, E. J.; Requejo, F. G. *J. Phys. Chem. B* **2001**, *105*, 4961-4966.
9. Phillips, D. C.; Sawhill, S. J.; Self, R.; Bussell, M. E. *J. Catal.* **2002**, *207*, 266-273.
10. Oyama, S. T.; Wang, X.; Requejo, F. G.; Sato, T.; Yoshimura, Y. *J. Catal.* **2002**, *209*, 1-5.
11. Wang, X.; Clark, P.; Oyama, S. T. *J. Catal.* **2002**, *208*, 321-331.
12. Oyama, S. T.; Wang, X.; Lee, Y.-K.; Bando, K.; Requejo, F. G. *J. Catal.* **2002**, *210*, 207-217.
13. Sawhill, S. J.; Phillips, D. C.; Bussell, M. E. *J. Catal.* **2002**, submitted for publication.
14. Korlann, S.; Diaz, B.; Bussell, M. E. *Chem. Mater.* **2002**, *14*, 4049-4058.

# Probe Reactions for C-C Bond Cleavage and Aromatic Hydrogenation over Mo-based Carbide and Sulfide Catalysts

Chunshan Song[1], Weilin Wang[1], Boli Wei[1], S. Ted Oyama[2], and Viviane Schwartz[2]*

(1) Clean Fuels and Catalysis Program, The Energy Institute, and Department of Energy & Geo-Environmental Engineering, Pennsylvania State University, 209 Academic Projects Building, University Park, PA 16802, Fax: 814-865-3248, csong@psu.edu
(2) Dept. of Chemical Engineering, Virginia Polytechnic Institute and State University, 140 Randolph Hall, Blacksburg, VA 24061

Introduction

Molybdenum based sulfide catalysts are widely used in hydroprocessing of petroleum fractions in refining industry. While these catalyst systems have been extensively studied [Topsoe et al., 1996], some fundamental issues remain to be addressed. Mo based carbide and bimetallic carbides have shown promises as new catalytic materials for hydroprocessing [Schwartz et al., 2000; Oyama et al., 1999; Dhandapani et al., 1998]. Knowledge on functionalities of these catalyst systems is still limited.

The present work deals with probe molecular reactions for C-C bond cleavage and aromatic ring hydrogenation over Mo-based carbide and sulfide catalysts. It is believed that cleavage of aromatic-aliphatic or aliphatic-aliphatic C-C bonds is very important for catalytic hydroprocessing and upgrading of heavy oil, and liquids derived from coal and coprocessing of heavy materials. There is little literature information on catalytic functionalities of Mo-based carbide and sulfide catalysts on C-C bond cleavage. As has been discussed in our recent report [Schmidt et al., 1996; Yoneyama and Song, 1999], 4-(1-naphthylmethyl)bibenzyl, abbreviated as NMBB, is a good model compound for examining activities and selectivities of various catalysts on hydrogenolysis and hydrogenation, since there are different types of potential cleavage sites of C-C bonds and both monocyclic and bicyclic aromatic moieties in the compound.
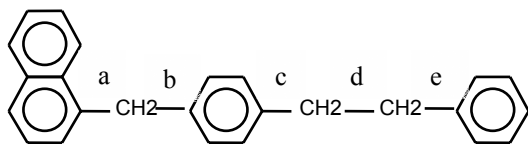
In this work, we employed this model compound to simulate the structure in heavy hydrocarbon resources. Hydrogenolysis and hydrogenation properties of multiple catalysts have been examined on this model structure at 375 °C and 400 °C. Two types of molybdenum catalysts have been tested to study the impact of different catalysts on the catalytic reaction of NMBB at 375°C and 400°C. One type is Mo carbide catalyst including Mo_2C and $NbMo_{1.6}C$, and the other type is sulfide catalyst including Mo sulfide from ATTM, Co-Mo/Al_2O_3, Ni-Mo/Al_2O_3.

Experimental

Three metal sulfide catalysts have been examined, including dispersed MoS_2 catalyst derived in-situ from ammonium tetrathiomolybdate [ATTM, $(NH_4)_2MoS_4$] and sulfided Co-Mo/Al_2O_3 (CR-344) and Ni-Mo/Al_2O_3 (CR-424) catalysts from Criterion. Before using these two commercial catalysts for model compound

reaction, they were sulfided in 100 ml autoclave using 6% CS_2 in *n*-tridecane under hydrogen pressure by a temperature-programmed manner: first at 250 °C for 2 h and then at 300 °C for 3 h. Our experience shows that such a procedure is effective for sulfidation in batch reactors. After sulfidation, the catalysts were kept in *n*-tridecane before use.

It should be noted that the molybdenum carbide catalysts were prepared at Virginia Tech and shipped to Penn State in a sealed ampoules with about 0.1 g sample in each ampoule. The carbide catalyst was charged into the reactor in the sealed glass ample, and broken in situ to avoid exposure to air.

All the reactions were conducted in a 25-ml horizontal micro-autoclave reactor under 1000 psig hydrogen pressure for 30 min plus 3 min for heat-up. The reactants charges were 0.2 g NMBB and 1 g solvent (*n*-tridecane) plus a given amount of catalyst for the single component reaction.

The sealed reactor was purged four times with H_2 and then pressurized up to 1000 psi H_2 at room temperature for all experiments. A preheated fluidized sand bath was used as the heating source, and the reactor was horizontally agitated to provide mixing (about 240 strokes/min). After the reaction, the micro-autoclave was quenched in cold water bath. The contents were washed out with 20-30 methylene dichloride, and filtered through a low speed filter paper for subsequent GC analysis.

After the reaction, the liquid was collected and analyzed by GC-MS. Quantitative analysis of products is computed according to the relative response factors that was pre-determined by using the reagent chemicals (relative to an internal standard). In this work, we used Shimadzu GC 17A gas chromatograph coupled with QP-5000 mass spectrometer. The column used for GC-MS was the Crossbond® 5% phenyl – extended temperature and inertness capillary column with 30 m long, 0.25 mm I.D., 0.25 μm. Dibenzofuran (DBF) was selected as an internal standard which has no overlap with the products from the reactions of the 5 different model compounds. The oven for GC-MS was programmed from 40 °C to 290 °C at a heating rate of 4 °C/min, with a initial holding time of 5 min and a final holding time of 10 min.

The conversion of reactants is defined as {[reactant (wt) charged – reactant (wt) recovered]/reactant (wt) charged]} × 100, the molar yields of products are defined as [product (mol)/reactant (mol) charged] × 100.

Results

Table 1 shows the active sites of different catalysts measured by chemisorption. In order to comparatively examine the functionalities of different catalysts on an uniform basis, the amount of catalyst was charged based on the equal number of active sites per gram of reactant feed. The measurements of active sites for the molybdenum sulfide catalysts were done in pulse mode with molecular oxygen in a stream of helium at dry ice/acetone temperature. The samples were pre-sulfided for 2 hrs at 415 °C in 10% H_2S/H_2. The CO uptake data was measured as active sites for the unsupported metal carbides.

Table 2 shows the product distribution of NMBB reactions over four different sulfide catalysts at 400°C. From Table 2, the total yields of naphthalene and tetralin were almost over 70% and 4-methylbibenzyl close to or over 50% in most catalytic runs, indicating that the cleavage of NMBB mainly products from 4-methylbibenzyl were also detected from the GC-occurs on the aromatic-aliphatic bond *a*. Some further cracking MS spectroscopy, such as toluene, ethylbenzene, *p*-xylene. In addition, some amount of methylnaphthalene, its hydrogenation isomers and bibenzyl also existed in the product pool, which represented that cracking also

Table 1. Active sites of catalyst by chemisorption

Catalyst	Catalyst/ Support	CoO (wt%)	NiO (wt%)	Mo (wt%)	Active Sites (micro-mol/g) on wt of catalyst used	Active Sites (micro-mol/g) on wt of catalyst recovered
ATTM	$(NH_4)_2MoS_4$	N/A	N/A	36.91	57.30	93.70
CR-344	Co-Mo/Al$_2$O$_3$	2.90	N/A	9.0(13.5*)	82.40	85.90
CR-424	Ni-Mo/Al$_2$O$_3$	N/A	3.00	8.7(13.0*)	92.30	95.00
Mo2C	Mo$_2$C	N/A	N/A	94.1	99.00	-
MoNb1.6C	NbMo$_{1.6}$C	N/A	N/A	59.4	22.00	-

* The content of MoO$_3$ within the commercial catalysts

Table 2 **Hydrogenolysis of NMBB** over Mo-based sulfide and carbide catalysts at 400 **°C**

	ATTM	S-Co-Mo/Al$_2$O$_3$	S-Ni-Mo/Al$_2$O$_3$	Mo$_2$C	NbMo$_{1.6}$C	Thermal
Experiment No.	1-014	1-023	1-024	1-025	1-026	1-013
Catalyst Amount, g	0.1636	0.0226	0.0203	0.1	0.125	
Active Sites, mcior-mol	9.37	1.86	1.87	9.90	2.75	
Catalyst loading, micro-mol/g	9.37	9.32	9.35	9.37	9.36	
Temperature, °C	400	400	400	400	400	400
Reactant, g NMBB	0.9997	0.1999	0.2003	1.0567	0.2939	0.2000
Yields, mol%						
Methylcyclohexane					5.5	
Toluene	4.6	5.1	6.2	6.6	8.7	2.2
Ethylbenzene		2.2	2.4	0.7	2.6	
p-Xylene	1.5	2.2	2.9	3.0	5.3	
Decalin				4.7	7.7	
Tetralin	62.9	43.7	41.5	64.7	46.9	
Naphthalene	8.2	28.9	42.8	4.6	3.6	2.0
MTHN isomers	5.1	4.6	4.8	1.8	2.3	
1-Methylnaphthalene		3.0	4.2	5.7	5.9	
Bibenzyl	9.9	8.7	9.8	5.9	3.4	
4-Methylbibenzyl	63.8	62.5	73.7	39.1	23.6	2.5
4-Methylhexahydrobibenzyl				18.6	16.8	
1,2-Dicyclhexylethane					5.9	
4-Methyl-1',2'-dicyclohexylethane				1.9	6.6	
1-Naphthyl-4-tolylmethane						0.7
NMBB Recovered						96.8
Conversion	**100.0**	**100.0**	**100.0**	**100.0**	**100.0**	**3.2**

Table 3   Hydrogenolysis of NMBB over Mo-based sulfide and carbide catalysts at 375°C

	ATTM	Co-Mo/Al$_2$O$_3$	Ni-Mo/Al$_2$O$_3$	Mo$_2$C	NbMo$_{1.6}$C	Thermal Baseline
Experiment No.	1-016	1-021	1-022	1-017	1-018	
Catalyst Amount, g	0.0326	0.0229	0.0203	0.1000	0.1140	N/a
Active Sites, mcior-mol	1.87	1.89	1.87	9.90	2.51	N/a
Catalyst loading,micro-mol/g	9.34	9.42	9.35	9.37	9.37	N/a
Temperature, °C	375	375	375	375	375	375
Reactant, g NMBB	0.2001	0.2003	0.2005	1.0567	0.2678	0.258
Yields, mol%						
Methylcyclohexane					12.7	
Toluene			1.4	1.9	5.4	
Ethylbenzene					2.1	
p-Xylene					6.0	
Decalin					10.2	
Tetralin	41.7	53.9	68.3	74.6	35.8	
Naphthalene	34.3	31.6	2.9	7.8	6.8	
MTHN isomers	1.8	1.4	1.6	3.7	4.0	
1-Methylnaphthalene	3.6	1.9		1.1		
Bibenzyl	9.8	10.2	9.4	12.0	4.4	
4-Methylbibenzyl	70.4	80.3	60.9	60.3	24.1	
4-Methylbibenzyl isomer	-					
4-Methylhexahydrobibenzyl	9.4		2.3	7.0	11.1	
1,2-dicyclhexylethane					10.0	
4-Methyl-1,2-dicyclohexylethane					8.9	
Tetrahydro-NMBB-1		5.2	4.0	5.9		
Tetrahydro-NMBB-2						
NMBB Recovered	11.0	0.0	0.0	0.0	0.0	
Conversion	**89.0**	**100.0**	**100.0**	**100.0**	**100.0**	**< 3%**

occurred on bond **b**. It is very obvious that no naphthyltolylmethane product were detected in all the catalytic reactions. In some catalytic runs, small amounts of hydrogenated NMBB products have been detected. Table 3 shows the results of catalytic runs at 375 °C.

   Baseline Runs.   Reaction of NMBB without added catalyst provides a baseline for comparison of all catalytic reactions. The results in Table 2 show that naphthalene and 4-methylbibenzyl are the main products at 400 °C. They were derived from hydrogenolysis at bond **a**. Some wall catalytic effect may be responsible for the observed conversion in the non-catalytic (thermal) runs.

      The small amount of 1-(naphthyl)-4-tolyl-methane and toluene indicated that bond **d** would be another cracking site under non-catalytic atmosphere. Naphthyltolylmethane, which was not found in catalytic reactions, is believed to be a product in non-catalytic reactions at 400 °C. It has been reported that, at least for temperature ≥410°C the dominant cleavage in thermal runs is at bond **d** [Farcasiu et al, 1990]. The low conversion observed in this reaction, 3.2%, agrees well with other values reported in our previous literature [Schmidt et al., 1996].

Discussion

   The results of single-component NMBB reaction (Table2 and Table 3) reveal that NMBB is a good model compound for examining the activity and selectivity of various catalysts for C-C bond hydrogenolysis and aromatic ring hydrogenation. The product distribution from NMBB catalytic hydrogenolysis indicates that the cleavage of NMBB mainly occurs on the aromatic-aliphatic C-C bond **a**, which is in distinct contrast to the non-catalytic and computational results which indicate the bond **d** in NMBB structure as the weakest linkage among the five potential C-C cleavage sites.

   Naphthalene, tetralin and 4-methylbibenzyl are the major products from reactions catalyzed over Mo sulfide catalysts under the specified reaction condition. The temperature has a significant effect on NMBB conversion. The higher the temperature, the higher the hydrogenolysis activity. The two commercial catalysts exhibit high hydrogenolysis activity even at low temperature compared to ATTM.

   Compared to Mo sulfide catalysts, Mo carbide catalysts possess different catalytic functionality. Some new hydrogenation products derived from bibenzyl and 4-methylbibenzyl, such as 1,2-

dicyclohexylethane, 4-methylhexahydrobibenzyl and 4-methyl-1,2'-dicyclohexylethane, were formed in the catalytic runs over NbMo$_{1.6}$C catalyst.

Among the Mo sulfide catalysts, ATTM exhibits highest hydrogenation ability on NMBB reaction at 400°C, while Ni-Mo/Al$_2$O$_3$ showed high activity on hydrogenation at 375°C. In addition, Ni-Mo/Al$_2$O$_3$ and Co-Mo/Al$_2$O$_3$ are more active to hydrogenolysis in terms of the yields of the secondary cracking products. Compared to Mo sulfide catalysts, Mo$_2$C and NbMo$_{1.6}$C carbide catalysts are extremely active to NMBB reaction in terms of hydrogenation ability. NbMo$_{1.6}$C catalyst shows hydrogenation ability twice as high as Ni-Mo/Al$_2$O$_3$ based on the same active sites of catalyst per gram NMBB. NbMo$_{1.6}$C also exhibits highest activity on hydrogenolysis among the examined Mo-based catalysts.

References

Dhandapani B, St Clair T.; Oyama S.T. Appl. Catal. A: Gen., 1998, 168 (2), 219

Farcasiu, M.; Smith, C.; Pradhan, V. R.; Wender, I. Fuel Process. Tech. 1991, 29, 199.

Oyama S.T.; Yu C.C.; Ramanathan S. J Catal., 1999, 184 (2), 535.

Schmidt, E.; Song, C.; Schobert, H. H. Energy Fuels, 1996, 10, 597.

Schwartz ,V.; Oyama S.T.; Chen JGG. J. Phys. Chem. B., 2000, 104 (37), 8800.

Topsoe, H.; Clausen, B. S.; Massoth, F. E. Hydrotreating Catalysis. Science and Technology. Springer-Verlag, Berlin, 1996, 310 pp.

Yoneyama, Y.; Song, C. Catal. Today 1999, 50, 19.

Catalysis by Mo-based Monometallic and Bimetallic Carbides and Sulfides for Simultaneous Hydrodesulfurization, Hydrodenitrogenation, and C-C Hydrogenolysis

Chunshan Song[1], Weilin Wang[1], Boli Wei[1], S. Ted Oyama[2], and Viviane Schwartz[2]*

(1) Clean Fuels and Catalysis Program, The Energy Institute, and Department of Energy & Geo-Environmental Engineering, Pennsylvania State University, 209 Academic Projects Building, University Park, PA 16802, Fax: 814-865-3248, csong@psu.edu
(2) Dept. of Chemical Engineering, Virginia Polytechnic Institute and State University, 140 Randolph Hall, Blacksburg, VA 24061

The present work deals with multi-probe molecular reactions for simultaneous hydrodesulfurization, hydrodenitrogenation, and C-C hydrogenolysis over Mo-based monometallic and bimetallic carbide and sulfide catalysts, in conjunction with the work on single-probe molecular reactions [Song et al., 2003]. Molybdenum based sulfide catalysts are widely used in hydroprocessing of petroleum fractions in refining industry. While these catalyst systems have been extensively studied [Topsoe et al., 1996], some fundamental issues remain to be addressed. Mo based carbide and bimetallic carbides have shown promises as new catalytic materials for hydroprocessing [Schwartz et al., 2000; Oyama et al., 1999; Dhandapani et al., 1998]. Knowledge on functionalities of these catalyst systems is still limited.

Table 1 shows the properties of the Mo-based monometallic and bimetallic carbide and sulfide catalysts. A multi-component model-feedstock was used to test catalytic functions for simultaneous hydrogenation, C-C bond hydrogenolysis, hydrodesulfurization, and hydrodenitrogenation. These reactions are precisely those involved in the conversion and processing of heavy hydrocarbon resources such as heavy oil, coal, and other residual materials. The multi-component feed includes 4-(1-naphthylmethyl)bibenzyl (NMBB), dibenzothiophene (DBT), quinoline, pyrene, and eicosane. The information feedback from model tests should be useful for selecting promising catalysts for hydroprocessing or coprocessing of coal and waste materials as well as petroleum resid in the future.

Table 2 and Tables 3 shows the results of multi-probe reactions at 400 °C and 375 °C, respectively. All the catalysts show certain activity for conversion of the five compounds under the reaction conditions compared to the thermal reaction. From the thermal reaction of 5-component model compounds, we can rank the five compounds in the following sequence in terms of reactivity: quinoline > NMBB > pyrene > DBT > eicosane.

ATTM and Co-Mo/Al$_2$O$_3$ and Ni-Mo/Al$_2$O$_3$ exhibit high activity on hydrogenolysis and hydrogenation properties. Among the Mo carbide catalysts and the Mo sulfide catalysts, NbMo$_{1.6}$C showed similar activity on quinoline and NMBB compared to the two commercial catalysts. Moreover, NbMo$_{1.6}$C exhibit slightly higher activity on the conversion of pyrene, which is consistent with its high hydrogenation ability. Co-reactants significantly influence NMBB conversion and the products derived. Many hydrogenation products from bibenzyl and 4-methylbibenzyl that were observed in single-component NMBB reaction in the presence of NbMo$_{1.6}$C, decline or disappear completely in the 5-component reaction.

It is noticed clearly that Mo$_2$C, unlike in the single-component reaction, shows low activity on the model compounds, indicating Mo$_2$C was strongly affected by the existence of other co-reactants.

Given the same active sites per gram reactant charges, NbMo$_{1.6}$C showed slightly higher hydrogenation ability on pyrene than Co-Mo/Al$_2$O$_3$ and Ni-Mo/Al$_2$O$_3$ catalysts at 400°C. Compared to the hydrogenation ability in single compound reactions, the co-reactants apparently change the catalytic activities of the various catalysts. The co-reactants significantly inhibit the hydrogenation of the products from NMBB cracking.

For all catalytic runs, quinoline is the most reactive among the 5 compounds, which was almost completely converted at 400°C. For DBT reaction, the two commercial Co-Mo/Al$_2$O$_3$ and Ni-Mo/Al$_2$O$_3$ catalysts showed high activity compared to ATTM-derived Mo catalyst. ATTM performs as a better catalyst precursor on HDN than even the commercial Co-Mo/Al$_2$O$_3$ and Ni-Mo/Al$_2$O$_3$ catalysts. However, Co-Mo/Al$_2$O$_3$ and Ni-Mo/Al$_2$O$_3$ catalysts show higher HDS ability on DBT than ATTM. Between the monometallic carbide Mo$_2$C and bimetallic carbide NbMo$_{1.6}$C catalyst, NbMo$_{1.6}$C catalyst is more active on HDN and HDS. NbMo$_{1.6}$C shows slightly higher activity on HDN than Ni-Mo/Al$_2$O$_3$ catalyst under the reaction condition.

The results from 5-component reactions indicate that the patterns of product distributions strongly depend on the type of catalysts, and the trends do not always parallel with those for single-component tests, indicating the influence of co-reactants. The catalytic properties of Mo$_2$C are significantly inhibited in the 5-component reaction. ATTM performs as a better catalyst on HDN even than the two commercial Co-Mo/Al$_2$O$_3$ and Ni-Mo/Al$_2$O$_3$ catalysts. However, Co-Mo/Al$_2$O$_3$ and Ni-Mo/Al$_2$O$_3$ catalysts show higher HDS ability on DBT than ATTM. NbMo$_{1.6}$C also shows high activity on hydrogenation and HDN.

The reaction temperature has a great effect on the product distribution. More hydrogenation products and very limited C-C cleavage products were obtained at 375°C, while higher yields of hydrocracking, and hydrogenated C-C cleavage products were detected at 400°C.

Overall, the unique reactivities and selectivities of the NbMo$_{1.6}$C carbide in hydrogenation and its HDN and HDS performance make the bimetallic Mo-based carbides promising candidates for further study in hydrocarbon processing.

References
Dhandapani B, St Clair T.; Oyama S.T. Appl. Catal. A: Gen., 1998, 168 (2), 219
Farcasiu, M.; Smith, C.; Pradhan, V. R.; Wender, I. Fuel Process. Tech. 1991, 29, 199.
Oyama S.T.; Yu C.C.; Ramanathan S. J Catal., 1999, 184 (2), 535.
Schmidt, E.; Song, C.; Schobert, H. H. Energy Fuels, 1996, 10, 597.
Schwartz ,V.; Oyama S.T.; Chen JGG. J. Phys. Chem. B., 2000, 104 (37), 8800.
Song, C.; Wang, W.; Wei, B.; Oyama S.T.; Schwartz ,V. Am. Chem. Soc. Div. Fuel Chem. Prepr., 2003, 48 (1), in press.
Topsoe, H.; Clausen, B. S.; Massoth, F. E. Hydrotreating Catalysis. Science and Technology. Springer-Verlag, Berlin, 1996, 310 pp.
Yoneyama, Y.; Song, C. Catal. Today 1999, 50, 19.

Table 1. Active sites of catalyst by chemisorption

Catalyst	Catalyst/ Support	CoO (wt%)	NiO (wt%)	Mo (wt%)	Active Sites (micro-mol/g) on wt of catalyst used	Active Sites (micro-mol/g) on wt of catalyst recovered
ATTM	$(NH_4)_2MoS_4$	N/A	N/A	36.91	57.30	93.70
CR-344	Co-Mo/Al$_2$O$_3$	2.90	N/A	9.0(13.5*)	82.40	85.90
CR-424	Ni-Mo/Al$_2$O$_3$	N/A	3.00	8.7(13.0*)	92.30	95.00
Mo2C	Mo$_2$C	N/A	N/A	94.1	99.00	-
NbMo1.6C	NbMo$_{1.6}$C	N/A	N/A	59.4	22.00	-

* The content of MoO$_3$ within the commercial catalysts

Table 2 Results of 5-Component Probe Reactions at 400 °C

Catalyst	ATTM	Co-Mo/Al2O3	Ni-Mo/Al2O3	Mo2C	NbMo1.6C	Thermal
Experiment No.	5-017	5-024	5-025	5-028	5-029	5-013
Temperature, oC	400	400	400	400	400	400
Quinoline						
Propylcyclohexane	60.2	34.8	50.0	2.1	25.6	
PropylBenzene	3.9	2.4	3.9	0.4	3.1	
Propenylcyclohexene	0.8	3.1	3.3	2.6	4.3	
1,2,3,4-tetrahydroquinoline		13.8	3.2	50.3	12.4	11.3
5,6,7,8-tetrahydroquinoline		3.3	0.9	12.4	3.6	
Decahydroquinoline				7.0	1.5	
2-propylbenzenamine	6.0	19.7	20.6	3.0	5.4	
Quinoline recovered		1.0	0.9	7.0	1.3	89.0
Conversion	**100.0**	**99.0**	**99.1**	**93.0**	**98.7**	**11.0**
DBT						
Benzene, cyclohexyl-	10.6	4.8	4.7		4.7	
Biphenyl	6.3	72.1	80.5	5.4	40.7	
TH-DBT	15.6					
DBT recovered	53.9	24.1	14.8	95.1	52.3	100.0
Conversion	**46.1**	**75.9**	**85.2**	**4.9**	**47.7**	**0.0**
NMBB						
Methylcyclohexane	5.0		1.8			
Toluene	3.5	3.5	3.8		5.5	1.5
p-Xylene			1.3		2.8	
Tetralin	49.2	23.6	30.7	0.9	25.6	
Naphthalene	15.9	30.9	31.8	25.5	47.9	
1-Methylnaphthalene			0.8		1.5	
Bibenzyl	5.3	2.1	2.2	1.2	3.9	
4-Methylbibenzyl	64.1	47.3	51.6	21.7	64.7	
4-Methyldicyclohexylethane	5.6		2.9		1.2	
1-Naphthyltolylmethane						0.8
TH-NMBB-1		7.7	5.6		2.5	
TH-NMBB-2	9.3	21.9	21.5		8.0	
NMBB recovered	6.1	14.9	6.5	59.9	15.3	96.9
Conversion	**93.9**	**85.1**	**93.5**	**40.1**	**84.7**	**3.1**
Pyrene						
4,5,9,10-tetrahydropyrene	2.5	3.7	3.3	0.5	2.9	
1,2,3,3a,4,5-hexahydropyrene	9.7	6.4	6.7		6.3	
1,2,3,6,7,8-hexahydropyrene	10.7	6.1	7.3	0.8	8.3	
4,5-Dihydropyrene	20.5	29.2	27.2	15.2	24.4	1.8
Pyrene recovered	42.4	60.9	64.7	83.5	53.6	99.1
Conversion	**57.6**	**39.1**	**35.3**	**16.5**	**46.4**	**0.9**
Eicosane						
n-C20 recovered	97.7	91.5	90.1	91.9	88.7	99.5
Conversion	**2.3**	**8.5**	**9.9**	**8.1**	**11.3**	**0.5**

Table 3 Results of 5-Component Probe Reactions at 375 °C

Catalyst	ATTM	Co-Mo/Al2O3	Ni-Mo/Al2O3	Mo2C	NbMo1.6C
Experiment No.	5-019	5-022	5-023	5-026	5-027
Temperature, oC	375	375	375	375	375
Quinoline					
Propylcyclohexane	30.4	10.9	20.2	0.6	13.6
PropylBenzene	2.1	0.4	0.7		2.0
Propenylcyclohexene	5.7	2.1	2.4	1.0	6.6
1,2,3,4-tetrahydroquinoline	16.9	54.0	46.7	77.7	30.3
5,6,7,8-tetrahydroquinoline	0.5	1.4	1.5	5.2	4.6
Decahydroquinoline				4.7	16.9
2-propylbenzenamine	13.1	12.5	17.1	1.8	1.0
Methylquinoline					0.3
Ethyl-THQ isomers				3.6	1.1
Ethylquinoline isomers				1.4	5.7
Quinoline recovered		2.3	1.3	5.7	2.0
Conversion	**100.0**	**97.7**	**98.7**	**94.3**	**98.0**
DBT					
cyclohexylbenzene	0.9	0.8	1.2		
Biphenyl	2.2	32.6	54.4	4.4	21.1
TH-DBT	8.8		0.3		
DBT recovered	88.1	66.3	44.7	95.8	78.9
Conversion	**11.9**	**33.7**	**55.3**	**4.2**	**21.1**
NMBB					
Methylcyclohexane					
Toluene					
p-Xylene					
Tetralin	6.7	2.4	4.8		3.3
Naphthalene	11.4	11.2	12.3	9.7	32.7
1-Methylnaphthalene		1.4	0.8	0.8	
Bibenzyl					1.3
4-methylbibenzyl	16.7	12.6	15.4	8.7	34.7
TH-NMBB-1	21.3	8.0	8.2		4.8
TH-NMBB-2	25.0	15.7	19.7		9.7
NMBB recovered	38.8	51.6	48.6	73.6	45.3
Conversion	**61.2**	**48.4**	**51.4**	**26.4**	**54.7**
Pyrene					
4,5,9,10-tetrahydropyrene	3.9	5.2	3.6	0.2	2.7
1,2,3,3a,4,5-hexahydropyrene	14.8	2.9	1.9		2.9
1,2,3,6,7,8-hexahydropyrene	21.0	2.2	1.9		4.1
4,5-dihydropyrene	27.4	36.1	32.3	7.6	26.8
1,3-dimethylpyrene					
Pyrene recovered	34.9	61.2	65.6	91.8	62.9
Conversion	**65.1**	**38.8**	**39.7**	**8.2**	**37.1**
Eicosane					
n-C20 recovered	90.0	93.9	98.3	98.8	90.4
Conversion	**10.0**	**6.1**	**1.7**	**1.2**	**9.6**

HYDRODESULFURIZATION OF THIOPHENE OVER CARBIDED MOLYBDENA-ALUMINA CATALYSTS

Masatoshi Nagai,[1] Hiroyuki Tominaga, Ryouko Abe, and Shinzo Omi

Graduate School of Bio-applications and Systems Engineering
Tokyo University of Agriculture and Technology
2-24 Nakamachi, Koganei, Tokyo 184-8588, Japan

Introduction

Molybdenum carbides supported on alumina and unsupported carbides with high surface area are recently being studied in order to prepare catalysts with high performance for hydrodesulfurization (1–3) and hydrodenitrogenation. McCrea *et al.* (1) studied the activities of Mo nitride, carbide, and sulfide supported on alumina in thiophene HDS and compared the order of the catalytic activity. The HDS activity depended on a high site density measured by CO adsorption as follows: β-Mo_2C > γ-Mo_2N > MoS_2. Miyao *et al.* (4) studied the relationship between the surface properties of carbided Mo/Al_2O_3 and the activity in carbazole HDN and reported that the Mo/Al_2O_3 carbided at 973 K was about 2.2 times more active than the reduced catalyst (per catalyst weight). Thus, Mo carbide was the most active catalyst of the three types of molybdenum catalysts during the hydrogenolysis reactions. However, few studies have been made at a higher activity of carbided Mo/Al_2O_3 per g-catalyst, then compared to sulfided Mo/Al_2O_3 and $CoMo/Al_2O_3$ catalysts for the HDS reaction. Furthermore, some of the sulfur removed during the HDS reaction accumulated on the surface to form a thin layer of sulfided molybdenum on the Mo carbide catalysts after 24 h (1). Little attention has been paid on how sulfur is adsorbed and changes the surface properties and activities during the HDS reaction, or on the behavior of the molybdenum and carbidic carbons of the Mo carbide catalysts. In this study, the activity of the carbided Mo/Al_2O_3 catalysts with various Mo loadings was studied during the HDS of thiophene at atmospheric pressure and compared to the sulfided Mo/Al_2O_3 and commercial CoMo catalysts. The relationship between the HDS activity and the atomic ratios of the molybdenum, carbidic carbon, and sulfur to aluminum and Mo oxidation states on the surface using X-ray photoelectron spectroscopy (XPS) is studied during the HDS reaction. The active species of the carbided Mo/Al_2O_3 during thiophene HDS are also discussed.

Experimental

Hydrogen was dried by passing it through a Deoxo unit (SUPELCO Co. Oxysorb) and a Linde 13X molecular sieve trap. 20% CH_4/H_2 and thiophene were used without further purification. 1.0–18.7 wt% MoO_3/Al_2O_3 were prepared as follows: γ-alumina (CSJ Reference catalyst, AL-04) was added to an aqueous solution of ammonium paramolybdate and the solution was boiled while being stirred. The MoO_3/Al_2O_3 sample was dried at 473 K for 24 h and calcined in air at 823 K for 3 h. After the MoO_3/Al_2O_3 catalyst (0.2 g) treated with 20% CH_4/H_2 from 573 to 973 K at a rate of 0.0167 K s^{-1} and held at the final temperature for 3 h. After the carburizing treatment, the catalyst was cooled to room temperature in flowing 20%CH_4/H_2 for surface property measurements or cooled to 623 K for HDS activity measurement. For the sulfided catalysts, $CoMo/Al_2O_3$ (Kejenefine124) and fresh and carbided 11.6 wt% MoO_3/Al_2O_3 were sulfided at 623 K for 3 h in flowing 10% H_2S/H_2 and they were purged with helium at 623 K. After the sulfiding treatment, the catalyst provided activity measurement at 623 K or the XPS measurement after it was cooled to room temperature in flowing helium. The rate of the HDS of thiophene over the carbided catalyst was measured at 623 K using a flow microreactor system at

atmospheric pressure. A 0.134 mol% thiophene in hydrogen mixture was introduced into the microreactor at 3.0 L h^{-1}. The reaction products were quantitatively analyzed using an FID gas chromatograph with a 2% Silicone DC-550 column for thiophene and tetrahydrothiophene at 393 K and a VZ-8 column for C4 hydrocarbon products.

The surface properties of the Mo/Al_2O_3 catalysts were analyzed before the reaction or at 0.167, 1, 3, and 8 h after the start by interrupting the reaction. The reactor was cooled to room temperature, both ends of the reactor closed, and then transferred to a glovebox which was pumped and backfilled with argon three times. The catalysts were removed from the reactor in argon and introduced to the XPS prechamber without exposure to air. The specific surface area (BET) of the catalysts was measured by nitrogen adsorption using a BET apparatus after the catalysts were evacuated at 473 K and 0.1 Pa for 2 h. The Mo loading (wt%) was measured using an atomic absorption spectroscope and represented as MoO_3-gram per sample-g. The quantity of chemisorbed CO on the catalysts was determined by the volumetric analyzer (Omnisorp 100CX) during evacuation. XPS spectra were obtained using a Shimadzu ESCA 3200 spectrometer with monochromatic MgK_α exciting radiation (1253.6 eV, 8 kV, 30 mA). The binding energies for the samples were referenced to Al 2p at 74.7 ± 0.2 eV. The analysis was done by argon etching using a nonlinear square method with a 100% Gaussian function, according to previously published XPS studies (5,6).
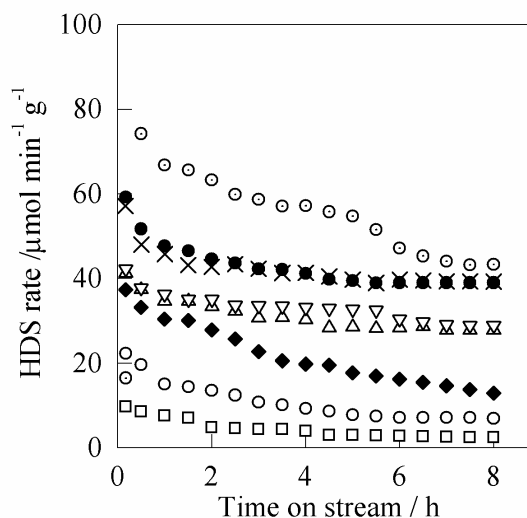

Figure 1. The HDS of thiophene over various Mo/Al_2O_3 catalysts with time on stream at 573 K and a total pressure of 10.1 MPa. ($\square$) 3.6 wt%, ($\bigcirc$) 4.8 wt%, ($\triangle$) 6.6 wt%, ($\triangledown$) 8.5 wt%, ($\bullet$) 11.6 wt%, and ($\times$) 18.7 wt% Mo/Al_2O_3 carbided at 973 K. ($\blacklozenge$) 11.6% Mo/Al_2O_3 and ($\odot$) $CoMo/Al_2O_3$ sulfided at 623 K.

Results and Discussion

HDS Activity of Carbided Mo/Al_2O_3. The rates of the HDS of thiophene over the 1.0–18.7 wt% Mo/Al_2O_3 catalysts carbided at 973 K with time on stream at 623 K and atmospheric pressure are shown in Fig. 1. The HDS rates for the 11.6 and 18.7 wt% Mo/Al_2O_3 catalysts were the highest of any carbided catalysts. As far as the same 11.6 wt% Mo loading was concerned, the HDS rate of the

carbided catalyst was 3 times higher than that of the sulfided catalyst. Although the HDS rate of the sulfided CoMo/Al$_2$O$_3$ catalyst was the highest of all the catalysts, it was decreased more rapidly than the carbided catalysts and then reached to a level similar to the carbided 11.6 and 18.7 wt% Mo/Al$_2$O$_3$ catalysts at 8 h on stream. The carburizing of the sulfided 11.6 wt% Mo/Al$_2$O$_3$ (sulfided/carbided) catalyst at 973 K improved the HDS activity of the sulfided catalyst. McCrea *et al.* (1) reported that the HDS rate (based on a weight) for a series of passivated 1.5–20 wt% Mo/Al$_2$O$_3$ catalyst carbided at 950 K was 1.5 times higher than that for a sulfided Mo/Al$_2$O$_3$ at atmospheric pressure. Moreover, the reaction products for thiophene HDS at 623 K were primarily *n*-butane and butenes with a trace of tetrahydrothiophene.
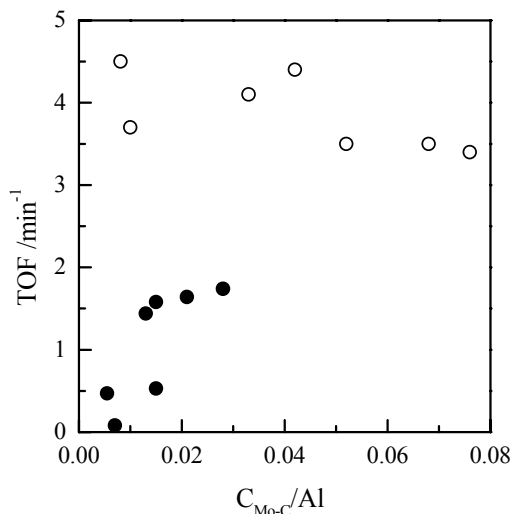
Figure 2. The relationship between TOFs and C$_{Mo-C}$/Al ratio of the carbided 1.0-18.7% Mo/Al$_2$O$_3$ (○) before the reaction and (●) at 8 h after the start.

Change in Surface Properties by XPS Analysis. X-ray photoelectron spectroscopy was used to provide information about the surface compositions of molybdenum, carbidic and carboneous carbons, and sulfur of the carbided and sulfided catalysts. The Mo/Al ratios were proportional up to an 11.6 wt% Mo loading, before raction. Mo carbides were dispersed on the surface except for the 18.7 wt% Mo catalyst that was agglomerated. Large Mo carbide particles were generated and agglomerated during the carburizing treatment but small Mo carbides were more likely dispersed during reaction, compared to those before the reaction. The C$_{Mo-C}$/Al ratio decreased 0.25-fold at 8 h after the start for more than 4.8 wt% Mo loadings. The C$_{Mo-C}$/Mo ratio was constant at 0.76±0.04 for the carbided catalysts in the entire range of Mo loading, indicating that the carbided catalysts before the reaction contained a similar type of molybdenum carbide species such as Mo$_2$C$_{1.5}$ or Mo oxycarbide. In combination of the TOF with the C$_{Mo-C}$/Al ratio (Fig. 2), the TOFs for the carbided catalysts were almost constant for various C$_{Mo-C}$/Al ratios before the reaction, while the TOFs and C$_{Mo-C}$/Al ratios decreased at 8 h after the start. As a result, the TOF of the catalysts with the 1.0–4.8 wt% Mo loadings were much lower than the higher Mo loadings catalysts. Two types of carbides of the carbided Mo/Al$_2$O$_3$ catalysts are present on the surface: Mo carbide and oxycarbide which interacted with alumina.

Molybdenum Oxidation States and Active Species. The distribution of the Mo oxidation states of the carbided 1.0–18.7 wt% Mo/Al$_2$O$_3$ catalysts, Mo^{3+} was mainly distributed at 26.6–39.3% together with Mo^{4+} and Mo^{5+} ions before the reaction. Mo^0 and Mo^{2+} were distributed at only a small percentage. In a previous paper (6), the carburization of 100% MoO$_3$ exhibited the total distribution of Mo^0 and Mo^{2+} at 80% in fresh carbided catalysts. As a result, higher values of the Mo oxidation state in the carbided Mo/Al$_2$O$_3$ catalysts are due to the interaction of molybdenum and alumina that are resistant to carbide. Furthermore, because the carbided 11.6 wt% Mo/Al$_2$O$_3$ was sulfided and had a S/Mo atomic ratio of more than 0.34 at 0.167 h after the start, the Mo 3d-S 2s envelope for the carbided catalysts during the reaction and the sulfided catalysts were curve-fitted. The Mo^{4+} species was also mainly distributed at 77.4% for the sulfided 11.6 wt% Mo/Al$_2$O$_3$ catalysts. This result is in good agreement with the Mo distribution obtained from the deconvolution of the Mo 3d spectra of MoS$_2$. The Mo^{4+} ion increased at 0.167 h after the start on the basis of the deconvolution of both the carbides and sulfides. Mo^{3+} ion was present on the carbided Mo/Al$_2$O$_3$ catalyst before the reaction and turned into Mo^{4+} (Mo sulfide) on the catalyst surface within 0.167 h. The TOF$_{8h}$ (number of thiophene molecules converted per exposed Mo atom per min at 8 h after the start) of the catalysts was linearly correlated with the presence of Mo^{4+} ion. Mo^{3+} on the carbided Mo/Al$_2$O$_3$ catalyst might be an active center at short time on stream but turned into Mo^{4+} (Mo sulfide) on the surface as a newer less active center than the Mo carbide, especially from 0.167 h after the start.

Conclusions

The activities of 1.0-18.7 wt% Mo/Al$_2$O$_3$ catalysts for thiophene HDS at 623 K and atmospheric pressure was correlated with the results of the XPS measurement. The HDS rates for the 11.6 and 18.7 wt% Mo/Al$_2$O$_3$ catalysts were the highest of any carbided catalysts. Concerning the same 11.6 wt% Mo loading, the HDS rate of the carbided catalyst was 3 times higher than that of the sulfided catalyst. Although the HDS of the sulfided CoMo/Al$_2$O$_3$ catalyst was the highest of all the catalysts, it was more rapidly reduced than the carbided catalysts and decreased to a level similar to the carbided 11.6 and 18.7 wt% Mo/Al$_2$O$_3$ catalysts at 8 h on stream. Carburizing of the sulfided 11.6 wt% Mo/Al$_2$O$_3$ catalyst at 973 K improved the HDS activity of the sulfided catalyst. The TOF$_{8h}$ of the catalysts was linearly correlated with the presence of the Mo^{4+} ion.

References
1. McCrea, K. R., Logan, J. W., Tarbuck, T. L., Heiser, J. L., and Bussell, M. E., *J. Catal.* **171**, 255 (1997).
2. Da Costa, P., Potvin, C., Manoi, J.-M., Lemberton, J.-L., Perot, G., and Djega-Mariadassou, G., *J. Mol. Catal. A* **184**, 323 (2002).
3. Dhandapani, B., Clair, T. St., and Oyama, S. T., *Appl. Catal. A* **168**, 219 (1998).
4. Miyao, T., Oshikawa, K., Omi, S., and Nagai, M., *Stud. Surf. Sci. Catal.* **106**, 255 (1997).
5. Quincy, R. B., Houalla, M., Proctor, A., and Hercules, D. M., *J. Phys. Chem.* **94**, 1520 (1990).
6. Oshikawa, K., Nagai, M., and Omi, S., *J. Phys. Chem.B* **105**, 9124 (2001).

In situ FT-IR spectroscopic studies of sulfur effect on Mo$_2$C/Al$_2$O$_3$ catalyst

Weicheng Wu, Zili Wu, Can Li*

State Key Laboratory of Catalysis, Dalian Institute of Chemical Physics, Chinese Academy of Sciences, P.O. Box 110, Dalian 116023, China

Introduction

Molybdenum carbide seems to be one of the most promising catalysts because it shows excellent catalytic activity for hydrogen-involved reactions.[1, 2] Especially, they have potential applications in hydrodesulfurization (HDS) [3-9] processes. However, transition metal carbides are found to be sensitive to sulfur species. Aegeter et al.[3] found by IR spectroscopy that Mo$_2$C/Al$_2$O$_3$ became sulfided at HDS temperatures. Their discussions were concentrated on the results of passivated carbide. It is noted that the passivation procedure causes a dramatic change in the carbide surface, i.e., from carbide to oxycarbide. Therefore, it is of significance to study how fresh carbide works under the reaction conditions. Thiophene is a typical representative of sulfur-containing hydrocarbons in hydrotreating reactions, so it is necessary to study the influence of thiophene on the surface property of carbide catalysts in order to get insight into the sulfur effect on the catalytic performance. In this work, we use *in situ* IR spectroscopy to characterise the surface nature of fresh Mo$_2$C/Al$_2$O$_3$ catalyst pretreated by thiophene/H$_2$. CO was employed to probe the sulfur effect of the catalyst surface.

Experimental

A MoO$_3$/Al$_2$O$_3$ sample with 10 wt % Mo was prepared by incipient impregnation method, a γ-Al$_2$O$_3$ (Degussa, S$_{BET}$ = 108 m^2 g^{-1}) impregnating with an aqueous solution of ammonium heptamolybdate, followed by a drying at 397 K overnight and calcination at 773 K for 4 h. The MoO$_3$/Al$_2$O$_3$ sample was pressed into a self-supporting wafer with a weight of approximately 15 mg/cm^2. The wafer was placed in a quartz IR cell equipped with CaF$_2$ windows, in which *in situ* carburization could be performed, and then carburized in a flowing 20% CH$_4$/H$_2$ mixture. The temperature was increased from room temperature to 573 K in 30 minutes and from 573 to 1033 K in 460 minutes, and then the temperature was maintained at 1033 K for 60 minutes. The carburized sample was cooled down to room temperature in flowing 20% CH$_4$/H$_2$ mixture.

The sample in the IR cell was treated with a thiophene/H$_2$ mixture (5/100 Torr) for 60 min at different temperatures (298, 373, 473, 573, 673 and 773 K) and detected by FT-IR spectroscopy, then evacuated to 10^{-5} Torr at 773 K for 60 min. Then the sample was cooled to RT and 10 Torr CO was introduced. The system was evacuated to 10^{-3} Torr in order that we could get the spectrum of chemisorbed CO.

All IR spectra were collected at room temperature on a Fourier transform infrared spectrometer (Nicolet Impect 410) with a resolution of 4 cm^{-1} and 64 scans in the region 4000-1000 cm^{-1}.

Results and Discussion

To investigate the sulfiding effect on Mo$_2$C/Al$_2$O$_3$ catalyst under different conditions, the catalyst was treated with a thiophene/H$_2$ mixture (5/100 Torr) at given temperatures for 60 min and then its surface nature was probed by CO adsorption at RT. Figure 1 exhibits the IR spectra of CO adsorbed on a fresh Mo$_2$C/Al$_2$O$_3$ sample and that sample treated with a thiophene/H$_2$ mixture. CO adsorbed on a fresh Mo$_2$C/Al$_2$O$_3$ sample gives two *characteristic* IR bands at 2055 and 2197 cm^{-1}. The detailed discussion will be done elsewhere.[10] The

intensity of the 2055-cm^{-1} band decreased dramatically. The 2197-cm^{-1} band disappeared and a strong band at 2100 cm^{-1} was observed when fresh sample was treated with the thiophene/H$_2$ mixture at 298 K. With the elevated treatment temperature, the intensity of the 2055-cm^{-1} decreased gradually and the 2100-cm^{-1} band become dominant. The band at 2100 cm^{-1} can be assigned to adsorbed CO on sulfide catalyst.[5, 11, 12] The results strongly suggest that the surface of the fresh Mo$_2$C/Al$_2$O$_3$ catalyst is significantly changed when treated with the thiophene/H$_2$ mixture above room temperature. The surface of the fresh Mo$_2$C/Al$_2$O$_3$ catalyst was partially sulfided.

The changes in the thiophene itself were also detected when the fresh Mo$_2$C/Al$_2$O$_3$ catalyst was treated with a thiophene/H$_2$ mixture at different temperatures (Figure 2). Upon exposure of a fresh Mo$_2$C/Al$_2$O$_3$ catalyst to a mixture of 5 Torr of thiophene and 100 Torr of H$_2$ at 473 K, the IR spectrum in the ν_{CH} region contains absorbance features at 2958, 2933, and 2879 cm^{-1}, and these are assigned to thiophene hydrodesulfurized on the catalyst surface.[13, 14] When treated at 673 K, a series of new bands at 3037, 3016, 2976, 2966, 2947, and 2922 cm^{-1} was observed. The two bands at 3037 and 3016 cm^{-1}, which can be assigned to the formation of alkene species, grow in intensity with the increase of treatment temperature. The process of hydrodesulfurization produced the bands at 2976, 2966, 2958, 2947, 2933, 2922, and 2879 cm^{-1}, which can be due to the attribution of saturated alkanes.[13, 14] These results indicated that when the fresh Mo$_2$C/Al$_2$O$_3$ catalyst was treated with a thiophene/H$_2$ mixture above 473 K, one or more hydrogenated species, exhibiting IR bands in the region 2870-2980 cm^{-1}, are produced. When the treatment temperature was increased to 673 K, some alkene species were formed. These species may be due to the decomposition of thiophene.
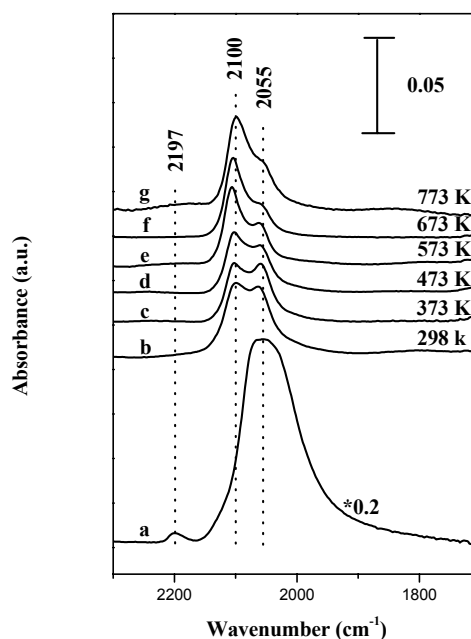
Figure 1. IR spectra of CO adsorbed at RT (a) on fresh Mo$_2$C/Al$_2$O$_3$ catalyst, and on the same catalyst after it was treated with a thiophene/H$_2$ (5/100 Torr) mixture at (b) 298 K, (c) 373 k, (d) 473 K, (e) 573 K, (f) 673 K, and (g) 773 K for 60 min.

(14) Wu, Z.; Chu, Y.; Yang, S.; Wei, Z.; Li, C.; Xin, Q. *J. Catal.* **2000**, 194, 23.
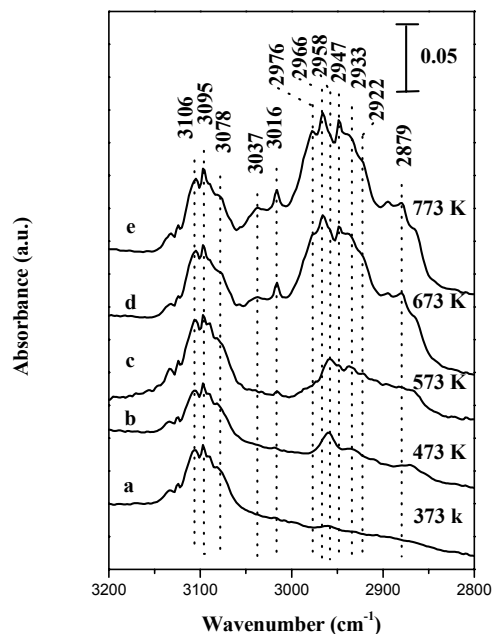
Figure 2. IR spectra in the ν_{CH} region for the fresh Mo_2C/Al_2O_3 catalyst treated with a thiophene/H_2 (5/100 Torr) mixture at (a) 373 k, (b) 473 K, (c) 573 K, (d) 673 K, (e) 773 K for 60 min.

Conclusions

The influence of thiophene on the surface state of the fresh Mo_2C/Al_2O_3 catalyst in the presence of H_2 has been studied by FT-IR spectroscopy combined with CO adsorption. The IR spectra of adsorbed CO suggest that thiophene can be easily hydrodesulfurized in the presence of H_2 on fresh Mo_2C/Al_2O_3 catalyst at temperatures as low as 473 K, at the expense of the sulfidation of the carbide catalyst.

References
(1) Oyama, S. T. *Catal. Today* **1992**, 15, 179.
(2) Chen, J. G. *Chem. Rev.* **1996**, 96, 1477.
(3) Lee, J. S.; Boudart, M. *Appl. Catal.* **1985**, 19, 207.
(4) Sajkowski, D. J.; Oyama, S. T. *Appl. Catal. A.* **1996**, 134, 339.
(5) Aegerter, P. A.; Quigley, W. W. C.; Simpson, G. J.; Ziegler, D. D.; Logan, J. W.; McCrea, K. R.; Glazier, S.; Bussell, M. E. *J. Catal.* **1996**, 164, 109.
(6) McCrea, K. R.; Logan, J. W.; Tarbuck, T. L.; Heiser, J. L.; Bussell, M. E. *J. Catal.* **1996**, 171, 255.
(7) Dhandapani, B.; Clair, T St.; Oyama, S. T. *Appl. Catal. A.* **1998**, 168, 219.
(8) Li, S.; Lee, J. S. *J. Catal.* **1998**, 178, 119.
(9) Costa, P. Da.; Potvin, C.; Manoli, J.-M.; Lemberton, J.-L.; Pérot, G.; Djéga-Mariadassou, G. *J. Mol. Cata. A: Chem.* **2002**, 184, 323.
(10) Manuscript in preparation.
(11) Müller, B.; Van Langeveld, A. D.; Moulijn, J. A.; Knözinger, H. *J. Phys. Chem.*, **1993**, 97, 9028.
(12) Mills, P.; Phillips, D. C.; Woodruff, B. P.; Main, R.; Bussell, M. E. *J. Phys. Chem.*, **2000**, 104, 3237.
(13) Tarbuck, T. L.; McCrea, K. R.; Logan, J. W.; Heiser, J. L.; Bussell, M. E. *J. Phys. Chem.*, **1998**, 102, 7845.

IR investigations on the surface sites of MoP/SiO$_2$ and their evolution under hydrodesulfurization conditions

Zili Wu*, Weicheng Wu, Zhaochi Feng, Qin Xin, Can Li*

State Key Laboratory of Catalysis, Dalian Institute of Chemical Physics, Chinese Academy of Sciences, P.O. Box 110, Dalian 116023, China. Email: ziliwu@dicp.ac.cn; canli@ms.dicp.ac.cn, Fax: 86-411-4694447

Introduction

In the last decades, there grows considerable interest in the development of new hydroprocessing catalysts because of the more stringent environmental legislation and the need of efficient conversion of low quality stocks into clean fuels. Since 1980s, transition metal nitrides and carbides has been attracted much attention as they show potential use in hydrotreating processes.[1] Recently, increasing studies show that transition metal phosphides have high catalytic activity for hydrodenitrogenation (HDN) [2,3] and hydrodesulfurization (HDS).[4,5] Among this class of catalysts, molybdenum phosphides, MoP, MoP/SiO$_2$ and MoP/Al$_2$O$_3$, were frequently studied and show better activity than conventional Mo sulfide catalysts in both HDN and HDS. It is interesting to note that molybdenum phosphides even increase in activity in the HDS of thiophene with steam on time,[5] which is different from the case of molybdenum nitride and carbide catalysts that readily deactivate in the presence of sulfur species.[6] In this work, in order to get insight into the nature of working surface of molybdenum phosphides under HDS reaction conditions, the surface sites of MoP/SiO$_2$ and their evolution in the presence of sulfur species were studied by IR spectroscopy using CO as the probe molecule.

Experimental

The precursor sample with Mo loading of 10 wt% was prepared by incipient wetness impregnation of SiO$_2$ with an aqueous solution of (NH$_4$)$_6$Mo$_7$O$_{24}$ and (NH$_4$)$_2$HPO$_4$. MoP/SiO$_2$ was prepared by reducing the oxide precursor in flowing hydrogen using temperature-programmed method.[2,5] The freshly prepared sample was passivated in a stream of 1% O$_2$/N$_2$ at room temperature (RT) and the passivated MoP/SiO$_2$ was obtained. In the IR study, a passivated sample was reduced in H$_2$ at different temperatures and then subjected to CO adsorption. The reduced sample was treated by thiophene (4 Torr), a mixture of thiophene/H$_2$ (4/400 Torr), or H$_2$S (5 Torr) at different temperatures, and the surface sites were probed by CO adsorption. All infrared spectra were collected on a Fourier transform infrared spectrometer (Nicolet Impact 410) with a resolution of 4 cm^{-1} and 64 scans.

Results and Discussion

Figure 1 presents the IR spectra of CO adsorbed on MoP/SiO$_2$ reduced at different temperatures. No IR band of adsorbed CO can be observed on the sample reduced at 673 K. Great changes of the spectra take place for the sample reduced at 723 K, a main band at 2050 cm^{-1} together with a weak shoulder at 2075 cm^{-1} appears. The band at 2050 cm^{-1} continues to increase in intensity with the elevated reduction temperatures, indicating that more surface sites for CO adsorption are generated owing to the deeper reduction. This band slight shifts to 2045 cm^{-1} and become the predominant band for the sample reduced at 923 K. According to the preparation process, the passivated MoP/SiO$_2$ reduced at 923 K can be regarded as fresh phosphide and it will be used in the following experiments. Therefore, adsobed CO on the surface of fresh MoP/SiO$_2$ owns an

characteristic band at around 2045 cm^{-1}. This band can be assigned to the linearly adsorbed CO on the surface molybdenum atom of MoP/SiO$_2$, which may be positively charged, i.e. Mo$^{\delta+}$ (0<δ<2).[7,8] To our knowledge, this is the first IR report for the nature of the surface sites of molybdenum phosphide.
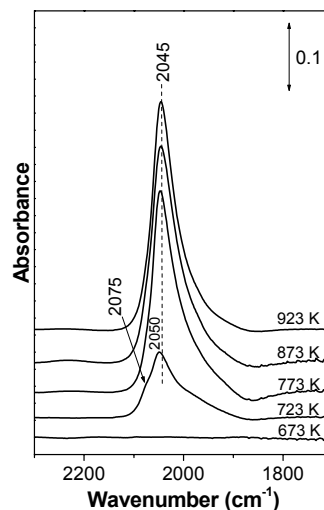

Figure 1. IR spectra of CO adsorbed on MoP/SiO$_2$ reduced by H$_2$ at different temperatures.

Figure 2 exhibits the IR spectra of CO adsorbed on MoP/SiO$_2$ sample treated with a thiophene/H$_2$ (4/400 Torr) mixture at different temperatures. The band at 2045 cm^{-1} shifts to higher frequencies when the treatment temperature is increased, e.g., to 2047 cm^{-1} at 373 K, to 2049 cm^{-1} at 473 K, to 2058 cm^{-1} at 573 K, and to 2096 cm^{-1} at 673 K. Meanwhile, a shoulder band at 2060 cm^{-1} is present for the sample treated at 673 K. The appearance of 2096 cm^{-1} indicates the sulfidation of the phospide surface because this is a characteristic band of CO adsorbed on sulfided Mo catalyst and has been assigned to linearly adsorbed CO on *cus* Mo^{2+} sites.[8] The results clearly show that the surface of the fresh MoP/SiO$_2$ catalyst is partially sulfided when treated with the thiophene/H$_2$ mixture at temperatures above RT.
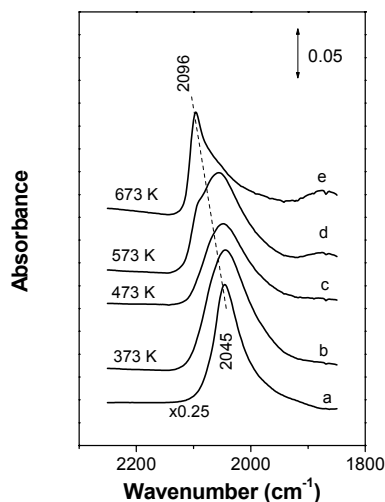

Figure 2. IR spectra of CO adsorbed on MoP/SiO$_2$ pretreated by a thiophene/H$_2$ mixture at different temperatures.

When MoP/SiO$_2$ sample was treated by thiophene alone, IR spectra of adsorbed CO imply that the surface keeps its phosphide nature even when it was treated by thiophene at 673 K, indicating that thiophene alone is quite stable on the surface of MoP/SiO$_2$.

The influence of H$_2$S on the nature of surface sites of MoP/SiO$_2$ is also studied by CO adsorption using IR spectroscopy. IR results show that the surface of MoP/SiO$_2$ is completely sulfided at the treatment temperature of 473 K.

Conclusions

The surface Mo$^{\delta+}$ ($0<\delta<2$) sites of MoP/SiO$_2$ catalyst has been probed by adsorbed CO using IR spectroscopy. IR results indicate that the surface of MoP/SiO$_2$ catalyst will be sulfided under HDS reaction conditions. With the presence of P atoms in the bulk of MoP, the composition of the sulfided MoP catalyst is somewhat similar to that of conventional Mo sulfides that adopt P as an additive. This could be the reason why MoP catalysts show good activities in HDS reactions.

References
(1) Oyama, S. T. *Catal. Today* **1992**, *15*, 179.
(2) Li, W.; Dhandapani, B.; Oyama, S. T. *Chem. Lett.* **1998**, 207.
(3) Stinner, C.; Prins, R.; Webber, T. *J. Catal.* **2001**, *202*, 187.
(4) Clark, P.; Wang, X.; Oyama, S. T. *J. Catal.* **2002**, *207*, 256.
(5) Phillips, D. C.; Sawhill, S. J.; Self, R.; Bussell, M. E. *J. Catal.* **2002**, *207*, 266.
(6) Wu, Z.; Chu, Y.; Yang, S.; Wei, Z.; Li, C.; Xin, Q. *J. Catal.* **2000**, *194*, 23.
(7) Yang, S.; Li, C.; Xu, J.; Xin, Q. *J. Phys. Chem. B* **1998**, *102*, 6986.
(8) Müller, B.; van Landeveld, A. D.; Moulijn, J. A.; Knözioger, H. *J. Phys. Chem*. **1993**, *97*, 9028.

HYDRODESULFURIZATION BEHAVIOR
OF Mo₂N CATALYST

Shuwen Gong, Haokan Chen, Wen Li, Baoqing Li

State Key Laboratory of Coal Conversion
Institute of Coal Chemistry Chinese Academy of Sciences
Taiyuan, China, 030001

Introduction

Since Volpe[1] synthesized γ - Mo$_2$N by temperature-programmed reaction of MoO$_3$ with NH$_3$, γ - Mo$_2$N as effective and selective hydrotreatment catalysts had been extensively studied[2-4]. Nagai[2] and co-workers reported the nitrided Mo/Al$_2$O$_3$ catalyst to be 1.1-1.2 times more active than a sulfided Mo/Al$_2$O$_3$ in the hydrodesulfurization(HDS) of dibenzothiophene and to be extremely selective in the C-S hydrogenolysis to form biphenyl. Also, Sajkowski and Oyama[3,5] found unsupported γ - Mo$_2$N to be nearly twofold as active as the commercial Ni-Mo/Al$_2$O$_3$ catalyst for HDS of coal-derived feed. Markel et al[6]. reported that unsupported molybdenum nitride was presented despite the sulfidation conditions in the catalytic reactor.

However, up to now, preparation of γ - Mo$_2$N is difficult, because all the reaction gases must be very high purity. Markel[6] synthesized γ - Mo$_2$N using matheson ammonia(99.9999%). Wise and his colleagues[7] synthesized γ - Mo$_2$N using mixture of N$_2$ and H$_2$(N$_2$ or H$_2$ is matheson and 99.9995%).

In this paper, we studied the HDS behavior of molybdenum nitride catalysts synthesized using low purity of reaction gases compared with previous reports in order to make the synthesis easy. Effects of reaction temperature and pretreatment method on the activities and structures of Mo$_2$N were also examined.

Experimental Section

Catalyst Synthesis. Mo$_2$N was produced by reaction of MoO$_3$(99%) and flowing mixture of N$_2$(99.9%) and commercial H$_2$. The gases were controlled using rotameters. MoO$_3$ powder was loaded in the center of 15mmID×20mmOD×60mm quartz tube reactor. The temperature was increased in three steps: first rapidly from room temperature to 300℃, then from 300℃ to 500℃ at 0.6℃/min, finally from 500℃ to 700℃ at 2℃/min and held at 700℃ for 2h. After the nitridation reaction, the reactor was cooled down to room temperature under N$_2$, and then passivated with a mixture of 1%O$_2$ in N$_2$ for 2h. We called it as passivated molybdenum nitride. Passivated Mo$_2$N was sulfided by the mixture of 3wt% CS$_2$ in cyclohexane and H$_2$ as the carrier gas at 350℃, which we called pre-sulfided Mo$_2$N. Passivated Mo$_2$N was employed in H$_2$ at 400℃ for 2h, which we called it as pre-reduced Mo$_2$N.

X-Ray Diffraction. The crystal structures of catalysts were determined using XRD, The diffraction patterns were collected using a DMAX-rA diffractometer and CuKα radiation(λ =1.542Å).

Evaluation of HDS Activities of Catalysts. The measurements of catalytic activities of Mo$_2$N were carried out using an atmospheric pressure flow reactor. A gas chromatograph equipped with a flame ionization detector was used to analyze thiophene and hydrocarbon products. Catalyst samples(≈0.2g) were loaded in the reactor. Thiophene was carried by H$_2$ using a bubbler apparatus. The major HDS products (1-butene, butadiene, cis-2-butene, trans-2-butene and butane) were calibrated with analytical gas standards to facilitate conversion calculations.

Results and Discussion

XRD Patterns of Passivated and After-reacted Mo₂N. The diffraction pattern for passivated Mo$_2$N showed peaks at 37.8°, 43.2°, 45.2°, 62.6°, 64.2°, 75.5°, 78.2°, and 80.5°(**Figure 1a**), which were assigned to the {111}, {200}, {002}, {220}, {202}, {311}, {113} and {222} reflections of bulk Mo$_2$N, respectively. They were obvious difference with γ - Mo$_2$N by JCPDS standard data and references[6-7]. There were not peaks attributed to Mo oxides and γ - Mo$_2$N, indicating that MoO$_3$ all transformed into Mo$_2$N, and passivation had no effects on bulk structure of Mo$_2$N. Therefore, it was concluded that passivation produced a protective, amorphous, surface oxide film which was slightly greater than one-monolayer thick like passivated γ - Mo$_2$N.
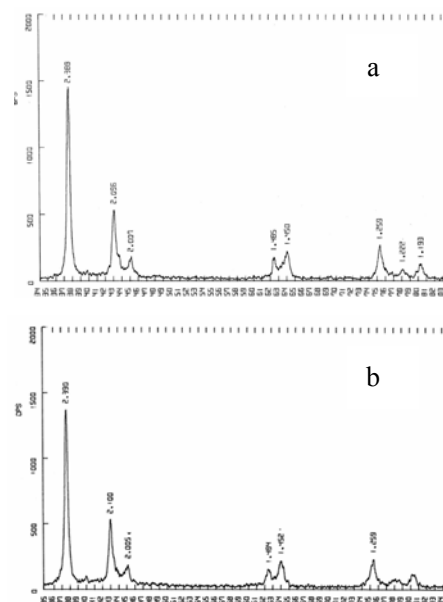
Figure1. XRD patterns of Mo$_2$N a: before-reaction
b : after-reaction.

After HDS reaction, Mo$_2$N was removed from the reactor and analyzed by X-ray diffraction. Diffraction pattern was presented in **Figure 1b**. Peak locations and relative intensities showed that the bulk structure of Mo$_2$N was unchanged, which meant that no traces of impurities, such as Mo sulfide, were found. This suggested that Mo$_2$N had strong resistance to sulfidation.

HDS Behavior of Mo₂N. HDS activity of passivated Mo$_2$N without pretreatment under different reaction temperature was showed in **Figure 2**. At 400℃ and 360℃ the HDS activities of Mo$_2$N deactivated with reaction time in the initial stage, and then retained about a constant. Because the bulk structure of Mo$_2$N was retained in the whole reaction, the deactivation of catalyst might be resulted from the change of Mo$_2$N surface properties.

It was also found that with the increase of the reaction temperature the amount of C4 products converted from thiophene was high(**Figure 2**). However, at 320℃ the HDS activities of Mo$_2$N were a little low.

Effect of Pretreatment on Mo₂N HDS Behavior. **Figure 3** showed the effect of pre-treatment on Mo$_2$N HDS activity. The

activity order was passivated nitride>sulfided nitride>reduced nitride, which indicated that pre-reduction and pre-sulfidation did not improve the activity of Mo$_2$N. But the sulfidation could improve the stability of catalytic activity. After 9h reaction, pretreated Mo$_2$N were removed from the reactor and analyzed by X-ray diffraction.
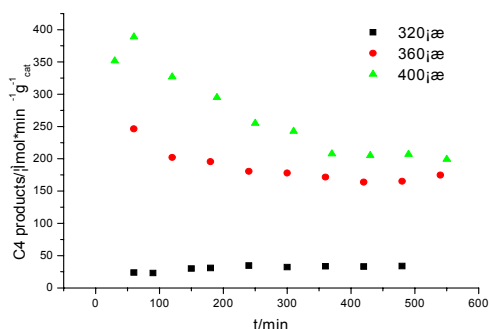

Figure 2. Catalytic activities of Mo$_2$N in HDS reaction
at different temperature.

XRD spectra of pre-reduced Mo$_2$N catalyst was presented in **Figure 4**. There were not obvious changes of peak locations compared with **Figure 1**, which indicated that no impurities such as Mo sulfide or Mo were found and pre-reduction had no effects on bulk structure of Mo$_2$N. Thus, pretreatment might affect the surface character of Mo$_2$N and deactivate the catalytic activity of Mo$_2$N. A possible reason might be that very thin metal Mo species film was formed on the surface. Logan[8] and Liu[9] reported similar result for the nitride catalysts which were reduced in H$_2$. Pre-sulfidation did not change the bulk structure of Mo$_2$N either. It suggested that Mo$_2$N had strong resistance to sulfidation. Sulfidation might only affect the surface properties which had great influence on the catalyst HDS activity. Markel[6] and McCrea[10] thought that a thin film of Mo sulfide formed on the surface of molybdenum nitrides in sulfidation condition. However, it should be noted that there were no satisfied explanation why deactivation of Mo$_2$N catalyst was also discovered after its pre-reduction and pre-sulfidation treatment.
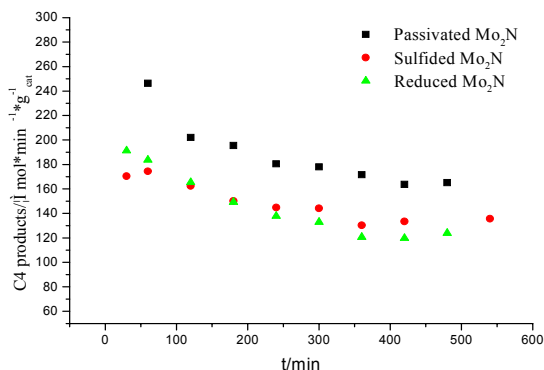
Figure 3. Catalytic activities of Mo$_2$N pretreated
by different methods.
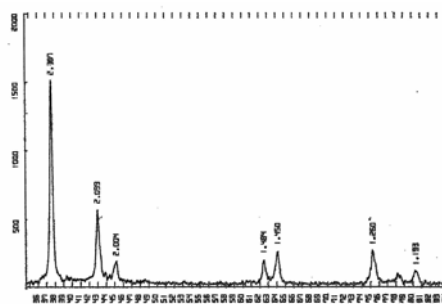
Figure 4. XRD pattern of pre-reduced molybdenum nitride.

Conclusions

1. Another crystal type Mo$_2$N that different from ɣ one was synthesized by temperature-programmed reaction between MoO$_3$(99%) and the mixture of N$_2$(99.9%) and commercial H$_2$. It had high thiophene HDS catalytic activity like ɣ - Mo$_2$N.

2. Mo$_2$N deactivated with reaction time at the initial stage of reaction, and then retained about a constant. The catalytic activity increased with increasing reaction temperature. X-ray diffraction pattern suggested that bulk structure of Mo$_2$N did not have change after reaction.

3. The HDS action of nitride catalyst was strongly dependent on the pretreatment of the catalyst. Pre-reduction and pre-sulfidation could deactivate the catalytic activity. However, the bulk structure of Mo$_2$N remained unchanged after pretreatment. The pretreatment might affect the surface properties of catalyst to deactivate the activity.

References
1. Volpe, L.; Boudart, M., J Solid State Chem., 1985, 59(3): 332-347
2. Nagai, M., Miyao, T.; Tuboi, T., Catal. Lett., 1993, 18(1): 9-14
3. Sajkowski, D. T.; Oyama, S. T., Appl. Catal. A, 1996, 134(1-2): 339-349
4. Colling, C. W.; Thompson, L. T., J. Catal., 1994, 146(1): 193-203
5. Sajkowski, D. T.; Oyama, S. T., Prepr. Am. Chem. Soc. Div. Pet. Chem., 1990, 35(2): 233-236
6. Markel, E. J.; Van Zee, J. W., J. Catal., 1990, 126 (2): 643-657
7. Wise, R. S.; Markel, E. J., J. Catal., 1994, 145(2): 344-355
8. Logan, J. W. Heiser, J. L., McCrea, K. R., Gates, B. D., Bussell, M. E. Catal., Lett., 1998, 56(4): 165-171
9. Liu, Y. Q., Liu, C. G., Que, G. H., Energy & Fuels, 2002, 16(3): 531-535
10. McCrea, K. R., Logan, J. W., Tarbuck, T. L., Heiser, J. l., Bussell, M. E., J. Catal., 1997,171(1):255-267